Masteroppgave

NTNU
Norges teknisk-naturvitenskapelige universitet
Fakultet for informasjonsteknologi og elektroteknikk
Institutt for elkrafftteknikk

Trond Markus Tutturen
Jørgen Nyhus-Solli

Towards Plug-and-Play Control of Wind Power Systems:

Scalable stability certificate guaranteeing large signal stability for entire wind parks

Masteroppgave i Energi og Miljø
Veileder: Gilbert Bergna-Diaz
Juni 2022

NTNU
Kunnskap for en bedre verden

Trond Markus Tutturen
Jørgen Nyhus-Solli

Towards Plug-and-Play Control of Wind Power Systems:

Scalable stability certificate guaranteeing large signal stability for entire wind parks

Masteroppgave i Energi og Miljø
Veileder: Gilbert Bergna-Diaz
Juni 2022

Norges teknisk-naturvitenskapelige universitet
Fakultet for informasjonsteknologi og elektroteknikk
Institutt for elkraftteknikk

NTNU
Kunnskap for en bedre verden

Abstract

To reduce global warming, power generation must transition from fossil sources to renewable energy sources with a lower carbon footprint. The traditional power grid structure is comprised of large fossil-fueled power plants often located in the vicinity of the power consumption, such as big cities. The transition to distributed renewable energy sources introduces new challenges. The renewables will be intermittently integrated into the power grid, potentially far away from where most of the power is consumed, causing less predictable power generation and more challenging transmission. Where traditional power generation is dominated by large synchronous generators with large inertia, most renewable energy sources are connected to the power grid through power electronic converters where the inertia cannot contribute to the stability of the power grid. The increasing penetration of renewables, therefore, has the *potential to jeopardize* the stability and the performance of the entire power system. Therefore, a new strategy for controlling power electronic converters is needed that allows for the continuous growth of distributed renewable energy sources without compromising the stability of the power system.

One of these converter-connected renewable energy sources is wind power, which might become one of the largest power sources in the future. This master thesis aims to develop a *scalable stability certificate* allowing for a *plug-and-play* philosophy for a wind park. By *scalable stability certificate*, it is meant as a set of criteria that guarantee *large signal stability* for a wind park that can be expanded to the desired size and connected to an external power grid without the risk of instability. The *plug-and-play* feature is meant as an connection strategy which enables a system to adapt to changes with minimal interventions. The derivation of the *stability certificate* is based on an analysis of a wind energy conversion system consisting of a permanent magnet synchronous generator connected to full scale back-to-back two-level voltage source converters. The system introduces three challenging non-linearities: in the generator dynamics, the mechanical torque generated by the wind, and in the power converters. It is shown how such a wind energy conversion system can be guaranteed to be stable for large disturbances by using design criteria for the damping in the generator and tuning conditions for passivity-based feedback control loops. It is proven that by satisfying these stability criteria *locally* at each wind turbine, a wind park consisting of these wind turbines will also be guaranteed to be stable for large disturbances. Thereby, a *scalable stability certificate* is found.

The derivation of the stability criteria relies on the following tools from *non-linear system theory*. *Passivity* is used as a starting point for control design in combination with *port-Hamiltonian* modeling formalism, which emphasizes the system dissipation, interconnection pattern, and the energy in the system dynamics. *Lyapunovs direct method* is used for the stability analysis, where the Lyapunov candidate function is inspired by the energy of the system. Lastly, *graph theory* is used to expand the model from one wind turbine to a wind park to investigate the stability of the entire system.

In addition, this thesis briefly compares PI-current control with PI-PBC, the performance and stability challenges with and without cascaded control structure, and how the damping in the generator improves the control performance.

Sammendrag

For å redusere den global oppvarming må kraftproduksjonen gå over fra fossile kilder til fornybare energikilder med lavere karbonavtrykk. Det tradisjonelle strømnettet består av store fossildrevne kraftverk som ofte plassert i nærheten av det største kraftforbruket, f.eks. nær storbyer. Overgangen til fornybare energikilder byr på nye utfordringer. De fornybare energikildene vil sporadisk bli integrert i kraftnettet, potensielt langt unna der det meste av kraften forbrukes, noe som forårsaker mindre forutsigbar kraftproduksjon og mer utfordrende kraftoverføring. Der tradisjonell kraftproduksjon domineres av store synkrongeneratorer med stort treghetsmoment, er de fleste fornybare energikilder koblet til kraftnettet gjennom kraftelektroniske omformere hvor treghetsmomentet ikke kan bidra til stabiliteten regulering i kraftnettet. Den økende innfasingen av fornybar energi har derfor potensialet til å redusere og i verste fall ødelegge stabiliteten og kraftoverføringsevnen til hele kraftsystemet. Derfor er det nødvendig med en ny strategi for å kontrollere kraftelektroniske omformere som muliggjør en kontinuerlig vekst av distribuerte fornybare energikilder uten at det går på bekostning a stabiliteten i kraftsystemet.

En av disse omformertilkoblede fornybare energikildene er vindkraft, som kan bli en av de største kildene til elektrisk energu i fremtiden. Denne masteroppgaven har som mål å utvikle et *skalerbart stabilitetssertifikat* som åpner for en *plug-and-play*-filosofi for en vindpark. Med *skalerbart stabilitetssertifikat* menes det som et sett med kriterier som garanterer *stor signalstabilitet* for en vindpark som kan bygges ut til ønsket størrelse og kobles til eksternt strømnett uten risiko for ustabilitet. *plug-and-play*-funksjonen er ment som en tilkoblingsstrategi som gjør det mulig for et system å tilpasse seg endringer med minimale inngrep. Utledningen av *stabilitetssertifikatet* er basert på en analyse av et vinkraftsystem bestående av en permanent magnet synkrongenerator koblet til fullskala back-to-back to-nivå spenningskildeomformere. Systemet introduserer tre utfordrende ulineæriteter: i generatordynamikken, det mekaniske dreiemomentet som genereres av vinden, og i kraftomformerne. Det vises hvordan et slikt vindkraftsystem kan garanteres å være stabilt for store forstyrrelser ved å bruke designkriterier for dempingen i generatoren og reguleringskrav for passivitetsbaserte tilbakekoblingskontrollsløyfer. Det er bevist at ved å tilfredsstille disse stabilitetskriteriene *lokalt* ved hver vindturbin vil en vindpark bestående av disse vindturbinene også være garantert stabil for store forstyrrelser. Derved er et *skalerbart stabilitetssertifikat* funnet.

Utledningen av stabilitetskriteriene er basert på følgende verktøy fra *ulineær systemteori*. *Passivity* brukes som utgangspunkt for kontrolldesign i kombinasjon med *port-Hamiltonian* modellering. *Lyapunovs direkte metode* brukes for stabilitetsanalysen, der Lyapunov-kandidatfunksjonen velges basert på energien i systemet. Til slutt brukes *grafteori* for å utvide modellen fra én vindturbin til en vindpark for å undersøke stabiliteten til et helt system.

I tillegg, sammenligner denne oppgaven i korthet PI-strømkontroll med PI-PBC, ytelses- og stabilitetsutfordringene med og uten kaskadekontrollstruktur, og hvordan dempingen i generatoren forbedrer kontrollytelsen.

Acknowledgement

The authors would like to send a special thanks to our supervisor, associate professor Gilbert Bergna-Diaz (Big G) at the department of Electric Power Engineering. Without his deep understanding of non-linear control theory and burning wish to educate others on this field, this work would not have been possible. Gilberts hospitality and the way he has continuously kept in touch since the beginning has had a major impact on the work and our motivation.

A special thanks to the group called "LUNSJ/BI". Without their humour and interesting view on life, this journey would have been less memorable and enjoyable.

Lastly we would like to thank our fellow students, who have been both a source of information, but more importantly have accompanied us on the journey to enlightenment.

Contents

List of Figures

List of Tables

List of Abbreviations

B2B - back-to-back

d-axis - direct axis

GGE - greenhouse gas emmsisions

GW - Gigawatt

IEA - International Energy Agency

LCF - Lyapunov candidate function

MPPT - maximum power point tracking

MW - Megawatt

PBC - passivity-based controller

PCC - point of common coupling

pH - port-Hamiltonian

PI - proportional integral

PMSG - permanent magnet synchronous generator

PV - Photovoltaics

PWM - Pulse width modulation

q-axis - quadrature axis

SG - synchronous generators

TS - turbine string

TSO - transmission system operator

TWh - Terrawatt-hour

WECS - wind energy conversion system

WTG - wind turbine generator

2l-VSC - two-level voltage source converter

Chapter 1

Introduction

The introduction chapter presents a motivation for this thesis along with a short description of our contribution to solving the challenges of integrating wind resources in the electrical grid. The chapter begins with a general overview of the demand for energy and follows up with a more specific description of the Status Quo for wind resources to highlight the area from which this thesis originate. Tools that seem able to deal with several of the challenges concerning wind energy are presented. Lastly, we present the contributions in this master thesis, more precisely the objectives, methodology, and limitations.

1.1 General Introduction

One of the International Energy Agency (IEAs) scenarios forecasts an increase in electricity consumption from 23 300 Terrawatt-hours (TWh) in 2021 to 30 000 TWh in 2030, an increase of more than 22 %. Electricity is, for most people, something they take for granted. When they plug into the wall sockets, they expect the electricity to start flowing. Going back not much further than a decade, few people, not counting those working with electricity generation, cared or even thought about where the electricity came from. This attitude has luckily changed over the last decade, and more people have started to take an interest in how the electricity is made [1]. As a result, companies that generate renewable power sell guarantees of origin to electricity companies, such that customers are able to support the renewable generation [2]. Measures like this are a good way to increase renewable power generation and are needed more than ever since the electricity demand is expected to increase over the following years. To reach the climate goals by reducing the greenhouse gas emissions (GGE) by at least 50-55 % in 2030 compared to the reference year in 1990, it is crucial that renewable energy sources meet this increased demand. In addition, a higher share of the already installed electricity capacity also needs to become renewable. Global CO_2 emissions from electricity generation increased by roughly 9% over the last decade, but the overall electricity demand rose by 25%. Therefore, meeting the increasing demand and not skyrocketing the emissions is a demanding challenge but not impossible [3].

The increase in electricity demand is tightly coupled with the desire to reduce greenhouse gases through electrification and the fact that more and more people get access to electricity [4]. Electrification of different sectors can drastically reduce the GGE. The transport sector counts for 16.2 % of the global GGE. The primary emissions from this sector come from the internal combusting engines burning petrol, and diesel [5]. Changing to electric vehicles arguably appears as a logical choice, and many countries have already implemented benefits for those willing to make the trade. One of the downsides of changing to electric vehicles is the increased pressure on electricity generation. In countries where the electricity is mainly produced by renewable energy sources with

low carbon footprint, the GGE declines. In countries where the electricity comes from fossil fuels on the other hand, the reduction of GGE declines less rapidly. The increase in electricity demand in such countries results in an increasing electricity production from fossil-fuelled based sources. The only solution that will be sustainable is to decarbonize the electricity supply, meaning all electricity has to come from renewable energy sources such as hydro, wind, solar, etc. However, the transition to renewable energy sources introduces new challenges.

Today's power grid is dominated by large synchronous generators (SG) with high inertia, often fuelled by fossil fuels. The grid frequency is decided by the transmission system operator (TSO), and a stable frequency is maintained by having all SGs electrically coupled and rotating at the same electrical frequency. The stability of the power grid relies on several factors, for instance the inertia of the SGs and the frequency regulation of SGs through the droop response of the speed controller to mention a few. [6].

Renewables such as wind and solar are connected to the power system through electrical power converters, and they have the potential to jeopardize the stable operation of the entire power system, especially under large disturbances, thus potentially limiting the timely-needed expansion of renewable energy sources [7]. A new strategy is needed to safely operate power systems with high integration of renewable sources. Amongst these renewables are wind power, which is anticipated to become one of the more dominating renewables in the future power grid. For that reason, wind power is the subject investigated in this thesis, and is more thoroughly introduced in the next section.

1.2 Wind Power

The global renewable capacity is expected to increase by about 305 Gigawatt (GW) annually between 2021 and 2026, according to the IEA main forecast [8]. Of the 305 GW per year, on average, 94 GW of the increase is expected to be wind power. The offshore share of wind power is expected to increase, from roughly 6.1 GW in 2020, reaching upwards to 76 GW by 2025 [9].

As mentioned, the offshore wind market is expected to keep increasing according to IEAs forecast. The increase in the offshore wind sector is due to several reasons. Decreasing offshore auction prices and new areas that were discarded because of the water depth are becoming more relevant, to mention a few. This is due to the technological advancement made in regards to the floating substructures. Offshore wind turbines also have higher rated power compared to onshore wind turbines. This implies fewer wind turbines to produce the same amount of power compared to the onshore ones [10]. For this reason, along with reducing encroachment on nature, offshore wind is becoming lucrative.

The Norwegian government has an ongoing initiative to promote offshore wind power. Phase one of the initiative is to increase the installed offshore capacity by 1500 Megawatt (MW), thereby increasing the electricity production by roughly 7 TWh per year. Phase two of the initiative also has a capacity of 1500 MW. However, some challenges regarding the grid connection need solving before this part sees the light of day [11].

The most promising wind energy conversion system (WECS) is the type 4 wind turbine generator (WTG) with a full scale back-to-back (B2B) power converter. In this configuration, the generator is completely decoupled from the power grid. By doing so, the speed of the generator is fully controllable, which allows for maximum power point tracking (MPPT) [12]. The downside of doing, the ability to rely on the inertia of the machine for stability regulation is lost. [13].

Today's conventional control and tuning strategies are often based on the linearization of the wind generation system. Linearization allows for simple analytical and numerical solutions for many control problems and ease the implementation of practical applications [14]. Unfortunately, most real-world control systems are nonlinear by nature. The generator dynamics, the wind itself, and the converters introduce nonlinearities in the WECS. To guarantee large signal stability, one has to take these nonlinearities into consideration.

The specialization project associated with this master thesis presented a detailed derivation of the equations describing a WECS. For completeness the derivation is included in Appendix B. The mechanical torque highly depends on the wind through the wind power coefficient C_p. The coefficient expresses the turbine's efficiency and is dependent on the tip speed ratio, which is a function of angular velocity, the wind speed, and the radius of the turbine blades. In addition, the wind power coefficient C_p is also dependent on the pitch angle β but is assumed to be constant and typically zero when the turbine operates in the regime of maximum aerodynamic efficiency [15].

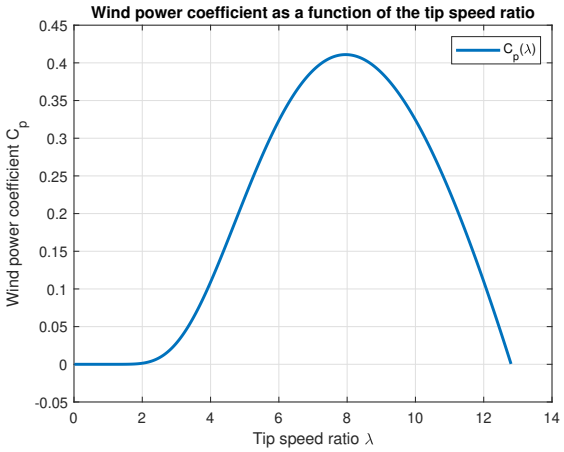

Figure 1.1: The wind power coefficient as a function of the tip speed ratio

From Figure 1.1, one can see the highly non-linear nature of the turbine coefficient, and to guarantee large signal stability without recurring to standard approximations, this non-linear property should ideally be taken into consideration when modeling and subsequently controlling the system.

To summarize, the offshore wind power is expected to increase drastically in the coming years, partly due to the technological advancements made on that front. The most promising system is the type 4 WTG, which makes it possible to control the speed of the generator, while the downside of doing so, however, is that one loses the ability to rely on the inertia for stability regulation and the non-linear nature of the wind power system introduces challenges. To guarantee large signal stability, one has to take these into consideration.

New procedures and methods need to be implemented to allow for a rapid change in the traditional power grid structure. A procedure that takes into account the nonlinearities of the renewables and their interfacing converters and that allows for a "*plug & play*" feature for a rapid expansion is therefore investigated in this master thesis. For that reason, a more detailed literature review highlighting some of the possible non-linear control theory tools contributing to this change is presented next.

1.3 State of the Art

The integration of power electronic converters in the power grid as a result of the change from centralized to more distributed generation has been a topic of extensive research [16]. Research that, amongst other, relate to photovoltaic (PV) systems integration in the grid [17] and on the challenges concerning grid integration of wind energy [18]. There are several challenges concerning wind energy. One of these is the output power prediction, as there is no ideal strategy to predict wind energy due to the challenging meteorological items to be forecasted. Another challenge is the reactive power/voltage support. For instance, the most utilized generator type is the induction generator which cannot produce reactive power of its own but only consume. Other challenges are the impact on the frequency due to the decoupling of the generators from the rest of the grid and harmonic injections. Nevertheless, the integration of wind energy into the power grid is happening at a level never seen before [8].

To overcome many of the issues regarding the integration of renewables and their overall impact on the large signal stability of the power grid, new methods are being investigated. In this regard, modeling techniques that highlight the passivity of the systems in combination with Lyapunov stability theory have shown promising results [15] [19]. One of these modeling techniques, and the one used in [15], is the Euler-Lagrange representation. In this thesis, however, the port-Hamiltonian (pH) modeling formalism is used since it allows for expansion and easy interconnection with other subsystems. The pH formalism has already been utilized in several fields of study, including the modeling of power converters [20] [21], modeling of synchronous generator [22] and modeling of an HVDC system [23].

As mentioned, the pH modeling formalism highlights the passivity of the system. Passivity is a key concept in stability analysis and is a useful starting point for control design, bringing the stored energy of the system to its minimum [24]. Passivity-based control has been around since the late 1980s [25] and was first introduced in the context of adaptive control of robot manipulators [26]. Passivity-based control is a control design method for non-linear systems that exploit the system's physical structure. More precisely, it exploits the fact that physical systems satisfy the energy balance. Stored energy is equal to the difference between supplied energy and dissipated energy, and the passivity-based controller (PBC) exploits this to arrive at a modified energy balance via control. The new energy balance consists of a desired stored energy which equals the difference between a new supplied energy and a desired dissipated energy. Passivity-based control is, therefore, an energy shaping and damping injection control method that accomplishes this by rendering the closed-loop passive with respect to some suitable storage function [19]. Passivity-based control is often found in combination with pH modeling, for instance, in [27].

By utilizing graph theory in combination with pH modeling, one is able to generalize the study of the interactions of n smaller pH systems connected together. The method is based on deriving the pH models for each individual component and then combining them all using power preserving interconnections with the help of the incidence matrix, which contains the network graph topology [28]. Graph theory has been around since the 17^{th} century, and its applications are well known and broadly spread to say at least [29]. For instance, in [30] a multi-carrier energy distribution system consisting of an electrical distribution system is coupled with a gas distribution system. Graph theory is in this paper used to integrate the network models into a pH model, and the model aims to create an application for energy management control and monitoring.

1.4 Contribution

This thesis is a continuation of the work done in the associated specialization project where a scalable *stability certificate* for a WECS was investigated. The *stability certificate* is a guarantee for the system to be stable for large disturbances and that the system can safely be connected to an external grid without jeopardizing its stability. The *main* contribution compared to our previous work is to include the two-level voltage source converter (2L-VSC) in a B2B configuration interfacing the permanent magnet synchronous generator (PMSG). In addition, the stability result is *generalized* by means of graph theory, making the result not only valid for a single wind turbine but for a complete wind park.

1.4.1 General objectives

The main objective of the thesis is to expand the *stability certificate* for a wind energy conversion system found in the specialization project by including the nonlinear dynamics of the back-to-back 2L-VSCs and generalizing the result to include any (multi-machine/converter) wind-park configuration. The *stability certificate* is developed using passivity in combination with port-Hamiltonian modeling and Lyapunov stability analysis.

1.4.2 Specific Objectives

More precisely, we aim to

- Derive the port-Hamiltonian model of a wind energy conversion system consisting of a wind turbine with a permanent magnet synchronous generator and full scale back-to-back converters.
- In combination with industry standard proportional integral (PI) controllers, use the *shifted* Hamiltonian as a Lyapunov candidate function to investigate the stability properties of the system and check if the conditions for stability are satisfied.
- Simulate the wind energy conversion system with the full back-to-back converters and validate the stability criteria. By use of simulation different control strategies are investigated such as comparison with traditional PI-current control, cascaded control structure and practical solutions to challenges introduced by cascaded control structure.
- Expand the stability analysis to apply for a wind park with the help of graph theory.

1.4.3 Methodology

To achieve our objectives, we:

- Derive a port-Hamiltonian model of a full back-to-back wind energy conversion system.
- Utilize the result presented in [31] for a *general* (rather abstract) class of (physical) systems and apply it to the specific case of the wind power system to find the stability criteria by means of Lyapunov stability theory.
- Derive a port-Hamiltonian model of the grid and expand the port-Hamiltonian model of the wind turbine, so it is comprised of several wind turbines.
- Connect the grid model and the new port-Hamiltonian model of the wind turbines through a power preserving interconnection with the help of graph theory
- Repeat the stability procedure done for the single wind turbine case for a wind park, i.e., utilize the result presented in [31] for a new Lyapunov function comprised of the shifted Hamiltonian of the grid and the shifted Hamiltonian of the wind turbines.
- Simulate the wind energy conversion system in Matlab/Simulink to validate our findings.

1.4.4 Limitations of Scope

Given the scope of the thesis, several simplification had to be made and are summarized below:

- The synchronous generator model is simplified to make the WECS easier to work with and simulate. The simplifications are that magnetic saturation is neglected, the magnetic field is evenly distributed in the generator, the resistance and the inductance in the generator and grid are independent of frequency, the permanent magnets create a sinusoidally distributed field, and hysteresis losses are neglected. These assumptions and simplifications are made, as their inclusion will not impact the control of the generator significantly.
- A damping coefficient, $'d'$, is introduced in the modeling of a synchronous generator. The damping is due to damper windings in the rotor of the synchronous generator. Only the damping effect is included in the model, as the effect on the flux linkages in the machine due to the damper windings would require a more advanced model. The damping due to friction is neglected in the model, as the friction loss is assumed to be very small.

- In the capacitors, a conductance $'G'$ is added to model the losses associated with the capacitor, as no physical element is loss-free. Switching losses are neglected, but one could argue that these could also be modeled in the conductance $'G'$.
- In the single converter model, the second converter and external grid are modeled as a current source on the DC-side of the converter for simplicity and to allow for a practical port-Hamiltonian structure.
- The external grid is modeled as a stiff voltage source in the two converter model in section 3.2.
- The HVDC-connection for the wind park in chapter 5 is modelled as a constant voltage source. It is assumed that the control of this modular multilevel converter keeps the voltage at the wind park connection constant.
- Due to time constraints, simulation of the wind park is left for future work.

1.4.5 Thesis Structure

This thesis is organized as follows. Chapter 2 is a short summary of the specialization project, which this thesis is a continuation of. Chapter 3 starts with the derivation of a *stability certificate* for a WECS with only the machine-side converter. Then the *stability certificate* is expanded to include the full back-to-back converter configuration. Towards the end of Chapter 3, the nonlinear dynamics of the wind are included. Chapter 4 begins with a theoretical part concerning the control of a wind turbine. Later, simulation results for different scenarios and a comparison of different control strategies and control structures are shown. In chapter 5, the certificate derived in chapter 3 is expanded for a more extensive system consisting of a wind park with multiple wind turbines. The thesis ends with conclusions and gives suggestions for future work in chapter 6.

Chapter 2

Summary of Specialization Project

This master thesis is a continuation of the work that was started in the specialization project "Towards Plug-and-Play control of Wind Power Systems: Tuning Criteria for Converter Connected PMSG Wind Turbine Guaranteeing Large Signal Stability". The aim of this project was to develop a so-called stability certificate for a PMSG-connected wind turbine. The stability certificate guarantees the PMSG-connected wind turbine to be stable even for large disturbances, and if the wind turbine is connected to a larger system, then the wind turbine will not jeopardize the stability of the larger system. As the master thesis is building on top of the result of this project, a short summary of the project is presented in this chapter for the sake of completeness.

2.1 Methodology

To attain a *stability certificate*, the methods introduced in [31] are applied to the wind energy conversion system described in [15]. The system is first shown to admit a port-Hamiltonian representation, and a Lyapunov candidate function (LCF) inspired by the Hamiltonian is chosen. The passive properties inherent to a port-Hamiltonian system are exploited to satisfy Lyapunov's stability conditions. The values of the tuning- and damping parameters of the WECS for the Lyapunov function to be satisfied yield the stability criterion.

2.2 The system, Analysis and Conclusions

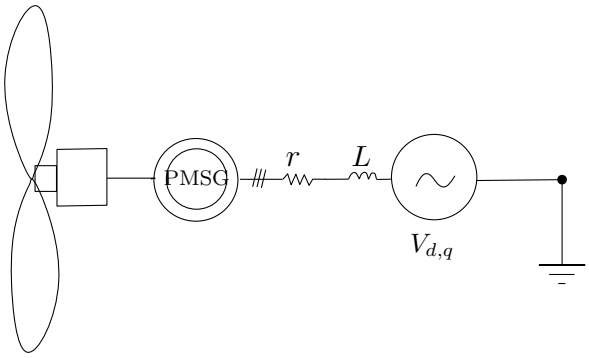

Figure 2.1: System under study in specialization project

The system that was investigated in the project is shown in Figure 2.1. The equations describing the system are:

$$\dot{\Psi}_d = L\dot{i}_d = -ri_d + Li_q\frac{P}{2}\omega_m - v_d \tag{2.1}$$

$$\dot{\Psi}_q = L\dot{i}_q = -ri_q - Li_d\frac{P}{2}\omega_m + \phi\frac{P}{2}\omega_m - v_q \tag{2.2}$$

$$\dot{\rho} = J\dot{\omega}_m = T_m - \frac{3}{2}\frac{P}{2}\phi i_q + d(\omega_{ref} - \omega_m) \tag{2.3}$$

where, Ψ_d and Ψ_q are the flux linkage, L is the inductances in the stator windings, P is the number of magnetic poles in the machine, i_d and i_q are the currents in the direct- and quadrature axis, respectively. ω_m is the angular velocity of the rotor, ω_{ref} is the reference angular speed of the rotor, ρ is the the angular momentum, ϕ is the magnetic flux from the permanent magnets and T_m is the mechanical torque.

Equation 2.3 is modified by a factor $\frac{2}{3}$ to make the system skew symmetric.

$$\dot{\rho}^* = J^*\dot{\omega}_m = T_m^* - \frac{P}{2}\phi i_q + d^*(\omega_{ref} - \omega_m) \tag{2.4}$$

The derivation of the system equations are shown in Appendix B. The system above admits the port-Hamiltonian representation:

$$\underbrace{\begin{bmatrix}\dot{\Psi}_d\\ \dot{\Psi}_q\\ \dot{\rho}^*\end{bmatrix}}_{\dot{x}} = \left(\underbrace{\frac{p}{2}\Phi\begin{bmatrix}0&0&0\\0&0&1\\0&-1&0\end{bmatrix}}_{J_0} + \underbrace{\frac{p}{2}L\begin{bmatrix}0&\omega_m&0\\-\omega_m&0&0\\0&0&0\end{bmatrix}}_{J(\omega)} - \underbrace{\begin{bmatrix}r&0&0\\0&r&0\\0&0&d^*\end{bmatrix}}_{R}\right)\underbrace{\begin{bmatrix}i_d\\ i_q\\ \omega_m\end{bmatrix}}_{\nabla\mathcal{H}(x)} + \underbrace{\begin{bmatrix}-1&0\\0&-1\\0&0\end{bmatrix}}_{G}\underbrace{\begin{bmatrix}v_d\\ v_q\end{bmatrix}}_{u} + \underbrace{\begin{bmatrix}0\\0\\T_m^* + d^*\omega_{ref}\end{bmatrix}}_{E} \tag{2.5}$$

which can be written in compact form as:

$$\dot{x} = \Big(\mathcal{J}_0 + \mathcal{J}(\omega_m) - \mathcal{R}\Big)\nabla\mathcal{H}(x) + Gu + E \tag{2.6}$$

An incremental model is needed as the system needs to have an equilibrium point different from the origin.[1] It was shown in the associated specialization project that for the LCF

$$\mathcal{V}(\widetilde{x}) = \mathcal{H}(\widetilde{x}) = \frac{1}{2}\widetilde{x}^\top Q\widetilde{x} \tag{2.7}$$

[1] This is since the equilibrium point in the origin is equivalent to the wind energy conversion system being shut off.

all four conditions for a Lyapunov function are satisfied, which implies that the system is asymptotically stable for large disturbances if the following criterion is satisfied:

$$d^* - \frac{(\bar{i}_q \frac{p}{2} L)^2}{4(r+\gamma)} \geq 0 \tag{2.8}$$

with d^* the damping coefficient representing the effect of the damper windings in the PMSG; γ a tunable control parameter constant [31], proportional to the gain in the PI current controllers. Criterion 2.8 states that the damping in the system must be larger then a certain value, $\frac{(\bar{i}_q \frac{p}{2} L)^2}{4(r+\gamma)}$, for the system to be guaranteed to be stable. By tuning the current controllers and increasing the gain, the term $\frac{(\bar{i}_q \frac{p}{2} L)^2}{4(r+\gamma)}$ can be reduced. The result is that the current controllers can reduce the required damping in the PMSG, and that linear PI current controllers that are widely used in industry today can be used to stabilize the nonlinear system.

The model that is shown above was later expanded to include the nonlinear relation between the mechanical torque T_m and the angular velocity

$$T_m(\omega_m) = \frac{1}{2}\rho A v^3 C_p \frac{1}{\omega_m}, \tag{2.9}$$

where ρ is the air density, A is the area swept by the turbine blades with length r_b, v is the wind speed and C_p is the wind power coefficient which is defined as $C_p = C_1(C_2\eta - C_5)e^{-C_6\eta}$. $\eta = \frac{1}{\lambda} - 0.035$ where λ is the tip speed ratio $\lambda = \frac{r_b\omega_m}{v}$ [15].

C_1	0.5
C_2	116
C_5	5
C_6	21

Table 2.1: Constants for the Wind power coefficient C_p

Inserting the expression for the wind power coefficient into 2.9 gives:

$$T_m(\omega_m) = \frac{1}{2}\rho A V^3 \frac{1}{\omega_m} C_1 \Big(C_2 (\frac{v}{r_b \omega_m} - 0.035) - C_5 \Big) e^{-C_6 (\frac{v}{r_b \omega_m} - 0.035)} \tag{2.10}$$

From the above equation, it is clear that mechanical torque has a nonlinear relation to the angular velocity and therefore motivates to investigate how this non-linearity is affecting the system's stability. The system model is thereby modified to:

$$\underbrace{\begin{bmatrix} \dot{\Psi}_d \\ \dot{\Psi}_q \\ \dot{\rho} \end{bmatrix}}_{\dot{x}} = \left(\underbrace{\frac{p}{2}\Phi \begin{bmatrix} 0 & 0 & 0 \\ 0 & 0 & 1 \\ 0 & -1 & 0 \end{bmatrix}}_{J_0} + \underbrace{\frac{p}{2} L \begin{bmatrix} 0 & \omega_m & 0 \\ -\omega_m & 0 & 0 \\ 0 & 0 & 0 \end{bmatrix}}_{J(\omega_m)} - \underbrace{\begin{bmatrix} r & 0 & 0 \\ 0 & r & 0 \\ 0 & 0 & d - \frac{T_m(\omega_m)}{\omega_m} \end{bmatrix}}_{R(\omega_m)} \right) \underbrace{\begin{bmatrix} i_d \\ i_q \\ \omega_m \end{bmatrix}}_{\nabla \mathcal{H}(x)} + \underbrace{\begin{bmatrix} -1 & 0 \\ 0 & -1 \\ 0 & 0 \end{bmatrix}}_{G} \underbrace{\begin{bmatrix} v_d \\ v_q \end{bmatrix}}_{u} + \underbrace{\begin{bmatrix} 0 \\ 0 \\ d\omega_{ref} \end{bmatrix}}_{E} \tag{2.11}$$

The LCF is chosen as before, $\mathcal{V}(\widetilde{x}) = \frac{1}{2}\widetilde{x}^\top Q \widetilde{x}$. By applying the methodology from [31], a stability criterion is derived.

$$\underbrace{d^*}_{\text{1.term}} - \underbrace{\frac{\partial T_m(\omega_m)}{\partial \omega_m}}_{\text{2.term}} - \underbrace{\frac{(\bar{i}_q \frac{p}{2} L)^2}{4(r+\gamma)}}_{\text{3.term}} \geq 0 \tag{2.12}$$

Comparing the new criterion for the system that includes the nonlinear dynamics introduced by the wind, with 2.8 which is the criterion for the system when the mechanical torque is a constant, it

is apparent that a new term has been introduced. The partial derivative of the mechanical torque with respect to angular velocity is given as:

$$\begin{aligned}\frac{\partial T_m(\omega_m)}{\partial \omega_m} &= \frac{1}{2}\rho A V^3 \frac{1}{\omega_m^2} C_1 \left(C_2(\tfrac{v}{r_b\omega_m} - 0.035) - C_5\right) e^{-C_6(\frac{v}{r_b\omega_m} - 0.035)} \\ &- \frac{1}{2}\rho A V^4 \frac{1}{r_b\omega_m^3} C_1 C_2 e^{-C_6(\frac{v}{r_b\omega_m} - 0.035)} \\ &+ \frac{1}{2}\rho A V^4 \frac{1}{r_b\omega_m^3} C_1 \left(C_2(\tfrac{v}{r_b\omega_m} - 0.035) - C_5\right) e^{-C_6(\frac{v}{r_b\omega_m} - 0.035)}\end{aligned} \tag{2.13}$$

It is not trivial to see whether the criterion 2.12 is satisfied or not due to the complexity of 2.13. To investigate stability, the criterion is plotted as a function of angular velocity for a given operating point. To clarify, this means that the other variables of the system, such as currents and mechanical torque, are assumed to be constant. For a wind speed of 15 m/s, the criterion is plotted in Figure 2.2, as a function of the angular velocity.

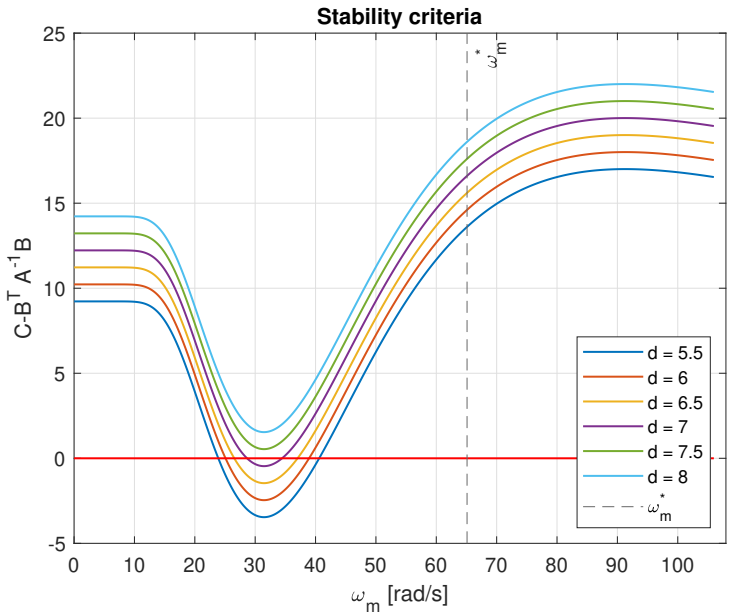

Figure 2.2: Plot of the stability criterion for different values of damping, $V = 15[m/s]$

In Figure 2.2, one can see the criterion for different damping coefficient values. The optimal operating point ω_m^* is drawn in with a dotted line. At the optimal operating point, the criterion is easily satisfied, however, during acceleration or deceleration of the wind turbine, a specific value of damping is required for the criterion to be satisfied. For the chosen scenario shown in Figure 2.2, a minimum damping $d = 7.25$ is required for the criterion to be satisfied for all values for the angular velocity.

The project also discussed how the required damping to guarantee stability varied with different parameters. An observation was that the damping required increased when the wind speed increased. The damping should therefore be designed for a worst-case scenario. The effect of tuning the current controllers is limited to only affecting the third term in criterion 2.12. It can be observed that the second term dominates the criterion, and tuning the controllers only has a limited effect, as can be seen in Figure 2.3.

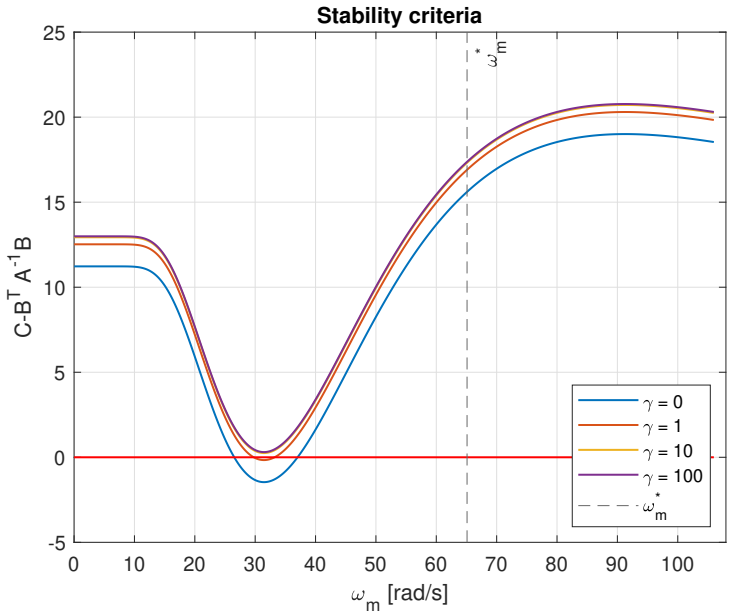

Figure 2.3: Plot of the stability criterion for different different values of γ

Therefore it can be concluded that when the non-linearities of the mechanical torque are included, tuning of the current controllers is not sufficient to guarantee stability. It is also necessary to design the machine with damping that satisfies $d^* \geq \frac{\partial T_m}{\partial \omega_m}$ for the system to be globally asymptotically stable, assuming that the current controllers are tuned such that the third term of 2.12 can be neglected.

End note

The specialization project was limited to developing a *stability certificate* for WECS only consisting of a PMSG connected to a constant voltage source. For the stability certificate to be of practical use, the WECS model must be expanded to contain the non-linear dynamics of the power converters. This is the starting point of this thesis.

Chapter 3

Deriving the *Stability Certificates*

The change from centralized to distributed generation demands a new strategy for interconnecting renewables to the power grid. Developing a stability certificate to guarantee large signal stability is therefore essential in today's world. The certificate designed in the specialization project excludes the nonlinear relationship of the power converters. As a consequence, the real-life applications of the certificate are less functional. Our contribution to the highly needed change in the power grid is, therefore, to create an innovative stability certificate including the nonlinear dynamics of the converters in combination with the mechanical and electrical relationship of a permanent magnet synchronous generator.

3.1 Single Converter + PMSG Model

The first step to studying the stability of the full back-to-back converter connected PMSG wind energy conversion system, is to expand the system analyzed in the specialization project and summarized in chapter 2 by including one of the two 2L-VSCs. Consequently, the second converter and the grid connection are modeled as a current source on the DC side of the converter. The system is shown in Figure 3.1.

3.1.1 Model Description

Our starting point will be the equations describing the electrical and mechanical aspects of the system derived in the specialization project. A detailed derivation of the equations can be found in Appendix B.

$$L\dot{i}_d = -ri_d + Li_q\frac{P}{2}\omega_m - v_d \tag{3.1}$$

$$L\dot{i}_q = -ri_q - Li_d\frac{P}{2}\omega_m + \phi\frac{P}{2}\omega_m - v_q \tag{3.2}$$

$$J\dot{\omega}_m = T_m - T_e = T_m - \frac{3}{2}\frac{P}{2}\phi i_q + d(\omega_{ref} - \omega_m) \tag{3.3}$$

The equations describe a WECS consisting of a wind turbine and a PMSG. The system investigated in the specialization project (Figure 2.1) will be expanded by first including a 2L-VSC acting as a rectifier.

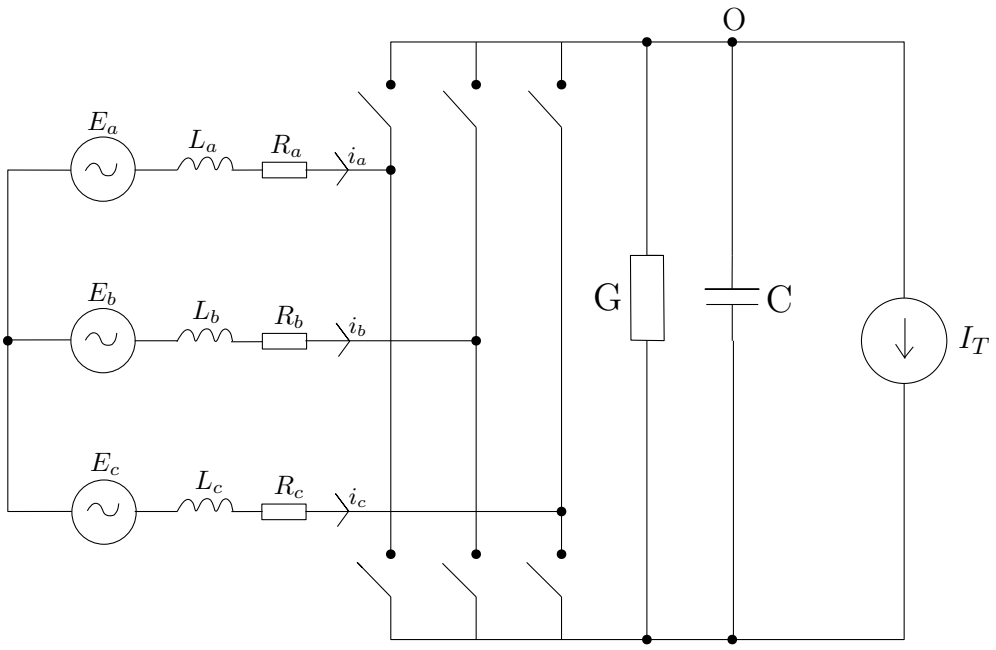

Figure 3.1: Wind energy conversion system with one 2L-VSC acting as a rectifier

A fourth equation describing the 2L-VSC is needed to complete the system. Kirchhoff's current law in node O above the capacitor (Figure 3.1) yields

$$\dot{q_c} = C\dot{V_c} = I_T - u_1 i_d - u_2 i_q - GV_c \tag{3.4}$$

where q_c is the charge in the capacitor. C is the capacitance, G is the conductance, V_c is the voltage across the converter, I_T is a constant current source representing the external grid, and u_1 and u_2 can be interpret as the duty cycles for the d and q-axis in the 2L-VSC, respectively. The last term, GV_c, represents the losses in the converter. Both switching losses and losses due to the components not being ideal. The new overall system will therefore take the form:

$$L\dot{i}_d = -ri_d + Li_q\frac{P}{2}\omega_m - u_1 V_c \tag{3.5}$$

$$L\dot{i}_q = -ri_q - Li_d\frac{P}{2}\omega_m + \phi\frac{P}{2}\omega_m - u_2 V_c \tag{3.6}$$

$$J\dot{\omega}_m = T_m - T_e = T_m - \frac{3}{2}\frac{P}{2}\phi i_q + d(\omega_{ref} - \omega_m) \tag{3.7}$$

$$C\dot{V}_c = u_1 i_d + u_2 i_q - GV_c - I_T \tag{3.8}$$

In the new set of equations

$$u_1 V_c = v_d \tag{3.9}$$

$$u_2 V_c = v_q \tag{3.10}$$

since the voltages in the d and q axis are now dependent on the dc voltage of the converter, as opposed to the specialization project where they were linear values. The third system equation, 3.7, is modified to ensure skew-symmetry. The modification consists of multiplying the equation with a factor $\frac{2}{3}$, due to the factor $\frac{3}{2}$ in the term $\frac{3}{2}\frac{P}{2}\phi i_q$. The factor $\frac{3}{2}$ is due to an amplitude invariant park transform being used in the derivation of the system model. The third equation then becomes:

$$J^*\dot{\omega}_m = T_m^* - \frac{P}{2}\phi i_q + d^*(\omega_{ref} - \omega_m)$$

where $J^* = \frac{2}{3}J$, $T_m^* = \frac{2}{3}T_m$ and $d^* = \frac{2}{3}d$. To simplify notation, from this point J, T_m and d are used instead of J^*, T_m^* and d^*.

To assess the system's stability, it is beneficial to write the system on a port-Hamiltonian form. Port-based modeling provides a unified framework for subsystems existing in different physical domains. For instance, electrical, thermal and mechanical [19].

A system on pH form has the general expression

$$\dot{x} = \big(\mathcal{J}(x) - \mathcal{R}(x)\big)\nabla\mathcal{H}(x) + G(x)u + E \tag{3.11}$$

where $x \in \mathbb{R}^n$ is a collection of the state variables, $\mathcal{J} \in \mathbb{R}^{n\times n}$ is the skew-symmetric interconnection matrix. Furthermore, $\mathcal{R} \in \mathbb{R}^{n\times n}$ is the symmetric and positive semidefinite dissipation matrix, $u \in \mathbb{R}^m$ is the control input vector and $G \in \mathbb{R}^{n\times m}$ is the control input matrix, $E \in \mathbb{R}^n$ is the disturbance matrix, and $\mathcal{H} \in \mathbb{R}$ is the Hamiltonian function describing the energy storage of the system.

The system, described in 3.5, 3.6, 3.7 and 3.8, written on a pH form then becomes:

$$\underbrace{\begin{bmatrix}\dot{\psi}_d\\ \dot{\psi}_q\\ \dot{\rho}\\ \dot{q}_c\end{bmatrix}}_{\dot{x}} = \left(\underbrace{\begin{bmatrix}0 & L\omega_m\frac{p}{2} & 0 & -u_1\\ -L\omega_m\frac{p}{2} & 0 & \frac{p}{2}\phi & -u_2\\ 0 & -\frac{p}{2}\phi & 0 & 0\\ u_1 & u_2 & 0 & 0\end{bmatrix}}_{J} - \underbrace{\begin{bmatrix}r & 0 & 0 & 0\\ 0 & r & 0 & 0\\ 0 & 0 & d & 0\\ 0 & 0 & 0 & G\end{bmatrix}}_{R}\right)\underbrace{\begin{bmatrix}i_d\\ i_q\\ \omega_m\\ V_c\end{bmatrix}}_{\nabla\mathcal{H}(x)} + \underbrace{\begin{bmatrix}0\\ 0\\ T_m + d\omega_{ref}\\ -I_T\end{bmatrix}}_{E} \tag{3.12}$$

The energy storage function $\mathcal{H}(x)$ will be on the form

$$\begin{aligned}\mathcal{H}(x) &= \frac{1}{2}x^\top Qx\\ &= \frac{1}{2}\begin{bmatrix}\psi_d & \psi_q & \rho & q_c\end{bmatrix}\begin{bmatrix}\frac{1}{L} & 0 & 0 & 0\\ 0 & \frac{1}{L} & 0 & 0\\ 0 & 0 & \frac{1}{J} & 0\\ 0 & 0 & 0 & \frac{1}{C}\end{bmatrix}\begin{bmatrix}\psi_d\\ \psi_q\\ \rho\\ q_c\end{bmatrix}\\ &= \frac{1}{2}(\frac{1}{L}\psi_d^2 + \frac{1}{L}\psi_q^2 + \frac{1}{J}\rho^2 + \frac{1}{C}q_c^2)\end{aligned} \tag{3.13}$$

The gradient of the Hamiltonian $\nabla\mathcal{H}(x)$ is thus:

$$\begin{aligned}\nabla\mathcal{H}(x) &= \begin{bmatrix}\frac{\partial}{\partial\psi_d}\\ \frac{\partial}{\partial\psi_q}\\ \frac{\partial}{\partial\rho}\\ \frac{\partial}{\partial q_c}\end{bmatrix}\frac{1}{2}(\frac{1}{L}\psi_d^2 + \frac{1}{L}\psi_q^2 + \frac{1}{J}\rho^2 + \frac{1}{C}q_c^2)\\ &= \begin{bmatrix}\frac{1}{L}\psi_d & 0 & 0 & 0\\ 0 & \frac{1}{L}\psi_q & 0 & 0\\ 0 & 0 & \frac{1}{J}q_c & 0\\ 0 & 0 & 0 & \frac{1}{C}\rho\end{bmatrix}\\ &= \underbrace{\begin{bmatrix}\frac{1}{L} & 0 & 0 & 0\\ 0 & \frac{1}{L} & 0 & 0\\ 0 & 0 & \frac{1}{J} & 0\\ 0 & 0 & 0 & \frac{1}{C}\end{bmatrix}}_{Q}\underbrace{\begin{bmatrix}\psi_d\\ \psi_q\\ \rho\\ q_c\end{bmatrix}}_{x}\\ &= Qx\end{aligned} \tag{3.14}$$

From Equation 3.12 one is able to write the system on the following form

$$\dot{x} = \big(\mathcal{J}(\omega_m) + \mathcal{J}_0 + u_1\mathcal{J}_1 + u_2\mathcal{J}_2 - \mathcal{R}\big)\nabla\mathcal{H}(x) + E \tag{3.15}$$

and written out this becomes:

$$\underbrace{\begin{bmatrix}\dot{\psi}_d\\ \dot{\psi}_q\\ \dot{\rho}\\ \dot{q}_c\end{bmatrix}}_{\dot{x}} = \left(\underbrace{\frac{P}{2}L\begin{bmatrix}0 & \omega_m & 0 & 0\\ -\omega_m & 0 & 0 & 0\\ 0 & 0 & 0 & 0\\ 0 & 0 & 0 & 0\end{bmatrix}}_{J(\omega)} + \underbrace{\frac{P}{2}\phi\begin{bmatrix}0 & 0 & 0 & 0\\ 0 & 0 & 1 & 0\\ 0 & -1 & 0 & 0\\ 0 & 0 & 0 & 0\end{bmatrix}}_{J_0} + u_1\underbrace{\begin{bmatrix}0 & 0 & 0 & -1\\ 0 & 0 & 0 & 0\\ 0 & 0 & 0 & 0\\ 1 & 0 & 0 & 0\end{bmatrix}}_{J_1} + u_2\underbrace{\begin{bmatrix}0 & 0 & 0 & 0\\ 0 & 0 & 0 & -1\\ 0 & 0 & 0 & 0\\ 0 & 1 & 0 & 0\end{bmatrix}}_{J_2} - \underbrace{\begin{bmatrix}r & 0 & 0 & 0\\ 0 & r & 0 & 0\\ 0 & 0 & d & 0\\ 0 & 0 & 0 & G\end{bmatrix}}_{R} \right) \underbrace{\begin{bmatrix}i_d\\ i_q\\ \omega_m\\ V_c\end{bmatrix}}_{\nabla\mathcal{H}(x)} + \underbrace{\begin{bmatrix}0\\ 0\\ T_m + d\omega_{ref}\\ -I_T\end{bmatrix}}_{E} \tag{3.16}$$

A set of dynamic equations describing a nonlinear systems can be written in several ways. A common form is

$$\dot{x} = f(x) + g(x)u \tag{3.17}$$
$$y = h(x) + j(x)u \tag{3.18}$$

Comparing Equation 3.17 and Equation 3.15, one is able to see that 3.15 can be split in the following way:

$$f(x) = \big(\mathcal{J}_0 + \mathcal{J}(\omega_m) - \mathcal{R}\big)\nabla\mathcal{H}(x) + E \tag{3.19}$$
$$g(x) = \begin{bmatrix}\mathcal{J}_1\nabla\mathcal{H}(x) & \mathcal{J}_2\nabla\mathcal{H}(x)\end{bmatrix} \tag{3.20}$$

where

$$u = \begin{bmatrix}u_1\\ u_2\end{bmatrix} \tag{3.21}$$

The stability of the system is investigated next, with the help of Lyapunov's direct method.

3.1.2 The Lyapunov Function

There are different ways to investigate the stability of a system. Some are concerned with linearization and ensuring the eigenvalues are located in the left half-plane. Since we are interested in large signal stability–and therefore avoiding any type of linearization–we use Lyapunov's direct method.
A Lyapunov function is defined as:

$\mathcal{V}$ is a lyapunov function for x = 0 if and only if:
$\mathcal{V}$ is continuously differentiable

(**I**) $\mathcal{V}(0) = 0$
(**II**) $\mathcal{V}(x) > 0 \; in \; D\backslash(0)$
(**III**) $\dot{\mathcal{V}}(0) = 0$
(**IV**) $\dot{\mathcal{V}}(x) \; < 0 \; in \; D\backslash(0)$

Condition (II) states that $\mathcal{V}$ is positive definite in D.
Condition (IV) states that $\dot{\mathcal{V}}$ is negative definite in D
If all of the conditions above are fulfilled, then $\mathcal{V}$ is a lyapunov function for x = 0.
In other words, a Lyapunov function has a single equilibrium point that is the minimum of the function. This is useful when analysing stability, since it can be shown that if a Lyapunov function for the system exists, then the system has a stable equilibrium point and is asymptotically stable.

The equilibrium point of interest is usually not at the origin, but with the help of a change of variables, one can shift any point of interest to the origin.

Consider the system

$$\dot{x} = f(x) \tag{3.22}$$

where $x \in \mathbb{R}^n$ are the state variables and $\dot{x} = \frac{dx}{dt}$
Say for instance $\bar{x} \neq 0$, then by introducing $y = x - \bar{x}$ and taking the derivative

$$\dot{y} = \dot{x} - \dot{\bar{x}} = \dot{x} = f(x) = f(y + \bar{x}) = g(y) \tag{3.23}$$

where $g(0) = 0$
The new variable y, now has an equilibrium at the origin. while $f(x)$ has an equilibrium at $\bar{x} \neq 0$

3.1.3 Analysis of the Incremental Model

Since the idea is to have an operating wind turbine, an equilibrium different from the origin is explored. Utilizing the trick described above, the incremental model of the pH system takes the form:

$$\begin{array}{rrr} & \dot{x} = & (\mathcal{J}_0 + \mathcal{J}(\omega_m) - \mathcal{R})Qx + g(x)u + E \\ - & 0 = & (\mathcal{J}_0 + \mathcal{J}(\bar{\omega}_m) - \mathcal{R})Q\bar{x} + g(\bar{x})\bar{u} + E \\ \hline & \dot{\widetilde{x}} = & \big(\mathcal{J}_0 - \mathcal{R}\big)Q\widetilde{x} + \mathcal{J}(\omega_m)Qx - \mathcal{J}(\bar{\omega}_m)Q\bar{x} + g(x)u - g(\bar{x})\bar{u} \end{array} \tag{3.24}$$

If one were to investigate the last two terms closer $g(x)u - g(\bar{x})\bar{u}$ one could see that they could be rewritten as

$$\begin{aligned} g(x)u - g(\bar{x})\bar{u} &= g(\widetilde{x} + \bar{x})(u) - g(\bar{x})\bar{u} \\ &= g(\widetilde{x})u + g(\bar{x})u - g(\bar{x})\bar{u} \\ &= g(\widetilde{x})u + g(\bar{x})\widetilde{u} \end{aligned} \tag{3.25}$$

And the incremental model of the pH system can be rewritten as:

$$\dot{\widetilde{x}} = \big(\mathcal{J}_0 - \mathcal{R}\big)Q\widetilde{x} + \mathcal{J}(\omega_m)Qx - \mathcal{J}(\bar{\omega}_m)Q\bar{x} + g(\widetilde{x})u + g(\bar{x})\widetilde{u} \tag{3.26}$$

and as

$$g(\widetilde{x}) = \begin{bmatrix} \mathcal{J}_1 Q\widetilde{x} & \mathcal{J}_2 Q\widetilde{x} \end{bmatrix}$$

the incremental model can be further rewritten as:

$$\dot{\widetilde{x}} = \left(\mathcal{J}_0 + \sum_{i=1}^{2} \mathcal{J}_i u_i - \mathcal{R}\right) Q\widetilde{x} + \mathcal{J}(\omega_m)Qx - \mathcal{J}(\bar{\omega}_m)Q\bar{x} + g(\bar{x})\widetilde{u} \tag{3.27}$$

Lyapunovs direct method and pH modeling formalism is tightly bound to the concept of passivity. Systems written on a pH form are by definition passive due to the underlying dirac structures of the Hamiltonian modeling [19]. Furthermore, passive systems cannot store more energy than what is being supplied to them. In other words, it cannot generate energy.

A dynamical system on state space form can be written as

$$\dot{x} = f(x, u) \tag{3.28}$$

$$y = h(x, u) \tag{3.29}$$

where f: $R^n \times R^p \to R^n$ is locally Lipschitz, h: $R^n \times R^p \to R^p$ is continuous and $f(0, 0) = h(0, 0) = 0$. The system represented by 3.28 and 3.29 is said to be passive if there exists a continuously differentiable positive semidefinite function $\mathcal{V}(x)$ such that

$$u^T y \geq \dot{\mathcal{V}} = \frac{\partial \mathcal{V}}{\partial t} f(x, u), \quad \forall (x, y) \ \epsilon \ R^n \times R^p \ \ [24] \tag{3.30}$$

The function $\mathcal{V}(x)$ is not necessarily straightforward to find. A good starting point however is the storage function or the Hamiltonian of the system $\mathcal{H}(x)$

As mentioned earlier, the equilibrium of interest is usually not at the origin. The starting point for the stability analysis and the Lyapunov function is therefore not the Hamiltonian of the system, but rather a function inspired by it, i.e., inspired by the energy of the system $\mathcal{H}(\widetilde{x}) = \mathcal{V}(x) = \frac{1}{2}\widetilde{x}^\top Q\widetilde{x}$

If the LCF satisfies all four conditions for Lyapunovs method, the system is globally asymptotically stable.

Condition I

$$\begin{aligned}\mathcal{V}(\bar{x}) &= \frac{1}{2}(\bar{x}-\bar{x})^\top Q(\bar{x}-\bar{x}) \\ &= 0\end{aligned}$$

is satisfied.

Condition II

$$\mathcal{V}(x) = \frac{1}{2}\widetilde{x}^\top Q\widetilde{x} > 0, \forall x \in D\backslash\{0\}$$

is satisfied as $\mathcal{V}$ is a quadratic function.

Condition III and IV concerns the derivative of the LCF, and the following procedure is inspired by the work done in [31]

$$\dot{\mathcal{V}}(x) = \frac{d\mathcal{H}(\widetilde{x})}{dt} = \nabla^\top \mathcal{H}(\widetilde{x})\frac{d\widetilde{x}}{dt} = \nabla^\top \mathcal{H}(\widetilde{x})\dot{\widetilde{x}} = \widetilde{x}^\top Q\dot{\widetilde{x}} \tag{3.31}$$

Notice that $\dot{\widetilde{x}} = \frac{d(x-\bar{x})}{dt} = \frac{dx}{dt} = \dot{x}$. Hence,

$$\dot{\mathcal{V}}(x) = \widetilde{x}^\top Q\dot{x} \tag{3.32}$$

By combining 3.27 and 3.32 derivative of the LCF becomes:

$$I: \quad \dot{\mathcal{V}} = \widetilde{x}^\top Q \left(\mathcal{J}_0 + \sum_{i=1}^{2} \mathcal{J}_i u_i - \mathcal{R} \right) Q\widetilde{x} + \widetilde{x}^\top Q\mathcal{J}(\omega_m)Qx - \widetilde{x}^\top Q\mathcal{J}(\bar{\omega}_m)Q\bar{x} + \widetilde{x}^\top Qg(\bar{x})\widetilde{u}$$

$$II: \quad \dot{\mathcal{V}} = \underbrace{\widetilde{x}^\top Q \left(\mathcal{J}_0 + \sum_{i=1}^{2} \mathcal{J}_i u_i \right) Q\widetilde{x}}_{0} - \widetilde{x}^\top Q\mathcal{R}Q\widetilde{x} + \widetilde{x}^\top Q\mathcal{J}(\omega_m)Qx - \widetilde{x}^\top Q\mathcal{J}(\bar{\omega}_m)Q\bar{x} + \widetilde{x}^\top Qg(\bar{x})\widetilde{u}$$

$$III: \quad \dot{\mathcal{V}} = -\widetilde{x}^\top Q\mathcal{R}Q\widetilde{x} + \widetilde{x}^\top Q\mathcal{J}(\omega_m)Qx - \widetilde{x}^\top Q\mathcal{J}(\bar{\omega}_m)Q\bar{x} + \underbrace{\widetilde{x}^\top Qg(\bar{x})}_{y^\top}\widetilde{u}$$

$$IV: \quad \dot{\mathcal{V}} = y^\top\widetilde{u} - \widetilde{x}^\top Q\mathcal{R}Q\widetilde{x} + \widetilde{x}^\top Q\mathcal{J}(\omega_m)Qx - \widetilde{x}^\top Q\mathcal{J}(\bar{\omega}_m)Q\bar{x}$$

$$V: \quad \dot{\mathcal{V}} = y^\top\widetilde{u} - \widetilde{x}^\top Q\mathcal{R}Q\widetilde{x} + \widetilde{x}^\top Q\mathcal{J}(\omega_m)Qx - \widetilde{x}^\top Q\mathcal{J}(\bar{\omega}_m)Q\bar{x} + \underbrace{\widetilde{x}^\top Q\mathcal{J}(\omega_m)Q\bar{x} - \widetilde{x}^\top Q\mathcal{J}(\omega_m)Q\bar{x}}_{0}$$

$$VI: \quad \dot{\mathcal{V}} = y^\top\widetilde{u} - \widetilde{x}^\top Q\mathcal{R}Q\widetilde{x} + \underbrace{\widetilde{x}^\top Q\Big(\mathcal{J}(\omega_m)Qx - \mathcal{J}(\omega_m)Q\bar{x}\Big)}_{0} - \widetilde{x}^\top Q\mathcal{J}(\bar{\omega}_m)Q\bar{x} + \widetilde{x}^\top Q\mathcal{J}(\omega_m)Q\bar{x}$$

$$VII: \quad \dot{\mathcal{V}} = y^\top\widetilde{u} + \widetilde{x}^\top Q\Big[\big(\mathcal{J}(\omega_m) - \mathcal{J}(\bar{\omega}_m)\big)Q\bar{x} - \mathcal{R}Q\widetilde{x}\Big]$$

$$VIII: \quad \dot{\mathcal{V}} = y^\top\widetilde{u} + \widetilde{x}^\top Q\Big[\big(\mathcal{J}(\omega_m) - \mathcal{J}(\bar{\omega}_m)\big)Q\bar{x} - \mathcal{R}Q\widetilde{x}\Big] + \underbrace{\widetilde{x}^\top Q\Big[\gamma g(\bar{x})g(\bar{x})^\top - \gamma g(\bar{x})g(\bar{x})^\top\Big]Q\widetilde{x}}_{0}$$

$$IX: \quad \dot{\mathcal{V}} = y^\top\widetilde{u} + \widetilde{x}^\top Q\Big[\big(\mathcal{J}(\omega_m) - \mathcal{J}(\bar{\omega}_m)\big)Q\bar{x} - \mathcal{R}Q\widetilde{x} - \gamma g(\bar{x})g(\bar{x})^\top Q\widetilde{x}\Big] + \gamma y^\top y$$

$$X: \quad \dot{\mathcal{V}} = y^\top\widetilde{u} + (z-\bar{z})^\top\Big[M(z) - M(\bar{z}) - \gamma g(\bar{x})g(\bar{x})^\top(z-\bar{z})\Big] + \gamma y^\top y$$

Step explanation

- I: By combining 3.27 and 3.32 the derivative of the LCF can be expressed as shown in I.
- II: Due to skew-symmetry of $\mathcal{J}_0 + \sum_{i=1}^{2} \mathcal{J}_i u_i$, the first term becomes zero.
- III: $y^\top$, the passive output of the system is defined as $\widetilde{x}^\top Qg(\bar{x})$.
- IV: Rearranging of the expression.
- V: Zero is added to the equation by adding and subtracting the term, $\widetilde{x}^\top Q\mathcal{J}(\omega_m)Q\bar{x}$. This way of proceeding is gotten from [31].
- VI: By rearranging the expression the term $\widetilde{x}^\top Q\Big(\mathcal{J}(\omega_m)Qx - \mathcal{J}(\omega_m)Q\bar{x}\Big)$ becomes zero due to skew-symmetry, since $Qx - Q\bar{x} = Q\widetilde{x}$.
- VII: The simplified expression is shown in VIII.
- VIII: Output feedback is added to enforce passivity in the system [31].
- X The expression is simplified and definition of the passive output is used, $\widetilde{x}^\top Qg(\bar{x})$.
- IX: A new variable z is introduced to simplify the notation, $z \triangleq \nabla\mathcal{V}(x) = x^\top Q$. A function $M(z)$ is defined as $M(z) \triangleq \mathcal{J}(z)\bar{z} - \mathcal{R}z$.

Condition IV

The expression for the time derivative of the Lyapunov function is:

$$\dot{\mathcal{V}} = \underbrace{y^\top\widetilde{u}}_{1.term} + \underbrace{(z-\bar{z})^\top\Big[M(z) - M(\bar{z}) - \gamma g(\bar{x})g(\bar{x})^\top(z-\bar{z})\Big]}_{2.term} + \underbrace{\gamma y^\top y}_{3.term} \tag{3.33}$$

The second term of Equation 3.33 needs to be negative semi-definite which is the case if $M(z) - M(\bar{z}) - \gamma g(\bar{x})g(\bar{x})^\top \tilde{z}$ is monotonically decreasing . It can be shown that this is the case if and only if

$$\nabla^\top M(z) + \nabla M(z) - 2\gamma g(\bar{x})g(\bar{x})^\top \leq 0 \tag{3.34}$$

This step might seem a bit overwhelming and not trivial. It is a step that is performed in [31] with a background in mathematical concepts from [32]. The reason for doing this is to investigate monotonicity by checking the definiteness of the gradient matrix. This is analogous to calculating the derivative of a scalar function to investigate the monotonicity of that function. As it is easier to understand the scalar case, it is included below to make the transition from investigating $(z - \bar{z})^\top [M(z) - M(\bar{z}) - \gamma g(\bar{x})g(\bar{x})^\top (z - \bar{z})]$ to investigating $\nabla^\top M(z) + \nabla M(z) - 2\gamma g(\bar{x})g(\bar{x})^\top$, smoother for the reader.

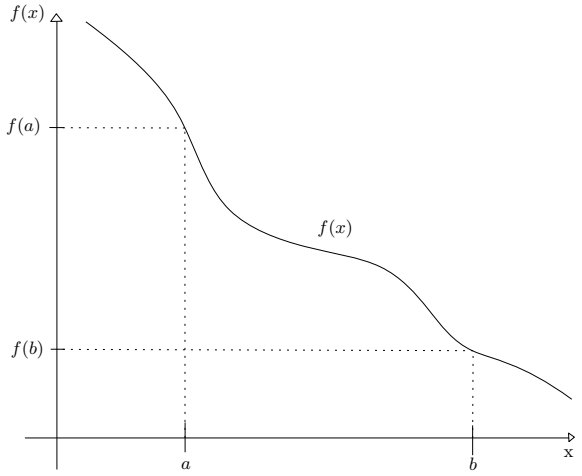

Figure 3.2: A monontonically decreasing function f

Given a function $f(x)$ that is continuous on an interval I. $f(x)$ is said to be monotonically decreasing if for any two points a and b on the interval I where $b > a$, $f(a) > f(b)$. This is equivalent to the derivative being negative $\frac{df(x)}{dx} < 0$.

proof:

$$\frac{df(x)}{dx} = \frac{f(b) - f(a)}{b - a} < 0 \tag{3.35}$$

as $f(b) - f(a) < 0$ and $b - a > 0$. QED

The expression $(b - a)\,[f(b) - f(a)] < 0$ when $\frac{df(x)}{dx} < 0$. The derivative can therefore be used to determine the monotonicity of $f(x)$ on the interval I. Likewise, to determine the monotonicity of $M(z) - M(\bar{z}) - \gamma g(\bar{x})g(\bar{x})^\top (z - \bar{z})$ the gradient $\nabla M(z)$ is investigated. Thereby, to check if $(z - \bar{z})[M(z) - M(\bar{z}) - \gamma g(\bar{x})g(\bar{x})^\top (z - \bar{z})]$ is negative definite, we instead investigate if

$$\nabla^\top M(z) + \nabla M(z) - 2\gamma g(\bar{x})g(\bar{x})^\top \leq 0 \tag{3.36}$$

where,

$$M(z) = \mathcal{J}(z)\bar{z} - \mathcal{R}z = \begin{bmatrix} 0 & L\omega_m \frac{P}{2} & 0 & 0 \\ -L\omega_m \frac{P}{2} & 0 & 0 & 0 \\ 0 & 0 & 0 & 0 \\ 0 & 0 & 0 & 0 \end{bmatrix} \begin{bmatrix} \bar{i}_d \\ \bar{i}_q \\ \bar{\omega}_m \\ \bar{V}_c \end{bmatrix} - \begin{bmatrix} r & 0 & 0 & 0 \\ 0 & r & 0 & 0 \\ 0 & 0 & d & 0 \\ 0 & 0 & 0 & G \end{bmatrix} \tag{3.37}$$

$$\nabla M(z) = \begin{bmatrix} -r & 0 & \bar{i}_q \frac{P}{2} L & 0 \\ 0 & -r & -\bar{i}_d \frac{P}{2} L & 0 \\ 0 & 0 & -d & 0 \\ 0 & 0 & 0 & -G \end{bmatrix} \tag{3.38}$$

From Equation 3.20 one is able to find the expression for $g(\bar{x})g(\bar{x})^\top$

$$g(\bar{x}) = \begin{bmatrix}\begin{bmatrix}0&0&0&-1\\0&0&0&0\\0&0&0&0\\1&0&0&0\end{bmatrix}\begin{bmatrix}\frac{\bar{\psi}_d}{L}\\\frac{\bar{\psi}_q}{L}\\\frac{\bar{p}}{J}\\\frac{\bar{q}_c}{c}\end{bmatrix} & \begin{bmatrix}0&0&0&0\\0&0&0&-1\\0&0&0&0\\0&1&0&0\end{bmatrix}\begin{bmatrix}\frac{\bar{\psi}_d}{L}\\\frac{\bar{\psi}_q}{L}\\\frac{\bar{p}}{J}\\\frac{\bar{q}_c}{c}\end{bmatrix}\end{bmatrix} = \begin{bmatrix}\frac{\bar{q}_c}{c} & 0\\0 & -\frac{\bar{q}_c}{c}\\0&0\\\frac{\bar{\psi}_d}{L} & \frac{\bar{\psi}_q}{L}\end{bmatrix} = \begin{bmatrix}-\bar{V}_c & 0\\0 & -\bar{V}_c\\0&0\\\bar{i}_d & \bar{i}_q\end{bmatrix} \tag{3.39}$$

$$g(\bar{x})g^\top(\bar{x}) = \begin{bmatrix}-\bar{V}_c & 0\\0 & -\bar{V}_c\\0&0\\\bar{i}_d & \bar{i}_q\end{bmatrix}\begin{bmatrix}-\bar{V}_c & 0 & 0 & \bar{i}_d\\0 & -\bar{V}_c & 0\bar{i}_q & \end{bmatrix} = \begin{bmatrix}\bar{V}_c^2 & 0 & 0 & -\bar{i}_d\bar{V}_c\\0 & \bar{V}_c^2 & 0 & \bar{i}_q\bar{V}_c\\0&0&0&0\\-\bar{V}_c\bar{i}_d & -\bar{V}_c\bar{i}_q & 0 & \bar{i}_d^2+\bar{i}_q^2\end{bmatrix} \tag{3.40}$$

Equation 3.36 can then be expressed:

$$\begin{bmatrix}-r&0&\bar{i}_q\frac{p}{2}L&0\\0&-r&-\bar{i}_d\frac{p}{2}L&0\\0&0&-d&0\\0&0&0&-G\end{bmatrix} + \begin{bmatrix}-r&0&0&0\\0&-r&0&0\\\bar{i}_q\frac{p}{2}L&-\bar{i}_d\frac{p}{2}L&-d&0\\0&0&0&-G\end{bmatrix} - 2\gamma\begin{bmatrix}\bar{V}_c^2&0&0&-\bar{i}_d\bar{V}_c\\0&\bar{V}_c^2&0&\bar{i}_q\bar{V}_c\\0&0&0&0\\-\bar{V}_c\bar{i}_d&-\bar{V}_c\bar{i}_q&0&\bar{i}_d^2+\bar{i}_q^2\end{bmatrix} \leq 0$$

$$= \begin{bmatrix}-2(r+\gamma\bar{V}_c^2)&0&\bar{i}_q\frac{P}{2}L&2\gamma\bar{i}_d\bar{V}_c\\0&-2(r+\gamma\bar{V}_c^2)&\bar{i}_d\frac{P}{2}L&2\gamma\bar{i}_q\bar{V}_c\\\bar{i}_q\frac{P}{2}L&\bar{i}_d\frac{P}{2}L&-2d&0\\2\gamma\bar{i}_d\bar{V}_c&2\gamma\bar{i}_q\bar{V}_c&0&-2(G+\gamma(\bar{i}_d^2+\bar{i}_q^2))\end{bmatrix} \leq 0$$

In the equilibrium point, it is desirable that $\bar{i}_d = 0$, to allow for maximum torque per ampere[1]. Inserting $\bar{i}_d = 0$ yields:

$$\begin{bmatrix}-2(r+\gamma\bar{V}_c^2)&0&\bar{i}_q\frac{P}{2}L&0\\0&-2(r+\gamma\bar{V}_c^2)&0&2\gamma\bar{i}_q\bar{V}_c\\\bar{i}_q\frac{P}{2}L&0&-2d&0\\0&2\gamma\bar{i}_q\bar{V}_c&0&-2(G+\gamma\bar{i}_q^2)\end{bmatrix} \tag{3.41}$$

To satisfy condition IV, expression 3.36 and thereby 3.41 needs to be negative semi-definite. To check for this, we partition the matrix as follows before computing the Schur complement [33].

$$-X = \begin{bmatrix}A & B\\B^\top & C\end{bmatrix} \tag{3.42}$$

To say that X is negative semi-definite, is the same as -X is positive semi-definite. Computing the Schur complement gives

$$\begin{aligned}C - B^\top A^{-1}B &= \begin{bmatrix}2d&0\\0&2(G+\gamma\bar{i}_q^2)\end{bmatrix} - \begin{bmatrix}-\bar{i}_q\frac{P}{2}L&0\\0&-2\gamma\bar{i}_q\bar{V}_c\end{bmatrix}\begin{bmatrix}\frac{1}{2(r+\gamma\bar{V}_c^2)}&0\\0&\frac{1}{2(r+\gamma\bar{V}_c^2)}\end{bmatrix}\begin{bmatrix}-\bar{i}_q\frac{P}{2}L&0\\0&-2\gamma\bar{i}_q\bar{V}_c\end{bmatrix}\\ &= \begin{bmatrix}2d-\frac{(\bar{i}_q\frac{P}{2}L)^2}{2(r+\gamma\bar{V}_c^2)}&0\\0&2(G+\gamma\bar{i}_q^2)-\frac{(2\gamma\bar{i}_q\bar{V}_c)^2}{2(r+\gamma\bar{V}_c^2)})\end{bmatrix}\end{aligned} \tag{3.43}$$

Given that we obtained a diagonal matrix, we then require each of the elements to be positive. In addition, the A matrix itself needs to be positive semi-definite.

$$A = \begin{bmatrix}2(r+\gamma\bar{V}_c^2)&0\\0&2(r+\gamma\bar{V}_c^2)\end{bmatrix} \tag{3.44}$$

From the definition of the A matrix above, one can see that this is true as long as

$$\gamma \geq -\frac{r}{V_c^2} \tag{3.45}$$

[1]Maximum torque per ampere is further explained in section 4.1

The condition related to the first diagonal term of the Schur complement

$$2d - \frac{(\bar{i}_q \frac{P}{2} L)^2}{2(r + \gamma \bar{V}_c^2)} \geq 0 \tag{3.46}$$

is similar to the expression found earlier in the specialization project–despite that back then, we did not include any converters in the analysis–and can be made to fulfill the negative semi-definite criteria by choosing a suitable damping coefficient d. The only difference in this new condition is the appearance of the converter voltage at the equilibrium $\bar{V}_c$, which turns out to be helpful due to the smaller damping d required to make the system stable. 3.46 is solved for γ, to attain a condition for the tuning, which reads:

$$\gamma \geq \frac{1}{\bar{V}_c^2} \left(\frac{(\bar{i}_q \frac{P}{2} L)^2}{4d} - r \right) \tag{3.47}$$

However, the presence of the power converter introduces an additional condition that needs to be met to ensure stability. The new condition is related to the other diagonal term resulting from the Schur complement, which reads:

$$2(G + \gamma \bar{i}_q^2) - \frac{(2\gamma \bar{i}_q \bar{V}_c)^2}{2(r + \gamma \bar{V}_c^2)} \geq 0, \tag{3.48}$$

which can be expanded to find a tuning criteria

$$\begin{aligned} 2G(2(r + \gamma \bar{V}_c^2)) + 2\gamma \bar{i}_q 2(r + \gamma \bar{V}_c^2) - (2\bar{V}_c \bar{i}_q \gamma)^2 &\geq 0 \\ 4Gr + 4G\gamma \bar{V}_c^2 + 4\gamma \bar{i}_q^2 r + 4\gamma^2 \bar{i}_q^2 \bar{V}_c^2 - 4\gamma^2 \bar{i}_q^2 \bar{V}_c^2 &\geq 0 \\ 4Gr + 4G\gamma \bar{V}_c^2 + 4\gamma \bar{i}_q^2 r &\geq 0 \end{aligned}$$

Solving for γ yields:

$$\gamma \geq \frac{-4Gr}{G\bar{V}_c^2 + \bar{i}_q^2 r} \tag{3.49}$$

This analysis resulted in three minimum conditions for γ. The three conditions are 3.45, 3.47 and 3.49. There can obviously be only one lower condition for γ. As 3.45 and 3.49 both have a negative lower limit for γ, 3.47 is the most strict condition for γ. And thus if 3.47 is satisfied, both 3.45 and 3.49 are both satisfied as well.
By choosing a suitable γ that satisfies 3.47, one is able to make the second term of Equation 3.33 negative semi-definite.

Hence, under the assumption that the above stability condition is being satisfied, Equation 3.33 can then be reformulated to

$$\dot{\mathcal{V}} \leq y^\top \widetilde{u} + \gamma y^\top y \tag{3.50}$$

Rearranging and assuming for simplicity the use of the proportional controller[2] Equation 3.50 becomes

$$\dot{\mathcal{V}} = -y^\top \left[K_P - \gamma I \right] y \leq 0, \text{ if } K_p > \gamma \tag{3.51}$$

Thereby, if the gain K_p is chosen larger than γ, the fourth lyapunov condition $\dot{\mathcal{V}}(x) \leq 0$ is satisfied.

To check if Condition III is satisfied, we first compute

$$\begin{aligned} y^\top(x) &= \widetilde{x}^\top Q g(\bar{x}) \\ &= \begin{bmatrix} i_d - \bar{i}_d & i_q - \bar{i}_q & \omega_m - \bar{\omega}_m & V_c - \bar{V}_c \end{bmatrix} \begin{bmatrix} -\bar{V}_c & 0 \\ 0 & -\bar{V}_c \\ 0 & 0 \\ \bar{i}_d & \bar{i}_q \end{bmatrix} \\ &= \begin{bmatrix} -\bar{V}_c(i_d - \bar{i}_d) + \bar{i}_d(V_c - \bar{V}_c) & -\bar{V}_c(i_q - \bar{i}_q) + \bar{i}_q(V_c - \bar{V}_c) \end{bmatrix} \end{aligned} \tag{3.52}$$

[2]This result can be easily extended for the case of a PI controller, by introducing some minor changes in the Lyapunov function in the lines of appendix C. $\tilde{u} = -K_P y$,

and notice that in the equilibrium point

$$\begin{aligned} y^\top(\bar{x}) &= \begin{bmatrix} -\bar{V}_c(\bar{i}_d - \bar{i}_d) + \bar{i}_d(\bar{V}_c - \bar{V}_c) & -\bar{V}_c(\bar{i}_q - \bar{i}_q) + \bar{i}_q(\bar{V}_c - \bar{V}_c) \end{bmatrix} \\ &= \begin{bmatrix} 0 & 0 \end{bmatrix} \end{aligned} \tag{3.53}$$

From this last expression one is able to show that condition III; i.e., $\dot{\mathcal{V}}(\bar{x}) = 0$ is satisfied

$$\begin{aligned} \dot{\mathcal{V}}(\bar{x}) &= y^\top(\bar{x})\widetilde{u} + \gamma y^\top(\bar{x}) y(\bar{x}) \\ &= 0 \end{aligned} \tag{3.54}$$

All four conditions for a Lyapunov function is satisfied. The LCF is therefore shown to be a Lyapunov function, when 3.46 is satisfied and $K_p > \gamma$.

3.1.4 Conclusion

This section has been concerned with finding a *stability certificate* for a WECS with only one 2L-VSC. From the mathematical derivation –Lyapunovs direct method– above, one can see how large signal stability can be guaranteed by choosing a suitable γ. The two criteria are summarized below.

$$\gamma \geq \frac{1}{\bar{V}_c^2}\left(\frac{(\bar{i}_q \frac{P}{2} L)^2}{4d} - r\right)$$
$$\gamma \geq \frac{-4Gr}{G\bar{V}_c^2 + \bar{i}_q^2 r}$$

The second criterion is fulfilled as long as γ is chosen to be positive. The stricter and thereby the determining stability criterion to be fulfilled is the first.

With the use of a proportional (integral) controller, one is able to render the system stable by making sure the proportional gain K_p is greater than γ, since

$$\dot{\mathcal{V}} = -y^\top \left[K_P - \gamma I\right] y \leq 0, \text{ if } K_p > \gamma$$

A *stability certificate* for a WECS with only one 2L-VSC, while the second 2L-VSC and the grid connection are modeled as a current source on the converter's DC side, can arguably be seen as an oversimplification when we are interested in real-world applications. For that reason, we expand the model by including the second 2L-VSC in the next section.

3.2 Two Converters in back-to-back + PMSG

As the system successfully has been expanded from the PMSG case investigated in the specialization project to the case of PMSG with one converter, and stability criteria for the expanded system can be found (refer to the previous section), we proceed to include the second converter in the analysis. The connection to the grid is now modeled as constant voltage sources V_a^G, V_b^G and V_c^G as can be seen in Figure 3.3.

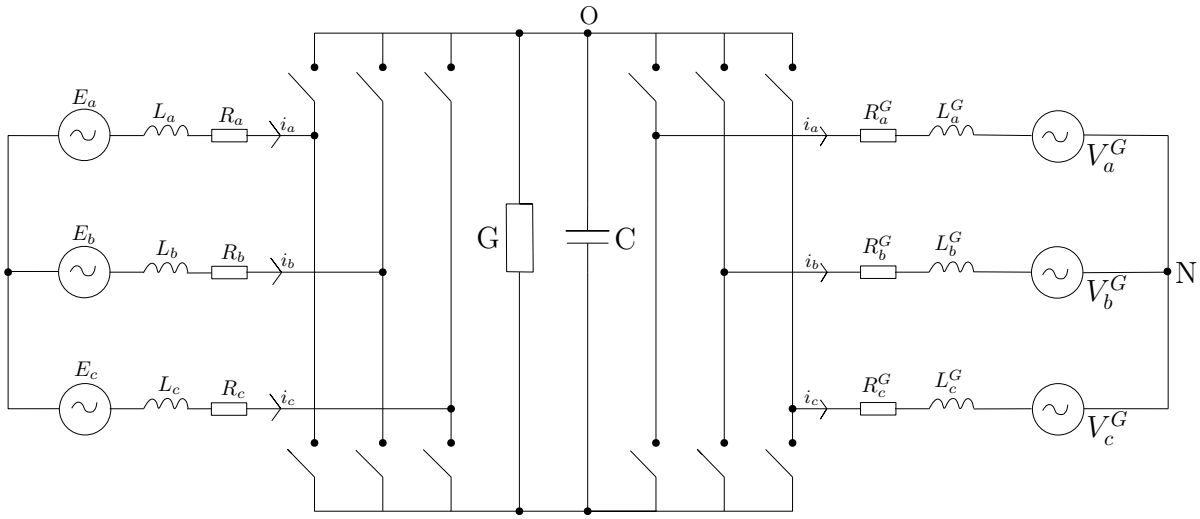

Figure 3.3: Wind energy conversion system with full scale 2L-VSCs in back-to-back configuration.

3.2.1 System Description

When developing the system equations, a rotating reference frame is used to get the dq-system equations with time-invariant solutions. The inclusion of the second converter adds two new state variables: the d- and q flux components. With the two new state variables, two new equations are also needed to describe the overall system. The equations describing the system shown in Figure 3.3 are:

$$L\dot{i}_d = -ri_d + Li_q\frac{P}{2}\omega_m - u_1V_c \tag{3.55}$$

$$L\dot{i}_q = -ri_q - Li_d\frac{P}{2}\omega_m + \phi\frac{P}{2}\omega_m - u_2V_c \tag{3.56}$$

$$J\dot{\omega}_m = T_m - \frac{P}{2}\phi i_q + d(\omega_{ref} - \omega_m) \tag{3.57}$$

$$C\dot{V}_c = u_1i_d + u_2i_q - u_3i_d^G - u_4i_q^G - GV_c \tag{3.58}$$

$$L_G\dot{i}_d^G = -r_Gi_d^G + \omega_GL_Gi_q^G + u_3V_c - V_d^G \tag{3.59}$$

$$L_G\dot{i}_q^G = -r_Gi_q^G - \omega_GL_Gi_d^G + u_4V_c - V_q^G \tag{3.60}$$

where u_3 and u_4 can be interpret as the duty cycles for the grid side converter. i_d^G and i_q^G are the currents from the grid side converter in the d- and q axis, respectively. L_G is the grid inductance and r_G is the grid resistance. ω_G is the angular grid frequency and V_d^G and V_q^G are the grid voltages.

As explained in section 3.1, the third system equation is modified to preserve skew-symmetry. The

system represented on a pH form becomes:

$$\underbrace{\begin{bmatrix}\dot{\psi}_d\\ \dot{\psi}_q\\ \dot{\rho}\\ \dot{q}_c\\ \dot{\psi}_d^G\\ \dot{\psi}_q^G\end{bmatrix}}_{\dot{x}} = \left(\underbrace{\begin{bmatrix} 0 & L\omega_m\frac{p}{2} & 0 & -u_1 & 0 & 0\\ -L\omega_m\frac{p}{2} & 0 & \frac{p}{2}\phi & -u_2 & 0 & 0\\ 0 & -\frac{p}{2}\phi & 0 & 0 & 0 & 0\\ u_1 & u_2 & 0 & 0 & -u_3 & -u_4\\ 0 & 0 & 0 & u_3 & 0 & \omega_G L_G\\ 0 & 0 & 0 & u_4 & -\omega_G L_G & 0\end{bmatrix}}_{\mathcal{J}(\omega_m,u)} - \underbrace{\begin{bmatrix} r & 0 & 0 & 0 & 0 & 0\\ 0 & r & 0 & 0 & 0 & 0\\ 0 & 0 & d & 0 & 0 & 0\\ 0 & 0 & 0 & G & 0 & 0\\ 0 & 0 & 0 & 0 & r_G & 0\\ 0 & 0 & 0 & 0 & 0 & r_G\end{bmatrix}}_{\mathcal{R}}\right)\underbrace{\begin{bmatrix} i_d\\ i_q\\ \omega_m\\ V_c\\ i_d^G\\ i_q^G\end{bmatrix}}_{\nabla\mathcal{H}(x)} + \underbrace{\begin{bmatrix} 0\\ 0\\ T_m + d\omega_{ref}\\ 0\\ V_d^G\\ V_q^G\end{bmatrix}}_{E} \tag{3.61}$$

The energy storage function, $\mathcal{H}(x)$ is:

$$\begin{aligned}\mathcal{H}(x) &= \frac{1}{2}x^\top Q x\\ &= \frac{1}{2}\begin{bmatrix}\psi_d & \psi_q & \rho & q_c & \psi_d^G & \psi_q^G\end{bmatrix}\begin{bmatrix}\frac{1}{L} & 0 & 0 & 0 & 0 & 0\\ 0 & \frac{1}{L} & 0 & 0 & 0 & 0\\ 0 & 0 & \frac{1}{J} & 0 & 0 & 0\\ 0 & 0 & 0 & \frac{1}{C} & 0 & 0\\ 0 & 0 & 0 & 0 & \frac{1}{L_G} & 0\\ 0 & 0 & 0 & 0 & 0 & \frac{1}{L_G}\end{bmatrix}\begin{bmatrix}\psi_d\\ \psi_q\\ \rho\\ q_c\\ \psi_d^G\\ \psi_q^G\end{bmatrix}\\ &= \frac{1}{2}(\frac{1}{L}\psi_d^2 + \frac{1}{L}\psi_q^2 + \frac{1}{J}\rho^2 + \frac{1}{C}q_c^2 + \frac{1}{L_G}\psi_d^{G^2} + \frac{1}{L_G}\psi_q^{G^2})\end{aligned} \tag{3.62}$$

Equation 3.61 can be expressed as:

$$\begin{aligned}\underbrace{\begin{bmatrix}\dot{\psi}_d\\ \dot{\psi}_q\\ \dot{\rho}\\ \dot{q}_c\\ \dot{\psi}_d^G\\ \dot{\psi}_q^G\end{bmatrix}}_{\dot{x}} = \Bigg(&\underbrace{\frac{P}{2}L\begin{bmatrix} 0 & \omega_m & 0 & 0 & 0 & 0\\ -\omega_m & 0 & 0 & 0 & 0 & 0\\ 0 & 0 & 0 & 0 & 0 & 0\\ 0 & 0 & 0 & 0 & 0 & 0\\ 0 & 0 & 0 & 0 & 0 & 0\\ 0 & 0 & 0 & 0 & 0 & 0\end{bmatrix}}_{\mathcal{J}(\omega_m)} + \underbrace{\frac{P}{2}\phi\begin{bmatrix} 0 & 0 & 0 & 0 & 0 & 0\\ 0 & 0 & 1 & 0 & 0 & 0\\ 0 & -1 & 0 & 0 & 0 & 0\\ 0 & 0 & 0 & 0 & 0 & 0\\ 0 & 0 & 0 & 0 & 0 & 0\\ 0 & 0 & 0 & 0 & 0 & 0\end{bmatrix}}_{\mathcal{J}_0} + u_1\underbrace{\begin{bmatrix} 0 & 0 & 0 & -1 & 0 & 0\\ 0 & 0 & 0 & 0 & 0 & 0\\ 0 & 0 & 0 & 0 & 0 & 0\\ 1 & 0 & 0 & 0 & 0 & 0\\ 0 & 0 & 0 & 0 & 0 & 0\\ 0 & 0 & 0 & 0 & 0 & 0\end{bmatrix}}_{\mathcal{J}_1} + u_2\underbrace{\begin{bmatrix} 0 & 0 & 0 & 0 & 0 & 0\\ 0 & 0 & 0 & -1 & 0 & 0\\ 0 & 0 & 0 & 0 & 0 & 0\\ 0 & 1 & 0 & 0 & 0 & 0\\ 0 & 0 & 0 & 0 & 0 & 0\\ 0 & 0 & 0 & 0 & 0 & 0\end{bmatrix}}_{\mathcal{J}_2}\\ &+ u_3\underbrace{\begin{bmatrix} 0 & 0 & 0 & 0 & 0 & 0\\ 0 & 0 & 0 & 0 & 0 & 0\\ 0 & 0 & 0 & 0 & 0 & 0\\ 0 & 0 & 0 & 0 & -1 & 0\\ 0 & 0 & 0 & 1 & 0 & 0\\ 0 & 0 & 0 & 0 & 0 & 0\end{bmatrix}}_{\mathcal{J}_3} + u_4\underbrace{\begin{bmatrix} 0 & 0 & 0 & 0 & 0 & 0\\ 0 & 0 & 0 & 0 & 0 & 0\\ 0 & 0 & 0 & 0 & 0 & 0\\ 0 & 0 & 0 & 0 & 0 & -1\\ 0 & 0 & 0 & 0 & 0 & 0\\ 0 & 0 & 0 & 1 & 0 & 0\end{bmatrix}}_{\mathcal{J}_4} + \omega_G L_G\underbrace{\begin{bmatrix} 0 & 0 & 0 & 0 & 0 & 0\\ 0 & 0 & 0 & 0 & 0 & 0\\ 0 & 0 & 0 & 0 & 0 & 0\\ 0 & 0 & 0 & 0 & 0 & 0\\ 0 & 0 & 0 & 0 & 0 & 1\\ 0 & 0 & 0 & 0 & -1 & 0\end{bmatrix}}_{\mathcal{J}_5} - \underbrace{\begin{bmatrix} r & 0 & 0 & 0 & 0 & 0\\ 0 & r & 0 & 0 & 0 & 0\\ 0 & 0 & d & 0 & 0 & 0\\ 0 & 0 & 0 & G & 0 & 0\\ 0 & 0 & 0 & 0 & r_G & 0\\ 0 & 0 & 0 & 0 & 0 & r_G\end{bmatrix}}_{R}\Bigg)\underbrace{\begin{bmatrix} i_d\\ i_q\\ \omega_m\\ V_c\\ i_d^G\\ i_q^G\end{bmatrix}}_{\nabla\mathcal{H}(x)}\\ &+ \underbrace{\begin{bmatrix} 0\\ 0\\ T_m + d\omega_{ref}\\ 0\\ V_d^G\\ V_q^G\end{bmatrix}}_{E}\end{aligned} \tag{3.63}$$

which abbreviated becomes:

$$\dot{x} = \big(\mathcal{J}(\omega_m) + \mathcal{J}_0 + u_1\mathcal{J}_1 + u_2\mathcal{J}_2 + u_3\mathcal{J}_3 + u_4\mathcal{J}_4 + \mathcal{J}_5 - \mathcal{R}\big)\nabla\mathcal{H}(x) + E \tag{3.64}$$

As in section 3.1, Equation 3.64 is separated in to two parts where one contain the control input to the system.

$$\dot{x} = f(x) + g(x)u$$

$$\dot{x} = \underbrace{\big(\mathcal{J}(\omega_m) + \mathcal{J}_0 + \mathcal{J}_5 - \mathcal{R}\big)\nabla\mathcal{H}(x) + E}_{f(x)} + \underbrace{\begin{bmatrix}\mathcal{J}_1\nabla\mathcal{H}(x) & \mathcal{J}_2\nabla\mathcal{H}(x) & \mathcal{J}_3\nabla\mathcal{H}(x) & \mathcal{J}_4\nabla\mathcal{H}(x)\end{bmatrix}}_{g(x)} \underbrace{\begin{bmatrix}u_1\\u_2\\u_3\\u_4\end{bmatrix}}_{\boldsymbol{u}} \tag{3.65}$$

3.2.2 Analysis of the Incremental Model

To investigate the system's stability with two converters, a LCF is chosen as the Hamiltonian of the shifted system, i.e., the Hamiltonian of the incremental model.

$$\mathcal{V}(\widetilde{x}) = \mathcal{H}(\widetilde{x}) = \frac{1}{2}\widetilde{x}^\top Q\widetilde{x} \tag{3.66}$$

Condition I and II for this LCF, are by definition satisfied as shown in section 3.1. To investigate condition III and IV, the time derivative of the LCF must be derived.

$$\dot{\mathcal{V}}(x) = \frac{d\mathcal{H}(\widetilde{x})}{dt} = \nabla^\top\mathcal{H}(\widetilde{x})\frac{d\widetilde{x}}{dt} = \nabla^\top\mathcal{H}(\widetilde{x})\dot{\widetilde{x}} = \widetilde{x}^\top Q\dot{\widetilde{x}} \tag{3.67}$$

The incremental model is derived as before, to obtain a LCF that has a minimum different from the origin.

$$\begin{array}{rrl} & \dot{x} = & \big(\mathcal{J}(\omega_m) + \mathcal{J}_0 + \mathcal{J}_5 - \mathcal{R})\big)\,Qx + E + g(x)u \\ - & 0 = & (\mathcal{J}(\bar{\omega}_m) + \mathcal{J}_0 + \mathcal{J}_5 - \mathcal{R})Q\bar{x} + E + g(\bar{x})\bar{u} \\ \hline & \dot{\widetilde{x}} = & (\mathcal{J}_0 + \mathcal{J}_5 - \mathcal{R})Q\widetilde{x} + \mathcal{J}(\omega_m)Qx - \mathcal{J}(\bar{\omega}_m)Q\bar{x} + g(x)u - g(\bar{x})\bar{u} \end{array} \tag{3.68}$$

As before, the term $g(x)u - g(\bar{x})\bar{u}$, can be reformulated to.

$$\begin{aligned} g(x)u - g(\bar{x})\bar{u} &= g(\widetilde{x} + \bar{x})(u) - g(\bar{x})\bar{u} \\ &= g(\widetilde{x})u + g(\bar{x})u - g(\bar{x})\bar{u} \\ &= g(\widetilde{x})u + g(\bar{x})\widetilde{u} \end{aligned}$$

where

$$g(\widetilde{x}) = \begin{bmatrix}\mathcal{J}_1\nabla\mathcal{H}(\widetilde{x}) & \mathcal{J}_2\nabla\mathcal{H}(\widetilde{x}) & \mathcal{J}_3\nabla\mathcal{H}(\widetilde{x}) & \mathcal{J}_4\nabla\mathcal{H}(\widetilde{x})\end{bmatrix}$$

Which results in that Equation 3.68 can be formulated as:

$$\begin{aligned} \dot{\widetilde{x}} &= \Big(\mathcal{J}_0 + u_1\mathcal{J}_1 + u_2\mathcal{J}_2 + u_3\mathcal{J}_3 + u_4\mathcal{J}_4 + \mathcal{J}_5 - \mathcal{R}\Big)Q\widetilde{x} + \mathcal{J}(\omega_m)Qx - \mathcal{J}(\bar{\omega}_m)Q\bar{x} + g(\bar{x})\widetilde{u} \\ &= \Big(\mathcal{J}_0 + \sum_{i=1}^{4}\mathcal{J}_i u_i + \mathcal{J}_5 - \mathcal{R}\Big)Q\widetilde{x} + \mathcal{J}(\omega_m)Qx - \mathcal{J}(\bar{\omega}_m)Q\bar{x} + g(\bar{x})\widetilde{u} \end{aligned} \tag{3.69}$$

The matrix $g(\bar{x})$ describes how the control of the converters is impacting the system. The converter closest to the PMSG controls the speed of the rotor and effectively the active power that is transferred to the grid. The converter on the grid-side of the dc-link, controls the voltage on the dc-link and has a free control variable that could be used to control the reactive power transferred to the grid. As was observed for the system with only one converter in section 3.1, condition 3.46 which is related to the PMSG, is the most strict condition. If this condition is satisfied, then the rest of the conditions will be satisfied by choosing $\gamma > 0$. An interesting hypothesis to investigate is, therefore, if it is enough to only use the converter closest to the PMSG to render the rest of the system passive.

Hypothesis: "*Only using the converter closest to the PMSG is enough to compensate for the lack of monotonicity inherent to the machine, and thus to render the rest of the system passive.*"

Towards this end, we first find it convenient to divide $g(\bar{x})$ into separate parts for the two converters, as:

$$\begin{aligned} g(\bar{x}) &= \begin{bmatrix} g(\bar{x})^{\text{PMSG}} & g(\bar{x})^{G} \end{bmatrix} \\ g(\bar{x})^{\text{PMSG}} &= \begin{bmatrix} \mathcal{J}_1 \nabla \mathcal{H}(\bar{x}) & \mathcal{J}_2 \nabla \mathcal{H}(\bar{x}) \end{bmatrix} \\ g(\bar{x})^{G} &= \begin{bmatrix} \mathcal{J}_3 \nabla \mathcal{H}(\bar{x}) & \mathcal{J}_4 \nabla \mathcal{H}(\bar{x}) \end{bmatrix} \end{aligned} \tag{3.70}$$

The time derivative of the LCF can then be expressed as

$$I: \quad \dot{\mathcal{V}}(x) = \widetilde{x}^\top Q\Big(\mathcal{J}_0 + \sum_{i=1}^{4} \mathcal{J}_i u_i + \mathcal{J}_5 - \mathcal{R}\Big) Q\widetilde{x} + \widetilde{x}^\top Q\mathcal{J}(\omega_m) Qx - \widetilde{x}^\top Q\mathcal{J}(\bar{\omega}_m) Q\bar{x} + \underbrace{\widetilde{x}^\top Q g(\bar{x})}_{y^\top} \widetilde{u}$$

$$II: \quad \dot{\mathcal{V}}(x) = y^\top \widetilde{u} - \widetilde{x}^\top Q\mathcal{R}Q\widetilde{x} + \widetilde{x}^\top Q\mathcal{J}(\omega_m) Qx - \widetilde{x}^\top Q\mathcal{J}(\bar{\omega}_m) Q\bar{x} + \underbrace{\widetilde{x}^\top Q\mathcal{J}(\omega_m) Q\bar{x} - \widetilde{x}^\top Q\mathcal{J}(\omega_m) Q\bar{x}}_{0}$$

$$III: \quad \dot{\mathcal{V}}(x) = y^\top \widetilde{u} - \widetilde{x}^\top Q\mathcal{R}Q\widetilde{x} + \underbrace{\widetilde{x}^\top Q\mathcal{J}(\omega_m)(Qx - Q\bar{x})}_{0} - \widetilde{x}^\top Q\mathcal{J}(\bar{\omega}_m) Q\bar{x} + \widetilde{x}^\top Q\mathcal{J}(\omega_m) Q\bar{x}$$

$$IV: \quad \dot{\mathcal{V}}(x) = y^\top \widetilde{u} + \widetilde{x}^\top Q\Big[\big(J(\omega_m) - \mathcal{J}(\bar{\omega}_m)\big) Q\bar{x} - \mathcal{R}Q\widetilde{x}\Big] + \widetilde{x}^\top Q\left(\gamma g(\bar{x})^{PMSG} g(\bar{x})^{PMSG^\top}\right) Q\widetilde{x}$$
$$- \widetilde{x}^\top Q\left(\gamma g(\bar{x})^{PMSG} g(\bar{x})^{PMSG^\top}\right) Q\widetilde{x}$$

$$V: \quad \dot{\mathcal{V}}(x) = y^\top \widetilde{u} + \widetilde{x}^\top Q\Big[\big(\mathcal{J}(\omega_m) - \mathcal{J}(\bar{\omega}_m)\big) Q\bar{x} - \mathcal{R}Q\widetilde{x} - \gamma g(\bar{x})^{PMSG} g(\bar{x})^{PMSG^\top} Q\widetilde{x}\Big] + y^{PMSG^\top} \gamma y^{PMSG}$$

$$VI: \quad \dot{\mathcal{V}}(x) = y^\top \widetilde{u} + y^{PMSG^\top} \gamma y^{PMSG} + (z - \bar{z})^\top \Big[M(z) - M(\widetilde{z}) - \gamma g(\bar{x})^{PMSG} g(\bar{x})^{PMSG^\top} (z - \bar{z})\Big]$$

$$VII: \quad \dot{\mathcal{V}}(x) = -y^\top K_p y + y^{PMSG^\top} \gamma y^{PMSG} + (z - \bar{z})^\top \Big[M(z) - M(\widetilde{z}) - \gamma g(\bar{x})^{PMSG} g(\bar{x})^{PMSG^\top} (z - \bar{z})\Big]$$

$$VIII: \quad \dot{\mathcal{V}}(x) = -y^\top \big[K_P^* - \Gamma\big] y + (z - \bar{z})^\top \Big[M(z) - M(\widetilde{z}) - \gamma g(\bar{x})^{PMSG} g(\bar{x})^{PMSG^\top} (z - \bar{z})\Big] 0$$

Step explanation

I $y^\top$, the passive output of the system is defined as $\widetilde{x}^\top Q g(\bar{x})$ and skew-symmetry cancels the terms involving $\mathcal{J}_0, \mathcal{J}_1, \mathcal{J}_2, \mathcal{J}_3, \mathcal{J}_4$ and $\mathcal{J}_5$

II Zero is added to the equation by adding and subtracting the term, $\widetilde{x}^\top Q\mathcal{J}(\omega_m) Q\bar{x}$. This way of proceeding is gotten from[31]

III The term $\widetilde{x}^\top Q\mathcal{J}(\omega_m)(Qx - Q\bar{x})$ is canceled due to skew-symmetry. This cancellation is what was desired by adding the zero term in II.

IV Output feedback is added to enforce passivity in the system [31]. It is only the passive output from the PMSG-connected converter that is used to render the system passive.

V $y^{PMSG^\top} = \widetilde{x}^\top Q g(\bar{x})^{PMSG}$

VI $z \triangleq Qx$ and $M(z) \triangleq J(\omega_m)\bar{z} - Rz$

VII The passive output is chosen as the input to the system to get a closed loop controller. $\widetilde{u} = -K_p y$

VIII The contraction of the two first terms are shown below and marked with "*".

$$* \quad \underbrace{\begin{bmatrix} y^{PMSG^\top} & y^{G^\top} \end{bmatrix}}_{y^\top} \left[\underbrace{\begin{bmatrix} K_p^{PMSG} & 0_{2x2} \\ 0_{2x2} & K_P^G \end{bmatrix}}_{K_P^*} - \underbrace{\begin{bmatrix} \gamma I_{2x2} & 0_{2x2} \\ 0_{2x2} & 0_{2x2} \end{bmatrix}}_{\Gamma} \right] \underbrace{\begin{bmatrix} y^{PMSG} \\ y^G \end{bmatrix}}_{y} \tag{3.71}$$

$$K_P^{PMSG} = \begin{bmatrix} K_d^{PMSG} & 0 \\ 0 & K_q^{PMSG} \end{bmatrix} \quad K_p^G = \begin{bmatrix} K_d^G & 0 \\ 0 & K_q^G \end{bmatrix}$$

An expression for the time derivative of the LCF is therefore:

$$\dot{\mathcal{V}}(x) = \underbrace{-y^\top \left[K_P^* - \Gamma\right] y}_{1.Term} + \underbrace{\tilde{z}^\top \left[M(z) - M(\tilde{z}) - \gamma g(\bar{x})^{PMSG} g(\bar{x})^{PMSG^\top} \tilde{z}\right]}_{2.Term} \tag{3.72}$$

As 3.72 needs to be negative semi-definite to satisfy condition IV for the LCF, the second term must be investigated further as the first term is negative definite when $K_p^* > \Gamma$. It can be shown that if $\left[M(z) - M(\tilde{z}) - \gamma g(\bar{x})^{PMSG} g(\bar{x})^{PMSG^\top}(z - \bar{z})\right]$ is monotonically decreasing, then the second term in 3.72 is negative semi-definite. This is equivalent to checking if $\nabla^\top M(z) + \nabla M(z) - 2\gamma g(\bar{x})^{PMSG} g(\bar{x})^{PMSG^\top}$ is negative semi-definite.

Checking for monotonicity

$$\nabla^\top M(z) + \nabla M(z) - 2\gamma g(\bar{x})^{PMSG} g(\bar{x})^{PMSG^\top} \leq 0 \tag{3.73}$$

$$M(z) = \mathcal{J}(z)\bar{z} - \mathcal{R}z = \frac{P}{2} L \begin{bmatrix} 0 & \omega_m & 0 & 0 & 0 & 0 \\ -\omega_m & 0 & 0 & 0 & 0 & 0 \\ 0 & 0 & 0 & 0 & 0 & 0 \\ 0 & 0 & 0 & 0 & 0 & 0 \\ 0 & 0 & 0 & 0 & 0 & 0 \\ 0 & 0 & 0 & 0 & 0 & 0 \end{bmatrix} \begin{bmatrix} \bar{i}_d \\ \bar{i}_q \\ \bar{\omega}_m \\ \bar{V}_c \\ \bar{i}_d^G \\ \bar{i}_q^G \end{bmatrix} - \begin{bmatrix} r & 0 & 0 & 0 & 0 & 0 \\ 0 & r & 0 & 0 & 0 & 0 \\ 0 & 0 & d & 0 & 0 & 0 \\ 0 & 0 & 0 & G & 0 & 0 \\ 0 & 0 & 0 & 0 & r_G & 0 \\ 0 & 0 & 0 & 0 & 0 & r_G \end{bmatrix} \begin{bmatrix} i_d \\ i_q \\ \omega_m \\ V_c \\ i_d^G \\ i_q^G \end{bmatrix} = \begin{bmatrix} \frac{P}{2} L \omega_m \bar{i}_q - r i_d \\ -\frac{P}{2} L \omega_m \bar{i}_d - r i_q \\ -d\omega_m \\ -G V_c \\ -r_G i_d^G \\ -r_G i_q^G \end{bmatrix}$$

$$\nabla M(z) = \begin{bmatrix} -r & 0 & \bar{i}_q \frac{P}{2} L & 0 & 0 & 0 \\ 0 & -r & -\bar{i}_d \frac{P}{2} L & 0 & 0 & 0 \\ 0 & 0 & -d & 0 & 0 & 0 \\ 0 & 0 & 0 & -G & 0 & 0 \\ 0 & 0 & 0 & 0 & -r_G & 0 \\ 0 & 0 & 0 & 0 & 0 & -r_G \end{bmatrix} \tag{3.74}$$

$$g(\bar{x})^{PMSG} = \begin{bmatrix} \begin{bmatrix} 0 & 0 & 0 & -1 & 0 & 0 \\ 0 & 0 & 0 & 0 & 0 & 0 \\ 0 & 0 & 0 & 0 & 0 & 0 \\ 1 & 0 & 0 & 0 & 0 & 0 \\ 0 & 0 & 0 & 0 & 0 & 0 \\ 0 & 0 & 0 & 0 & 0 & 0 \end{bmatrix} \begin{bmatrix} 0 & 0 & 0 & 0 & 0 & 0 \\ 0 & 0 & 0 & -1 & 0 & 0 \\ 0 & 0 & 0 & 0 & 0 & 0 \\ 0 & 1 & 0 & 0 & 0 & 0 \\ 0 & 0 & 0 & 0 & 0 & 0 \\ 0 & 0 & 0 & 0 & 0 & 0 \end{bmatrix} \end{bmatrix} \begin{bmatrix} \bar{i}_d \\ \bar{i}_q \\ \bar{\omega}_m \\ \bar{V}_c \\ \bar{i}_d^G \\ \bar{i}_q^G \end{bmatrix} = \begin{bmatrix} -\bar{V}_c & 0 \\ 0 & -\bar{V}_c \\ 0 & 0 \\ \bar{i}_d & \bar{i}_q \\ 0 & 0 \\ 0 & 0 \end{bmatrix} \tag{3.75}$$

$$g(\bar{x})^{PMSG} g(\bar{x})^{PMSG^\top} = \begin{bmatrix} -\bar{V}_c & 0 \\ 0 & -\bar{V}_c \\ 0 & 0 \\ \bar{i}_d & \bar{i}_q \\ 0 & 0 \\ 0 & 0 \end{bmatrix} \begin{bmatrix} -\bar{V}_c & 0 & 0 & \bar{i}_d & 0 & 0 \\ 0 & -\bar{V}_c & 0 & \bar{i}_q & 0 & 0 \end{bmatrix} = \begin{bmatrix} \bar{V}_c^2 & 0 & 0 & -\bar{i}_d \bar{V}_c & 0 & 0 \\ 0 & \bar{V}_c^2 & 0 & -\bar{i}_q \bar{V}_c & 0 & 0 \\ 0 & 0 & 0 & 0 & 0 & 0 \\ -\bar{V}_c \bar{i}_d & -\bar{V}_c \bar{i}_q & 0 & \bar{i}_d^2 + \bar{i}_q^2 & 0 & 0 \\ 0 & 0 & 0 & 0 & 0 & 0 \\ 0 & 0 & 0 & 0 & 0 & 0 \end{bmatrix} \tag{3.76}$$

Inserting 3.74, 3.75 and 3.76 into 3.73;

$$\begin{bmatrix} -2(r + \gamma \bar{V}_c^2) & 0 & \bar{i}_q \frac{P}{2} L & 2\gamma \bar{i}_d \bar{V}_c & 0 & 0 \\ 0 & -2(r + \gamma \bar{V}_c^2) & -\bar{i}_d \frac{P}{2} L & 2\gamma \bar{i}_q \bar{V}_c & 0 & 0 \\ \bar{i}_q \frac{P}{2} L & -\bar{i}_d \frac{P}{2} L & -2d & 0 & 0 & 0 \\ 2\gamma \bar{i}_d \bar{V}_c & 2\gamma \bar{i}_q \bar{V}_c & 0 & -2\left(G + \gamma(\bar{i}_d^2 + \bar{i}_q^2)\right) & 0 & 0 \\ 0 & 0 & 0 & 0 & -2r_G & 0 \\ 0 & 0 & 0 & 0 & 0 & -2r_G \end{bmatrix} \leq 0 \tag{3.77}$$

At the equilibrium point it is desired that the d-component of the current in the first converter is zero, $\bar{i}_d = 0$. 3.77 is thereby simplified to 3.78.

$$\begin{bmatrix} -2(r+\gamma\bar{V}_c^2) & 0 & \bar{i}_q\frac{P}{2}L & 0 & 0 & 0 \\ 0 & -2(r+\gamma\bar{V}_c^2) & 0 & 2\gamma\bar{i}_q\bar{V}_c & 0 & 0 \\ \bar{i}_q\frac{P}{2}L & 0 & -2d & 0 & 0 & 0 \\ 0 & 2\gamma\bar{i}_q\bar{V}_c & 0 & -2\left(G+\gamma\bar{i}_q^2\right) & 0 & 0 \\ 0 & 0 & 0 & 0 & -2r_G & 0 \\ 0 & 0 & 0 & 0 & 0 & -2r_G \end{bmatrix} \leq 0 \tag{3.78}$$

The Schur compliment is used to check whether 3.78 is negative semi-definite or not. When applying the Schur complement to Equation 3.78, one can choose the A-matrix equal to 3.41, which is already proven to be negative definite by choosing γ according to 3.47 in section 3.1. The C-matrix must be chosen as $C = \begin{bmatrix} -2r_G & 0 \\ 0 & -2r_G \end{bmatrix}$, which also is negative definite. It can therefore be concluded that 3.78 is negative definite. The condition 3.73 is therefore satisfied, and the term $\left[M(z) - M(\widetilde{z}) - \gamma g(\bar{x})^{PMSG} g(\bar{x})^{PMSG^\top}(z-\bar{z})\right]$ is monotonically decreasing.

The time derivative of the LCF, 3.72, can therefore be expressed as:

$$\dot{\mathcal{V}}(x) = -y^\top \begin{bmatrix} K_p^* & - & \Gamma \end{bmatrix} y + \underbrace{(z-\bar{z})^\top \left[M(z) - M(\widetilde{z}) - \gamma g(\bar{x})^{PMSG} g(\bar{x})^{PMSG^\top}(z-\bar{z})\right]}_{\leq 0}$$

$$\dot{\mathcal{V}}(x) \leq -y^\top \begin{bmatrix} K_p^* & - & \Gamma \end{bmatrix} y$$

$$\dot{\mathcal{V}}(x) \leq 0, \text{ IFF } K_p^* \geq \Gamma$$

By choosing $K_p^* \geq \Gamma$, the time derivative of the LCF is satisfying condition IV. In appendix A the proof for condition IV, $\dot{\mathcal{V}} \leq 0$, is repeated but the passive feedback from both converters are included.

Condition I, II, and IV are therefore satisfied. Next we check if condition III, $\dot{\mathcal{V}}(0) = 0$ is satisfied.

Proof: Condition III

$$\dot{\mathcal{V}}(x) \leq y^{\top *} \begin{bmatrix} K_p^* & - & \Gamma \end{bmatrix} y^*$$

$$\dot{\mathcal{V}}(x) \leq \begin{bmatrix} y^{PMSG^\top} & y^{G^\top} \end{bmatrix} \left[\begin{bmatrix} K_p^{PMSG} & 0_{2x2} \\ 0_{2x2} & K_P^G \end{bmatrix} - \begin{bmatrix} \gamma I_{2x2} & 0_{2x2} \\ 0_{2x2} & 0_{2x2} \end{bmatrix} \right] \begin{bmatrix} y^{PMSG} \\ y^G \end{bmatrix}$$

$$\dot{\mathcal{V}}(x) \leq \begin{bmatrix} \widetilde{x}^\top Q g(\bar{x})^{PMSG} & \widetilde{x}^\top Q g(\bar{x})^G \end{bmatrix} \left[\begin{bmatrix} K_p^{PMSG} & 0_{2x2} \\ 0_{2x2} & K_P^G \end{bmatrix} - \begin{bmatrix} \gamma I_{2x2} & 0_{2x2} \\ 0_{2x2} & 0_{2x2} \end{bmatrix} \right] \begin{bmatrix} g^\top(\bar{x})^{PMSG} Q\widetilde{x} \\ g^\top(\bar{x})^G Q\widetilde{x} \end{bmatrix}$$

$$\dot{\mathcal{V}}(x) \leq \widetilde{x}^\top Q \begin{bmatrix} g(\bar{x})^{PMSG} & g(\bar{x})^G \end{bmatrix} \left[\begin{bmatrix} K_p^{PMSG} & 0_{2x2} \\ 0_{2x2} & K_P^G \end{bmatrix} - \begin{bmatrix} \gamma I_{2x2} & 0_{2x2} \\ 0_{2x2} & 0_{2x2} \end{bmatrix} \right] \begin{bmatrix} g^\top(\bar{x})^{PMSG} \\ g^\top(\bar{x})^G \end{bmatrix} Q\widetilde{x}$$

$$\dot{\mathcal{V}}(\bar{x}) = \underbrace{(\bar{x}-\bar{x})^\top}_{=0} Q \begin{bmatrix} g(\bar{x})^{PMSG} & g(\bar{x})^G \end{bmatrix} \left[\begin{bmatrix} K_p^{PMSG} & 0_{2x2} \\ 0_{2x2} & K_P^G \end{bmatrix} - \begin{bmatrix} \gamma I_{2x2} & 0_{2x2} \\ 0_{2x2} & 0_{2x2} \end{bmatrix} \right] \begin{bmatrix} g(\bar{x})^{PMSG} \\ g(\bar{x})^G \end{bmatrix} Q \underbrace{(\bar{x}-\bar{x})}_{=0}$$

$$\dot{\mathcal{V}}(x) = 0$$

All four conditions for a Lyapunov function are therefore satisfied. The LCF is thereby shown to be a Lyapunov function, and the system is therefore proven to be asymptotically stable. The hypothesis "*Only using the converter closest to the PMSG is enough to compensate for the lack of monotonicity inherent to the machine, and thus to render the rest of the system passive*" is thereby valid.

3.2.3 Conclusion

In this section, we have found stability criteria for a PMSG wind energy conversion system with full scale B2B 2L-VSCs. We showed that it is possible to compensate for the lack of monotonicity

for the machine by imposing some tuning requirements on the proportional control parameter of a single converter. In addition to this, we also showed that –although potentially less practical from a plug-and-play viewpoint– we can share the tuning conditions among both converters, as can be seen in Appendix A. To ensure the stability of the system, the same criterion found in section 3.1 must be satisfied.

$$2d - \frac{(\bar{i}_q \frac{P}{2} L)^2}{2(r + \gamma \bar{V}_c^2)} \geq 0$$

which gives the following restriction for γ

$$\gamma \geq \frac{1}{\bar{V}_c^2} \left(\frac{(\bar{i}_q \frac{P}{2} L)^2}{4d} - r \right) \tag{3.79}$$

The tuning requirements can then be found as $K_P^* > \Gamma$.

$$K_P^* = \begin{bmatrix} K_d^{PMSG} & 0 & 0 & 0 \\ 0 & K_q^{PMSG} & 0 & 0 \\ 0 & 0 & K_d^G & 0 \\ 0 & 0 & 0 & K_q^G \end{bmatrix} \geq \Gamma = \begin{bmatrix} \gamma & 0 & 0 & 0 \\ 0 & \gamma & 0 & 0 \\ 0 & 0 & 0 & 0 \\ 0 & 0 & 0 & 0 \end{bmatrix} \tag{3.80}$$

$$K_d^{PMSG} \geq \gamma \tag{3.81}$$

$$K_q^{PMSG} \geq \gamma \tag{3.82}$$

$$K_d^G \geq 0 \tag{3.83}$$

$$K_q^G \geq 0 \tag{3.84}$$

By tuning the proportional gain in the PI-controllers according to 3.81, 3.82, 3.83 and 3.84, the system is guaranteed to be stable even if being subjected to large disturbances. The design of the passive controllers is further explained in subsection 4.1.3.

In conclusion, we presented tuning criteria that guarantee *global asymptotic* stability for the (non-linear) WECS with back-to-back voltage source converters. Surprisingly enough, stability can be achieved by imposing stricter tuning conditions to only the machine-side converter–while the other only needs to have positive controller gains–. This observation is potentially useful for integrating more wind power into the electricity grid. The stricter tuning condition on the machine-side converter guarantees large signal stability. As a result, adding new turbines to the power grid without jeopardizing the stability is simpler, and the potential tuning of the second converter for performance can be done without risking instability. This *plug & play* philosophy eases the necessary change from a centralized to a more distributed energy system dominated by renewables.

In section 3.1 and section 3.2 the mechanical torque has been modelled as a constant which is indeed a simplification. As explained in chapter 2, the mechanical torque is, in reality, a non-linear function of angular velocity. In the next section, this non-linearity is included in the derivation of a stability certificate.

3.3 Including the Dynamics of the Wind

In the previous sections, the mechanical torque has been modeled as a constant. In reality, the torque the turbine generates from the wind is a function of angular velocity.

$$T_m(\omega_m) = \frac{1}{2}\rho A v_{wind}^3 C_p(\lambda)\frac{1}{\omega_m} \tag{3.85}$$

where ρ is the air density, $A = \pi r_b^2$ is the area swept by the turbine blades, v_{wind} is the wind speed, C_p is the wind power coefficient, and λ is the tip speed ratio.

$$\lambda = \frac{r_b \omega_m}{v_{wind}} \tag{3.86}$$

$$C_p = C_1\left(C_2(\tfrac{1}{\lambda} - 0.035) - C_5\right) e^{-C_6(\frac{1}{\lambda}-0.035)} \tag{3.87}$$

It is apparent that the mechanical torque is a non-linear function of the angular velocity of the rotor shaft, ω_m. The system model from section 3.2 must be updated. The third system equation, Equation 3.57 then becomes:

$$J\dot{\omega}_m = T_m(\omega_m) - \frac{P}{2}\phi i_q + d(\omega_{ref} - \omega_m) \tag{3.88}$$

The port-Hamiltonian formulation of the system becomes:

$$\begin{aligned}
\underbrace{\begin{bmatrix}\dot{\psi}_d\\ \dot{\psi}_q\\ \dot{\rho}\\ \dot{q}_c\\ \dot{\psi}_d^G\\ \dot{\psi}_q^G\end{bmatrix}}_{\dot{x}} = \Bigg(& \underbrace{\frac{P}{2}L\begin{bmatrix}0 & \omega_m & 0&0&0&0\\ -\omega_m & 0 & 0&0&0&0\\ 0&0&0&0&0&0\\0&0&0&0&0&0\\0&0&0&0&0&0\\0&0&0&0&0&0\end{bmatrix}}_{\mathcal{J}(\omega_m)} + \underbrace{\frac{P}{2}\phi\begin{bmatrix}0&0&0&0&0&0\\0&0&1&0&0&0\\0&-1&0&0&0&0\\0&0&0&0&0&0\\0&0&0&0&0&0\\0&0&0&0&0&0\end{bmatrix}}_{\mathcal{J}_0} + u_1\underbrace{\begin{bmatrix}0&0&0&-1&0&0\\0&0&0&0&0&0\\0&0&0&0&0&0\\1&0&0&0&0&0\\0&0&0&0&0&0\\0&0&0&0&0&0\end{bmatrix}}_{\mathcal{J}_1} + u_2\underbrace{\begin{bmatrix}0&0&0&0&0&0\\0&0&0&-1&0&0\\0&0&0&0&0&0\\0&1&0&0&0&0\\0&0&0&0&0&0\\0&0&0&0&0&0\end{bmatrix}}_{\mathcal{J}_2}\\
& + u_3\underbrace{\begin{bmatrix}0&0&0&0&0&0\\0&0&0&0&0&0\\0&0&0&0&0&0\\0&0&0&0&-1&0\\0&0&0&1&0&0\\0&0&0&0&0&0\end{bmatrix}}_{\mathcal{J}_3} + u_4\underbrace{\begin{bmatrix}0&0&0&0&0&0\\0&0&0&0&0&0\\0&0&0&0&0&0\\0&0&0&0&0&-1\\0&0&0&0&0&0\\0&0&0&1&0&0\end{bmatrix}}_{\mathcal{J}_4} + \omega_e L_G\underbrace{\begin{bmatrix}0&0&0&0&0&0\\0&0&0&0&0&0\\0&0&0&0&0&0\\0&0&0&0&0&0\\0&0&0&0&0&1\\0&0&0&0&-1&0\end{bmatrix}}_{\mathcal{J}_5} - \underbrace{\begin{bmatrix}r&0&0&0&0&0\\0&r&0&0&0&0\\0&0&d-\frac{T_m(\omega_m)}{\omega_m}&0&0&0\\0&0&0&G&0&0\\0&0&0&0&r_G&0\\0&0&0&0&0&r_G\end{bmatrix}}_{R(\omega_m)}\Bigg)\underbrace{\begin{bmatrix}i_d\\i_q\\\omega_m\\V_c\\i_d^G\\i_q^G\end{bmatrix}}_{\nabla\mathcal{H}(x)}\\
& + \underbrace{\begin{bmatrix}0\\0\\d\omega_{ref}\\0\\V_d^G\\V_q^G\end{bmatrix}}_{E}
\end{aligned} \tag{3.89}$$

which abbreviated becomes:

$$\dot{x} = \left(J(\omega_m) + \mathcal{J}_0 + u_1\mathcal{J}_1 + u_2\mathcal{J}_2 + u_3\mathcal{J}_3 + u_4\mathcal{J}_4 + \mathcal{J}_5 - \mathcal{R}(\omega_m)\right)\nabla\mathcal{H}(x) + E$$

$$\dot{x} = \underbrace{\left(\mathcal{J}(\omega_m) + \mathcal{J}_0 + \mathcal{J}_5 - \mathcal{R}(\omega_m)\right)\nabla\mathcal{H}(x) + E}_{f(x)} + \underbrace{\begin{bmatrix}\mathcal{J}_1\nabla\mathcal{H}(x) & \mathcal{J}_2\nabla\mathcal{H}(x) & \mathcal{J}_3\nabla\mathcal{H}(x) & \mathcal{J}_4\nabla\mathcal{H}(x)\end{bmatrix}}_{g(x)}\underbrace{\begin{bmatrix}u_1\\u_2\\u_3\\u_4\end{bmatrix}}_{\boldsymbol{u}} \tag{3.90}$$

3.3.1 Analysis of the Incremental Model

The shifted model, that is the incremental model, becomes:

$$\begin{array}{rll} & \dot{x} = & \left(\mathcal{J}(\omega_m) + \mathcal{J}_0 + \mathcal{J}_5 - \mathcal{R}(\omega_m)\right) Qx + E + g(x)u \\ - & 0 = & \left(\mathcal{J}(\bar{\omega_m}) + \mathcal{J}_0 + \mathcal{J}_5 - \mathcal{R}(\bar{\omega}_m)\right) Q\bar{x} + E + g(\bar{x})\bar{u} \\ \hline & \dot{\widetilde{x}} = & (\mathcal{J}_0 + \mathcal{J}_5)Q\widetilde{x} + \mathcal{J}(\omega_m)Qx - \mathcal{J}(\bar{\omega}_m)Q\bar{x} - \mathcal{R}(\omega_m)Qx + \mathcal{R}(\bar{\omega}_m)Q\bar{x} + g(x)u - g(\bar{x})\bar{u} \end{array} \tag{3.91}$$

As explained in section 3.2, the expression 3.91 can be reformulated to:

$$\dot{\widetilde{x}} = \Big(\mathcal{J}_0 + \sum_{i=1}^{4} \mathcal{J}_i u_i + \mathcal{J}_5\Big) Q\widetilde{x} + \mathcal{J}(\omega_m)Qx - \mathcal{R}(\omega_m)Qx - \mathcal{J}(\bar{\omega}_m)Q\bar{x} + \mathcal{R}(\bar{\omega}_m)Q\bar{x} + g(\bar{x})\widetilde{u} \tag{3.92}$$

The LCF is chosen as $\mathcal{V}(x) = \frac{1}{2}\widetilde{x}^\top Q\widetilde{x}$, and to check the Lyapunov conditions, the same procedure as shown section 3.2 is performed. By this choice of LCF, the two first conditions are satisfied by definition as shown in section 3.1. The same procedure shown in both section 3.1 and section 3.2 is performed to derive the expression for the time derivative for the LCF. For the sake of brevity, the derivation of this expression is omitted, and the final result is shown below.

$$\dot{\mathcal{V}}(x) = y^\top \widetilde{u} + {y^{PMSG}}^\top \gamma y^{PMSG} + (z-\bar{z})^\top \Big[M(z) - M(\bar{z}) - \gamma g(\bar{x})^{PMSG} {g(\bar{x})^{PMSG}}^\top (z-\bar{z})\Big] \tag{3.93}$$

where

$$M(z) \triangleq \mathcal{J}(z)\bar{z} - \mathcal{R}(z)z \tag{3.94}$$

We begin by analyzing when the third term in 3.93 is negative semi-definite. Towards this end, it is enough to check if the function inside the parenthesis is monotonically decreasing, which is equivalent to.

$$\nabla^\top M(z) + \nabla M(z) - 2\gamma g(\bar{x})^{PMSG} {g(\bar{x})^{PMSG}}^\top \leq 0 \tag{3.95}$$

where

$$M(z) = \mathcal{J}(z)\bar{z} - \mathcal{R}(z)z = \frac{P}{2}L \begin{bmatrix} 0 & \omega_m & 0 & 0 & 0 & 0 \\ -\omega_m & 0 & 0 & 0 & 0 & 0 \\ 0 & 0 & 0 & 0 & 0 & 0 \\ 0 & 0 & 0 & 0 & 0 & 0 \\ 0 & 0 & 0 & 0 & 0 & 0 \\ 0 & 0 & 0 & 0 & 0 & 0 \end{bmatrix} \begin{bmatrix} \bar{i}_d \\ \bar{i}_q \\ \bar{\omega}_m \\ \bar{V}_c \\ \bar{i}_q^G \\ \bar{i}_q^G \end{bmatrix} - \begin{bmatrix} r & 0 & 0 & 0 & 0 & 0 \\ 0 & r & 0 & 0 & 0 & 0 \\ 0 & 0 & d - \frac{T(\omega_m)}{\omega_m} & 0 & 0 & 0 \\ 0 & 0 & 0 & G & 0 & 0 \\ 0 & 0 & 0 & 0 & r_G & 0 \\ 0 & 0 & 0 & 0 & 0 & r_G \end{bmatrix} \begin{bmatrix} i_d \\ i_q \\ \omega_m \\ V_c \\ i_d^G \\ i_q^G \end{bmatrix} = \begin{bmatrix} \frac{P}{2}L_m \bar{i}_q - r i_d \\ -\frac{P}{2}L\omega_m \bar{i}_d - r i_q \\ -d\omega_m + T_m(\omega_m) \\ -GV_c \\ -r_G i_d^G \\ -r_G i_q^G \end{bmatrix}$$

$$\nabla M(z) = \begin{bmatrix} -r & 0 & \bar{i}_q \frac{P}{2}L & 0 & 0 & 0 \\ 0 & -r & -\bar{i}_d \frac{P}{2}L & 0 & 0 & 0 \\ 0 & 0 & -d - \frac{\partial T_m(\omega_m)}{\partial \omega_m} & 0 & 0 & 0 \\ 0 & 0 & 0 & -G & 0 & 0 \\ 0 & 0 & 0 & 0 & -r_G & 0 \\ 0 & 0 & 0 & 0 & 0 & -r_G \end{bmatrix} \tag{3.96}$$

The matrix ${g(\bar{x})^{PMSG}} {g(\bar{x})^{PMSG}}^\top$ is the same as 3.76. Inserting 3.96 and 3.76 into 3.95 yields the matrix below:

$$\begin{bmatrix} -2(r+\gamma\bar{V}_c^2) & 0 & \bar{i}_q \frac{P}{2}L & 2\gamma\bar{i}_d\bar{V}_c & 0 & 0 \\ 0 & -2(r+\gamma\bar{V}_c^2) & -\bar{i}_d \frac{P}{2}L & 2\gamma\bar{i}_q\bar{V}_c & 0 & 0 \\ \bar{i}_q \frac{P}{2}L & -\bar{i}_d \frac{P}{2}L & -2d + 2\frac{\partial T_m(\omega_m)}{\partial \omega_m} & 0 & 0 & 0 \\ 2\gamma\bar{i}_d\bar{V}_c & 2\gamma\bar{i}_q\bar{V}_c & 0 & -2\left(G + \gamma(\bar{i}_d^2 + \bar{i}_q^2)\right) & 0 & 0 \\ 0 & 0 & 0 & 0 & -2r_G & 0 \\ 0 & 0 & 0 & 0 & 0 & -2r_G \end{bmatrix} \leq 0 \tag{3.97}$$

As before $\bar{i}_d = 0$, which simplifies 3.97 to:

$$\begin{bmatrix} -2(r+\gamma\bar{V}_c^2) & 0 & \bar{i}_q\frac{P}{2}L & 0 & 0 & 0 \\ 0 & -2(r+\gamma\bar{V}_c^2) & 0 & 2\gamma\bar{i}_q\bar{V}_c & 0 & 0 \\ \bar{i}_q\frac{P}{2}L & 0 & -2d+2\frac{\partial T_m(\omega_m)}{\partial\omega_m} & 0 & 0 & 0 \\ 0 & 2\gamma\bar{i}_q\bar{V}_c & 0 & -2\left(G+\gamma\bar{i}_q^2\right) & 0 & 0 \\ 0 & 0 & 0 & 0 & -2r_G & 0 \\ 0 & 0 & 0 & 0 & 0 & -2r_G \end{bmatrix} \leq 0 \tag{3.98}$$

To check if 3.98 is negative semi-definite, the Schur complement method is used. The submatrices are chosen as follows:

$$A = \begin{bmatrix} 2(r+\gamma\bar{V}_c^2) & 0 & -\bar{i}_q\frac{P}{2}L & 0 \\ 0 & 2(r+\gamma\bar{V}_c^2) & 0 & -2\gamma\bar{i}_q\bar{V}_c \\ -\bar{i}_q\frac{P}{2}L & 0 & 2d-2\frac{\partial T_m(\omega_m)}{\partial\omega_m} & 0 \\ 0 & -2\gamma\bar{i}_q\bar{V}_c & 0 & 2\left(G+\gamma\bar{i}_q^2\right) \end{bmatrix} \tag{3.99}$$

$$B^\top = \begin{bmatrix} 0 & 0 & 0 & 0 \\ 0 & 0 & 0 & 0 \end{bmatrix} \tag{3.100}$$

$$C = \begin{bmatrix} 2r_G & 0 \\ 0 & 2r_G \end{bmatrix} \tag{3.101}$$

For (3.98) to be negative definite, we require 3.99 to be positive definite which again can be investigated using the Schur complement. The sub-matrices of A are in turn chosen as follows:

$$A_1 = \begin{bmatrix} 2(r+\gamma\bar{V}_c^2) & 0 \\ 0 & 2(r+\gamma\bar{V}_c^2) \end{bmatrix} \tag{3.102}$$

$$B_2 = \begin{bmatrix} -\bar{i}_q\frac{P}{2}L & 0 \\ 0 & -2\gamma\bar{i}_q\bar{V}_c \end{bmatrix} = B_2^\top \tag{3.103}$$

$$C_1 = \begin{bmatrix} 2d-2\frac{\partial T_m(\omega_m)}{\partial\omega_m} & 0 \\ 0 & 2\left(G+\gamma\bar{i}_q^2\right) \end{bmatrix} \tag{3.104}$$

The Schur compliment for 3.99 yields:

$$\begin{aligned} \frac{X_1}{A_1} &= C_1 - B_1^\top A_1^{-1} B_1 \\ &= \begin{bmatrix} 2d-2\frac{\partial T_m(\omega_m)}{\partial\omega_m} & 0 \\ 0 & 2\left(G+\gamma\bar{i}_q^2\right) \end{bmatrix} - \begin{bmatrix} -\bar{i}_q\frac{P}{2}L & 0 \\ 0 & -2\gamma\bar{i}_q\bar{V}_c \end{bmatrix} \begin{bmatrix} \frac{1}{2(r+\gamma\bar{V}_c^2)} & 0 \\ 0 & \frac{1}{2(r+\gamma\bar{V}_c^2)} \end{bmatrix} \begin{bmatrix} -\bar{i}_q\frac{P}{2}L & 0 \\ 0 & -2\gamma\bar{i}_q\bar{V}_c \end{bmatrix} \\ &= \begin{bmatrix} 2d-2\frac{\partial T_m(\omega_m)}{\partial\omega_m} & 0 \\ 0 & 2\left(G+\gamma\bar{i}_q^2\right) \end{bmatrix} - \begin{bmatrix} \frac{\left(\bar{i}_q\frac{P}{2}L\right)^2}{2(r+\gamma\bar{V}_c^2)} & 0 \\ 0 & \frac{\left(2\gamma\bar{i}_q\bar{V}_c\right)}{2(r+\gamma\bar{V}_c^2)} \end{bmatrix} \\ &= \begin{bmatrix} 2d-2\frac{\partial T_m(\omega_m)}{\partial\omega_m} - \frac{\left(\bar{i}_q\frac{P}{2}L\right)^2}{2(r+\gamma\bar{V}_c^2)} & 0 \\ 0 & 2\left(G+\gamma\bar{i}_q^2\right) - \frac{\left(2\gamma\bar{i}_q\bar{V}_c\right)}{2(r+\gamma\bar{V}_c^2)} \end{bmatrix} \end{aligned} \tag{3.105}$$

The matrix 3.105 is positive definite if the two diagonal terms are positive. This yields two criteria:

$$2d-2\frac{\partial T_m(\omega_m)}{\partial\omega_m} - \frac{\left(\bar{i}_q\frac{P}{2}L\right)^2}{2(r+\gamma\bar{V}_c^2)} \geq 0 \tag{3.106}$$

$$2\left(G+\gamma\bar{i}_q^2\right) - \frac{\left(2\gamma\bar{i}_q\bar{V}_c\right)}{2(r+\gamma\bar{V}_c^2)} \geq 0 \tag{3.107}$$

The criterion 3.106 is the same as found in specialization project when the converter was modeled as a constant voltage source.–see 2.12 for comparison– 3.106 is the design criterion for the PMSG

as the damping must be higher than the derivative of the torque. The third term of 3.106 can be potentially neglected when γ is chosen high enough. The criterion 3.107 is the same as 3.48, and is shown to be positive for $\gamma \geq 0$. If criteria 3.106 and 3.107 are satisfied, and matrix A_1 is positive definite –a prerequisite for using the Schur complement– then matrix 3.99 is positive definite . Matrix A_1 is positive definite when $\gamma > 0$, which is the case when 3.107 is satisfied. When these are satisfied, the Schur compliment for 3.98 yields:

$$\begin{aligned} -X &= \begin{bmatrix} A & B \\ B^\top & C \end{bmatrix} \\ \frac{-X}{A} &= C - B^\top A^{-1} B = \begin{bmatrix} 2r_G & 0 \\ 0 & 2r_G \end{bmatrix} > 0 \end{aligned} \tag{3.108}$$

The negative of matrix 3.98 is positive definite, which is equivalent to 3.98 being negative definite. By satisfying criteria 3.106 and 3.107, the term $\left[M(z) - M(\bar{z}) - \gamma g(\bar{x})^{PMSG} g(\bar{x})^{PMSG^\top}(z - \bar{z})\right]$ is monotonically decreasing and consequently 3.93 can be formulated as:

$$\dot{\mathcal{V}}(x) \leq y^\top \widetilde{u} + y^{PMSG^\top} \gamma y^{PMSG} \tag{3.109}$$

As in section 3.2, a P(I) controller can be designed with $K_p > \gamma$ which results in condition IV for the LCF being satisfied. In section 3.2, it is shown that condition III for a Lyapunov function is satisfied for the choice of the LCF that is done in this section. The system is therefore guaranteed to be stable when 3.106 and 3.107 are satisfied and $K_p > \gamma$.

3.3.2 Conclusion

In this section, it is shown that the inclusion of the nonlinear dynamics of the mechanical torque modifies the stability criteria for the system. It is criterion 3.106 that is of the most significant importance as criterion 3.107 is satisfied when $\gamma > 0$. Comparing 3.106 with the criterion found in the specialization project -chapter 2-, it is apparent that the only difference is in the denominator of the third term.

$$\begin{aligned} \text{Back-to-back converter}: \quad & 2d - 2\frac{\partial T_m(\omega_m)}{\partial \omega_m} - \frac{\left(\bar{i}_q \frac{P}{2} L\right)^2}{2(r + \gamma \bar{V}_c^2)} \geq 0 \\ \text{Constant voltage source}: \quad & 2d - 2\frac{\partial T_m(\omega_m)}{\partial \omega_m} - \frac{\left(\bar{i}_q \frac{P}{2} L\right)^2}{2(r + \gamma)} \geq 0 \end{aligned}$$

Moreover, γ is a constant that is proportional to the minimum gain of K_p of the controllers. By sufficiently increasing γ, the third term can be neglected. The damping in the generator can then be designed to ensure stability by calculating a worst-case scenario for the second term in the criterion. A result of this is that the stability of the WECS can be guaranteed when designing the damping of the generator. *Thus, feedback controllers can be used to help stabilize the system but cannot guarantee stability due to the non-linear behavior of the mechanical torque.* In the specialization project, the term $\frac{\partial T(\omega_m)}{\partial \omega_m}$ was investigated further, and it was found that when the angular velocity was close to the operating point, the contribution from the mechanical torque does not cause issues to the stability. It is during acceleration that the greatest damping is demanded to guarantee stability and is what the damping should be ideally designed for. This is visualized in Figure 2.2. A suggested method for calculating the damping and how it could be designed too meet the requirement is presented in the next section.

In conclusion, stability can be guaranteed by satisfying criteria 3.106 and 3.107. These are a design criterion and a tuning criterion.

3.3.3 The Damping Coefficient d

The damping coefficient d represents electromechanical damping due to damper windings on the rotor in the generator. The damper windings have multiple purposes in a synchronous machine. The most important is to suppress hunting and damp oscillations caused by aperiodic shocks due to short circuits or switching [34]. How damper windings work can be briefly explained as follows. When the rotor rotates at speed different from the speed of the rotating magnetic field put up by the currents flowing in the stator, then the damper windings will experience a changing magnetic field which will induce currents in the damper windings. The current-carrying damper windings will then experience a torque according to Lenz law. The torque will pull the rotor towards the synchronous speed of the magnetic field put up by the stator currents. The damper windings will speed up the rotor if the rotor is lagging the synchronous speed and slow the rotor down if the rotor is rotating too fast.

The *stability certificate* developed in this chapter heavily relies on the value of the damping, as can be seen in 3.106. If the stability is to be guaranteed, the damping must be higher than the partial derivative of the torque with respect to the angular velocity. It is therefore of great significance to be able to calculate the damping for the PMSG. A comparison of different methods for estimating the damping coefficient C_D for different types of synchronous machines is carried out in [35]. The coefficient C_D is linked to the damping coefficient d used in this thesis through the relation:

$$C_D = \frac{\frac{P}{2} \cdot d}{T_r} \tag{3.110}$$

where T_r is the rated torque for the electrical machine. One of the methods for calculating the damping d is found in [36]:

$$d \approx \frac{mV_t^2}{\frac{P}{2}\omega_m^2 R_d} \tag{3.111}$$

where m is the number of phases, V_t is the terminal line to ground voltage, P is the number of poles, ω_m is the angular velocity, and R_d is the damper resistance. Using this formula, the damping can be expressed as a function of the resistance in the damper windings. From 3.111, it is clear that a lower resistance in the damper windings will increase the damping effect. This can, for instance, be achieved by using thicker conductors. By calculating the worst-case scenario for the partial derivative of the mechanical torque with respect to the angular velocity, the required resistance, or rather, the conductance in the damper windings, can be calculated.

Whether 3.111 is a reasonable estimation of the damping or not is not investigated further in this thesis but is a topic for future work.

End note

In this chapter stability criteria for a wind energy conversion system with full scale back-to-back 2L-VSC including the non-linear dynamics of the wind, has been found. However, it is not yet shown that a equilibrium can be found, or how the passivity based control structure is implemented to ensure stability or how the control performance will be. These topics will be investigated in the next chapter.

Chapter 4

Control of Wind Turbine and Simulation

With a theoretical stability certificate in place, the next step is to implement the stability certificate in a WECS and run simulations to validate it. It is also of great interest to look at the performance of the WECS with the stability certificate implemented and compare it to traditional PI-current control. Firstly, it is looked at how a WECS is controlled and if an equilibrium point actually can be found.

4.1 Control of a Wind Turbine

Power electronics have made it possible to connect generators and motors to the power grid without the electrical machines running at synchronous speed. The speed and power of the machine can be fully controlled through converters such as a 2L-VSC with cascaded control structures. The advantage is that the machines can be controlled at the desired speed and optimal efficiency. On the other hand, the disadvantage is that inertia in the machines cannot be relied on for stability regulation in the power system through the converter connection.

4.1.1 Control Objectives

The wind energy conversion system consists of a PMSG and two 2L-VSC. Each 2L-VSC has two degrees of freedom, meaning they can have two control objectives each.

Speed control

The speed of rotation for a wind turbine should be controlled according to the torque-speed characteristic [37]. In short, this means that the speed of the turbine should follow the speed of the wind such that maximum torque is generated. A control objective is, therefore, to make the speed of the rotor follow a reference calculated based on the torque-speed characteristic of the wind turbine.

Maximum torque per Ampere

The system equations are on the time-invariant dq-format, which is achieved by using a rotating reference frame[38]. For the generator, the reference used is the rotor flux which is defined as the direct axis (d-axis). The force produced is the cross product between the current and the magnetic field, according to the Lorentz force law [39]. The maximum force is produced when the current is 90 degrees shifted relative to the rotor flux. Current in the d-axis will not contribute to generating torque, as the cross product between current and magnetic field is zero when they are in phase. The maximum torque per ampere is therefore achieved when all the current is in the q-axis, and the d-current component is zero [40]. To keep the d-axis current zero is the second control objective for the generator-connected VSC.

DC-link voltage

For a voltage source converter to operate, the voltage on the DC-side must be more than double the peak voltage of the AC-voltage [41]. When it is assumed that the converter is synchronized with the grid voltage, it can be shown that the DC-link voltage can be controlled by using the d-current component[42]. To have the VSC operating as desired, regulating the DC-link voltage to the desired value becomes the first control objective of the grid-connected VSC.

Reactive power transfer

To control the reactive power flow to the grid, the quadrature axis (q-axis) current is used. It is assumed that the q-component of the voltage is zero, $v_q = 0$. The apparent power can be expressed as:

$$\begin{aligned} s &= \underbrace{v_d \cdot i_d + v_q \cdot i_q}_{P} + j\,\underbrace{(-v_d \cdot i_q + v_q \cdot i_d)}_{Q} \\ s &= \underbrace{v_d \cdot i_d}_{P} - j\,\underbrace{v_d \cdot i_q}_{Q} \end{aligned} \tag{4.1}$$

4.1 shows that the q-axis component of the current is controlling the reactive power transferred to the grid. This is the second control objective for the grid-connected VSC.

The main objective of an offshore wind park is to deliver power to the mainland, however, delilvering reactive power is also important to sustain satisfacotry power quality [43]. As wind power is becoming an increasing participant in power production, it is reasonable for wind parks to also provide ancillary services. [44]. To accurately keep the voltage at the correct level, continuous and fast interventions need to take place. The type 4 WTG can provide this due to the pulse-width-modulation control [44], [45] and can deliver or consume reactive power to sustain the desired voltage level.

4.1.2 Equilibrium Calculation

For a stability analysis to be relevant, there must exist an equilibrium point for the system. This section shows that an equilibrium point for the system exists and how it is calculated. The system equations defining the system shown in Figure 4.1 are shown in section 3.2, but are repeated here for convenience:

$$L\dot{i}_d = -ri_d + Li_q\frac{P}{2}\omega_m - u_1V_c \tag{4.2}$$

$$L\dot{i}_q = -ri_q - Li_d\frac{P}{2}\omega_m + \phi\frac{P}{2}\omega_m - u_2V_c \tag{4.3}$$

$$J\dot{\omega}_m = T_m - \frac{P}{2}\phi i_q + d(\omega_{ref} - \omega_m) \tag{4.4}$$

$$C\dot{V}_c = u_1i_d + u_2i_q - u_3i_d^G - u_4i_q^G - GV_c \tag{4.5}$$

$$L_G\dot{i}_d^G = -r_Gi_d^G + \omega_GL_Gi_q^G + u_3V_c - V_d^G \tag{4.6}$$

$$L_G\dot{i}_q^G = -r_Gi_q^G - \omega_GL_Gi_d^G + u_4V_c - V_q^G \tag{4.7}$$

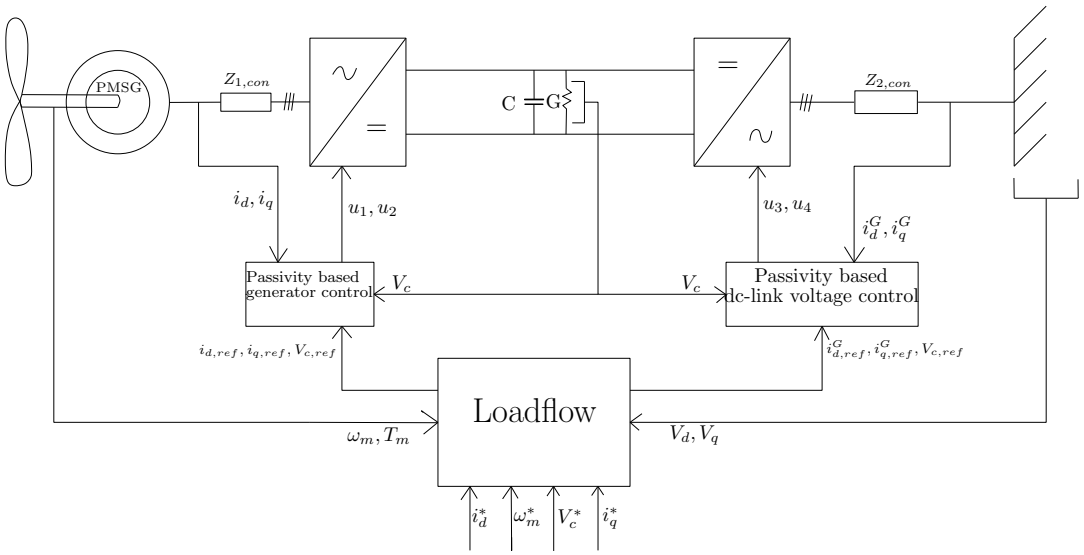

Figure 4.1: Control structure of a wind energy conversion system with two passivity-based controllers

The system has six coenergy variables ($i_d, i_q, \omega_m, V_c, i_d^G, i_q^G$), four control variables (u_1, u_2, u_3, u_4) and four known inputs $T_m, \omega_{ref}, V_d^G, V_q^G$. In the previous section, the four control objectives are described and are assumed to be achieved when calculating an equilibrium point for the system. At the equilibrium, four coenergy variables are already known along with the four inputs to the system. Using the above six listed system equations, the missing two coenergy variables and the four control variables can be calculated for the system.

Known coenergy variables		Known inputs	
d-axis current PMSG	$\bar{i}_d$	Mechanical torque	T_m
Angular velocity	$\bar{\omega}_m$	Angular velocity reference	ω_{ref}
DC-link voltage	$\bar{V}_c$	d-axix grid voltage	V_d^G
q-axis current Grid	$\bar{i}_q^G$	q-axis grid voltage	V_q^G

Table 4.1: Known coenergy variables and inputs at the equilibrium

At the equilibrium point, the left side of the system equations is all zero as the system is in a

steady state. ($\frac{\partial x}{\partial t} = 0$).

$\bar{i}_q$, q-axis current in the PMSG

4.4 can be used to calculate steady state q-axis current component in the PMSG. At the equilibrium, the angular velocity is equal to the reference ($\bar{\omega}_m = \omega_{ref}$).

$$\bar{i}_q = \frac{T_m}{\frac{P}{2}\phi} \tag{4.8}$$

i_d^G, d-axis current component in the grid connection

To obtain the steady-state expression for the d-axis current component in the grid connection, multiple of the system equations must be combined. Another approach is to use power conservation to find the expression, and is what is done in this thesis. Ultimately the two approaches give the same expression of the d-axis current, which is as expected.

$$\underbrace{T_m\omega_m}_{P_{in}} = \underbrace{i_d^G V_d^G + i_q^G V_q^G}_{P_{out}} + \underbrace{r(i_d^2 + i_q^2) + GV_c^2 + r_G({i_d^G}^2 + {i_q^G}^2)}_{P_{loss}} \tag{4.9}$$

Solving 4.9 for i_d^G, the d-axis current in the grid-side converter at steady state yields:

$$\bar{i}_d^G = \frac{-V_d^G}{2r_G} + \frac{1}{2r_G}\sqrt{{V_d^G}^2 - 4r_G\left(\bar{i}_q^G V_q^G + r_G{\bar{i}_q^G}^2 + G\bar{V}_c^2 + r(\bar{i}_d^2 + \bar{i}_q^2) - T_m\bar{\omega}_m\right)} \tag{4.10}$$

For the equilibrium point to exist, the term inside the square-root need to be positive.

$${V_d^G}^2 - 4r_G\left(\bar{i}_q^G V_q^G + r_G{\bar{i}_q^G}^2 + G\bar{V}_c^2 + r(\bar{i}_d^2 + \bar{i}_q^2) - T_m\bar{\omega}_m\right) > 0 \tag{4.11}$$

By taking a closer look at the terms, they can be sorted as follows:

$$\underbrace{T_m\bar{\omega}_m}_{P_{in}} - \underbrace{\bar{i}_q^G V_q^G}_{P^*_{out}} - \underbrace{r_G{\bar{i}_q^G}^2 + G\bar{V}_c^2 + r(\bar{i}_d^2 + \bar{i}_q^2)}_{P^*_{loss}} + \underbrace{\frac{{V_d^G}^2}{4r_G}}_{\hat{P}} > 0 \tag{4.12}$$

where

$$P^*_{out} = 0, V_d^G = 0 \text{ due to SRF}^1$$
$$P^*_{loss} < P_{loss}$$

Thereby the conditions for an equilibrium to exist can be rewritten as:

$$\underbrace{P_{in} + \hat{P}}_{>P_{in}} > P^*_{loss} \tag{4.13}$$

Condition 4.13 says a term that is larger than the power input to the system must be greater than a term smaller than the loss in the system. This is satisfied for all physically possible operating conditions for the system. Therefore, an equilibrium point can be found for all possible working conditions for the system.

[1] It is assumed that the synchronous reference is used where the d-axis is aligned with the voltage vector. The q-axis component of the voltage is thereby zero.

u_1, control variable 1

u_1 can be interpreted as the duty cycle for the d-axis components for the generator connected voltage source converter using pulse width modulation (PWM). The control variable can take values in the interval $u_1 \in [-\frac{1}{2}, \frac{1}{2}]$. 4.2 can be used to calculate u_1

$$u_1 = \frac{-r\bar{i}_d + L\frac{P}{2}\bar{\omega}_m\bar{i}_q}{\bar{V}_c} \tag{4.14}$$

u_2, control variable 2

Similarly to u_1, u_2 can be interpreted as the duty cycle for the q-axis components for the generator connected voltage source converter using PWM. The control variable can take values in the interval $u_2 \in [-\frac{1}{2}, \frac{1}{2}]$. 4.3 can be used to calculate u_2

$$u_2 = \frac{-r\bar{i}_q - L\bar{i}_d\frac{P}{2}\bar{\omega}_m + \phi\frac{P}{2}\bar{\omega}_m}{\bar{V}_c} \tag{4.15}$$

u_3, control variable 3

u_3 can be interpreted as the duty cycle for the d-axis components for the grid-connected voltage source converter using PWM. The control variable can take values in the interval $u_3 \in [-\frac{1}{2}, \frac{1}{2}]$. 4.5 can be used to calculate u_3. In 4.5 the three other control variables are included and must therefore be calculated last. It is possible to find an expression for u_3 that only consists of coenergy variables and inputs. However, this expression is more complex, so it is decided to include only the expression below.

$$u_3 = \frac{u_1\bar{i}_d + u_2\bar{i}_q - G\bar{V}_c - u_4\bar{i}_q^G}{\bar{i}_d^G} \tag{4.16}$$

u_4, control variable 4

u_4 can be interpreted as the duty cycle for the q-axis component for the grid connected voltage source converter using PWM. The control variable can take values in the interval $u_4 \in [-\frac{1}{2}, \frac{1}{2}]$. 4.7 can be used to calculate u_4.

$$u_4 = \frac{r_g\bar{i}_q^G + \omega_G L_G\bar{i}_d^G + V_q^G}{\bar{V}_c} \tag{4.17}$$

Using the expressions above, all the coenergy and control variables can be calculated at the equilibrium point. PBCs will calculate the control variables when implementing the control structure in a wind energy conversion system. The passivity-based control is briefly explained in the next subsection, along with how they are designed for the back-to-back wind energy conversion systems shown in Figure 4.1.

4.1.3 P(I) Passivity-based Control Implementation

Passivity-based control, as introduced in section 1.3 exploits the physical structure of a system and renders the closed loop passive with respect to some suitable storage function [19]. The aim of this subsection is, therefore, to design a control system that will result in a suitable LCF to ensure stability.

In section 3.2, y, the passive output of the system is defined as

$$y = g(\bar{x})^\top Q\widetilde{x} \tag{4.18}$$

where

$$g(\bar{x})^\top = \begin{bmatrix} -\bar{V}_c & 0 & 0 & \bar{i}_d & 0 & 0 \\ 0 & -\bar{V}_c & 0 & \bar{i}_q & 0 & 0 \\ 0 & 0 & 0 & -\bar{i}_d^G & \bar{V}_c & 0 \\ 0 & 0 & 0 & -\bar{i}_q^G & 0 & \bar{V}_c \end{bmatrix}$$

The passive output of the system entering the PBC will then become:

$$y = g(\bar{x})^\top Q\widetilde{x}$$

$$y = \begin{bmatrix} -\bar{V}_c & 0 & 0 & \bar{i}_d & 0 & 0 \\ 0 & -\bar{V}_c & 0 & \bar{i}_q & 0 & 0 \\ 0 & 0 & 0 & -\bar{i}_d^G & \bar{V}_c & 0 \\ 0 & 0 & 0 & -\bar{i}_q^G & 0 & \bar{V}_c \end{bmatrix} \begin{bmatrix} \widetilde{i}_d \\ \widetilde{i}_q \\ \widetilde{\omega} \\ \widetilde{V}_c \\ \widetilde{i}_d^G \\ \widetilde{i}_q^G \end{bmatrix}$$

$$y = \begin{bmatrix} -\bar{V}_c\widetilde{i}_d + \widetilde{V}_c\bar{i}_d \\ -\bar{V}_c\widetilde{i}_q + \widetilde{V}_c\bar{i}_q \\ -\bar{i}_d^G\widetilde{V}_c + \bar{V}_c\widetilde{i}_d^G \\ -\bar{i}_q^G\widetilde{V}_c + \bar{V}_c\widetilde{i}_q^G \end{bmatrix} = \begin{bmatrix} -\bar{V}_c(i_d - \bar{i}_d) + \bar{i}_d(V_c - \bar{V}_c) \\ -\bar{V}_c(i_q - \bar{i}_q) + \bar{i}_q(V_c - \bar{V}_c) \\ -\bar{i}_d^G(V_c - \bar{V}_c) + \bar{V}_c(i_d^G - \bar{i}_d^G) \\ -\bar{i}_q^G(V_c - \bar{V}_c) + \bar{V}_c(i_q^G - \bar{i}_q^G) \end{bmatrix}$$

Simplifying yields the final expression:

$$y = \begin{bmatrix} -i_d\bar{V}_c + \bar{i}_dV_c \\ -i_q\bar{V}_c + \bar{i}_qV_c \\ -\bar{i}_d^GV_c + i_d^G\bar{V}_c \\ -\bar{i}_q^GV_c + i_q^G\bar{V}_c \end{bmatrix} \tag{4.19}$$

The passive output from the system is chosen as the input to the controllers in the closed loop, $u = -K_p y + \bar{u}$.

$$u = -\begin{bmatrix} K_d^{PMSG} & 0 & 0 & 0 \\ 0 & K_q^{PMSG} & 0 & 0 \\ 0 & 0 & K_d^G & 0 \\ 0 & 0 & 0 & K_q^G \end{bmatrix} \begin{bmatrix} -i_d\bar{V}_c + \bar{i}_dV_c \\ -i_q\bar{V}_c + \bar{i}_qV_c \\ -\bar{i}_d^GV_c + i_d^G\bar{V}_c \\ -\bar{i}_q^GV_c + i_q^G\bar{V}_c \end{bmatrix} = \begin{bmatrix} K_d^{PMSG}\left(-i_d\bar{V}_c + \bar{i}_dV_c\right) \\ K_q^{PMSG}\left(-i_q\bar{V}_c + \bar{i}_qV_c\right) \\ K_d^G\left(-\bar{i}_d^GV_c + i_d^G\bar{V}_c\right) \\ K_q^G\left(-\bar{i}_q^GV_c + i_q^G\bar{V}_c\right) \end{bmatrix} = \begin{bmatrix} u_1 \\ u_2 \\ u_3 \\ u_4 \end{bmatrix} \tag{4.20}$$

Equation 4.20 shows the output from the P(I)-PBCs, which is the input to the converters.

It hast been shown that a equilibrium point can be found for any realistic operating conditions, and it is shown how the PBCs are designed and implemented. The next step is to simulate the WECS in Matlab/Simulink to investigate the stability criterias validity and performance.

4.2 Simulation

To support the mathematical proofs found in the previous chapter, simulations are conducted to validate the stability criteria. The simulations are done for the full back-to-back system.

As explained in subsection 4.1.2, for a stability analysis to be of any use, there must exist an equilibrium point the system can obtain. Calculating the equilibrium point requires a perfect system model and therefore has some drawbacks in real-world applications. The constant recalculation of the equilibrium point due to the ever-changing nature of the wind makes it less robust. Therefore, other solutions to cope with rapid changes should be investigated, therefore simulations done without and with outer loops are presented.

In the simulations, a constant wind speed is assumed for simplicity. The controllers dynamics are assumed to be sufficiently faster than the winds, and thereby the input to the control loops will be seen as constant regardless of a time-varying wind input. This simplification was done to ease the models implementation and reduce the computational processing power necessary since a rapidly changing wind input demands an almost constant recalculation of the equilibrium points. Due to the fact that we are only concerned about stability and not performance, a time-varying wind input is of less importance.

The choice of parameters are based on the wind energy conversion system investigated in [15] and are listed in Table 4.2

Item	**Symbol**	**Nominal value**
Inertia	J	7.856 $[kgm^2]$
Poles	P	28
Synchronous resistance	r	0.3676 $[\Omega]$
Synchronous inductance	L	3.55 $[mH]$
Permanent magnet flux	ϕ	0.2867 $[Wb]$
Damping	d	0.5 $[\frac{Nm}{rad/s}]$
d-axis current	$\tilde{i}_d$	0 $[A]$
Mechanical torque	T_m	200 $[Nm]$
Mechanical angular velocity	ω_m	200 $[rpm]$
DC-link conductance	G	10 $[\mu S]$
DC-link capacitance	C	3.3 $[mF]$
DC-link voltage	V_c	660 $[V]$
Grid resistance	r_G	0.2$[\Omega]$
Grid inductance	L_G	2 $[mH]$
Grid angular frequency	ω_G	$2\pi \cdot 50[\frac{rad}{s}]$
Gird q-axis current	i_q^G	2 $[A]$
Grid d-axis voltage	V_d^G	$230\sqrt{2}$ $[V]$
Grid q-axis voltage	V_q^G	0 $[V]$

Table 4.2: Model parameters and input values for the simulation

Some of the values in Table 4.2 are not found in [15], as the system in that paper does not include a second converter and a grid connection. The grid in this section is modeled as a stiff voltage source in a synchronous reference frame such that the q-axis voltage component is zero, $V_q^G = 0$ [V]. The value for the d-axis voltage component is set to $\sqrt{2} \cdot 230$[V] as it is assumed that the grid has rms-voltage of 230[V]. The grid frequency is 50 [Hz]. The DC-link voltage is set to 660[V] as this is more than double the peak grid voltage, as is required. The conductance G is assumed to be small, as it is assumed that the losses in the converter are quite small. The grid resistance and inductance are assumed to be small and are chosen as 0.2[Ω] and 2 [mH], respectively. It is assumed that at the time of simulation, it is required that reactive power must be supplied to the grid. i_q^G is therefore set to 2 [A]. The wind turbine has a nominal power of 5 [kVA]. It is assumed that the wind conditions during simulation cause the power to be below this rating. The mechanical torque generated by the turbine blades is assumed to be 200 [Nm], and the angular velocity is 200 [rpm], which constitutes a power of 4.19 [kW]

4.2.1 Implementation of the *Stability Certificate*

The first scenario that is simulated is testing the hypothesis from section 3.2,"*Only using the converter closest to the PMSG is enough to compensate for the lack of monotonicity inherent to the machine, and thus to render the rest of the system passive.*". Therefore, we only implement a passivity-based controller for the generator-connected converter–while, for simplicity, we begin by operating the second VSC under open-loop control.– Indeed, this is not a very realistic scenario as there would be closed-loop controllers on both converters in practical applications. The reasoning for doing this preliminary study is to show that we can guarantee stability with the minimum amount of feedback possible and at the *earliest* point possible. This is practical for designing the rest of the system, as it can be optimized for performance knowing the system is guaranteed to be stable. The values for control variable 3 and 4 (u_3 and u_4) are calculated as shown in subsection 4.1.2 and are fed directly into the grid-side converter.

Criterion 3.106 and 3.107 needs to be fulfilled to guarantee the system to be stable. Criterion 3.107 is satisfied as long K_p is chosen to be positive. Solving criterion 3.106 for γ yields:

$$2d - \frac{(\bar{i}_q \frac{P}{2} L)^2}{2(r + \gamma \bar{V}_c^2)} \geq 0$$

$$\gamma \geq \frac{(\bar{i}_q \frac{P}{2} L)^2 - 4dr}{4d\bar{V}_c^2}$$

$\bar{i}_q$ is calculated with the help of the swing equation

$$\begin{aligned} J\dot{\bar{\omega}}_m &= T_m - \frac{P}{2}\phi\bar{i}_q \\ \bar{i}_q &= \frac{T_m}{\frac{P}{2}\phi} \\ \bar{i}_q &= \frac{200}{\frac{28}{2} \cdot 0.2867} \\ \bar{i}_q &= 48.828A \end{aligned}$$

γ then becomes

$$\gamma \geq \frac{(48.828 \cdot \frac{28}{2} \cdot 3.55 \cdot 10^{-3})^2 - 4 \cdot 0.5 \cdot 0.3676}{4 \cdot 0.5 \cdot 660^2}$$

$$\gamma \geq 6.1956 \cdot 10^{-6}$$

$K_p > 6.1956 \cdot 10^{-6}$ is therefore needed to render the rest of the system passive and subsequently to guarantee stability.

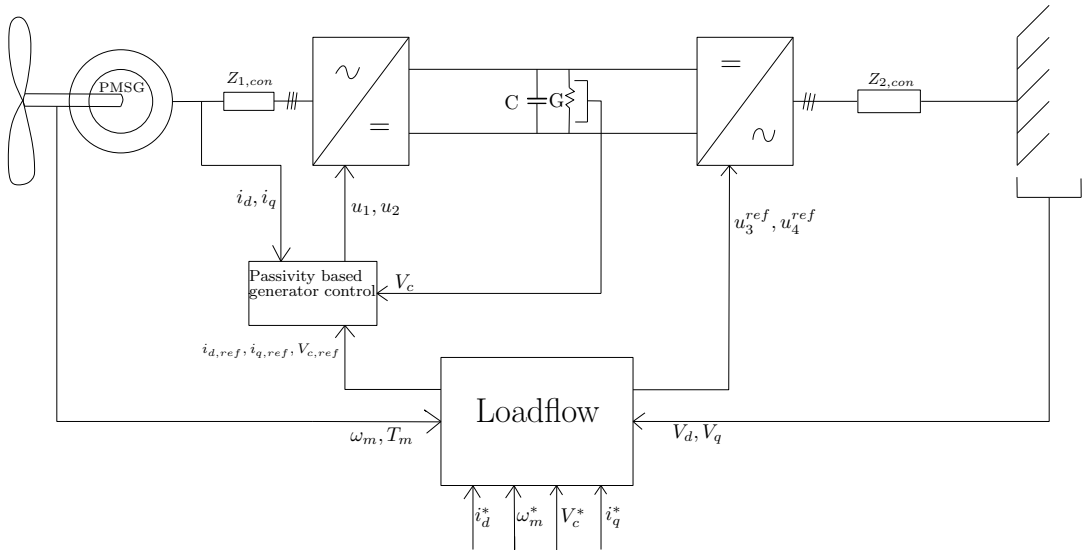

Figure 4.2: Control structure of a wind energy conversion system without outer loops and one passivity-based controller

Passivity-based controller for only machine-side converter

The following simulation, depicted in Figure 4.3, shows how the tuning of the passivity-based controller can make a system preserve its stability after a disturbance. A step in torque input and a step in angular velocity happen at $t = 30$ [s]. Simulation results are presented without and with the fulfillment of the stability criteria Equation 3.79.

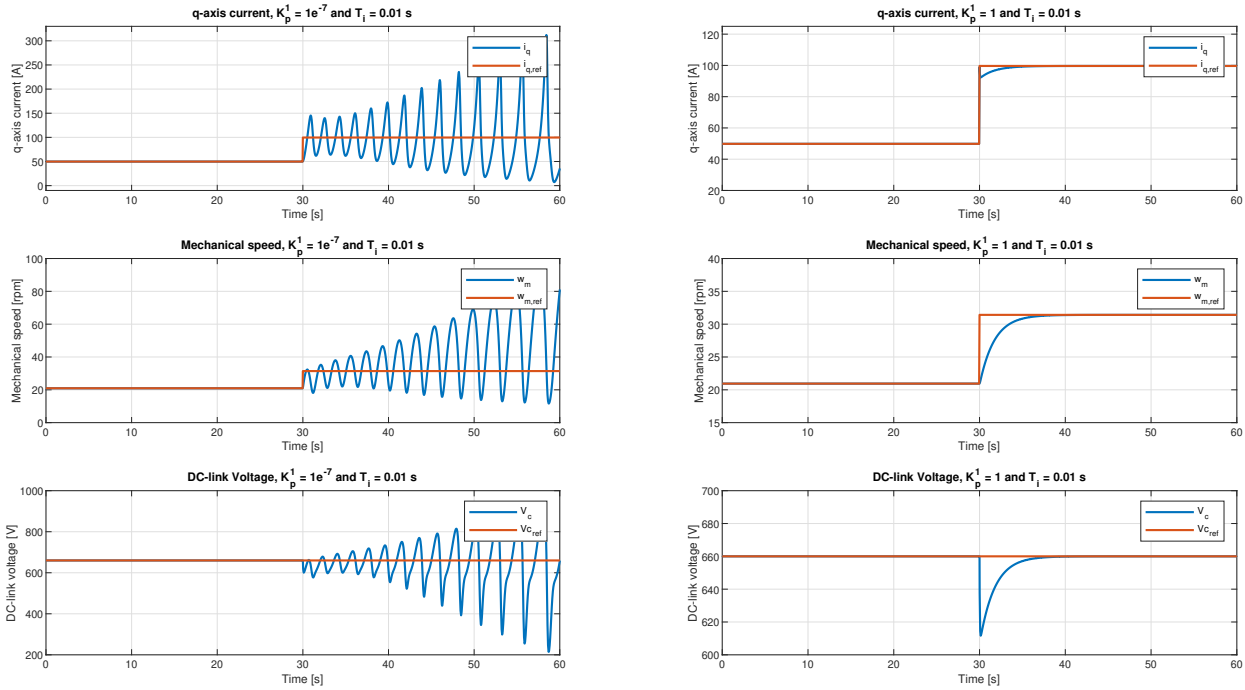

Figure 4.3: Initially the system is stable, and then a step in torque input and angular velocity happens at t = 30 [s]. When $K_p = 1e^{-7} < \gamma$ [left], the system becomes unstable. When $K_p = 1 > \gamma$ [right], the step does not affect the stability of the system.

A clear difference in system behavior is noticed. With $K_p < \gamma$, a step in torque and angular velocity make the system unstable, while with $K_p > \gamma$, the stability of the system is preserved regardless of the disturbances. This is in line with the stability certificate, which guarantees stability for the system when criteria 3.79 is satisfied. The simulation case was based on the fact that an increase in wind speed will affect the blades' mechanical torque and the angular velocity. The wind speeds are constantly changing, so a sudden increase in wind speed or direction must be considered when studying wind turbines' stability.

The *stability certificate* ensure that the passivity-based controller is guaranteed to render the system stable. On the other hand, the *stability criteria* do not disclose what happens when the gain is selected to be smaller than γ, meaning when the criteria is not satisfied. The system could be unstable but also stable. A simulation was done to demonstrate this. A step in the torque input was applied at $t = 30s$. The gain is chosen to be $K_p = 1 \cdot 10^{-7}$, which is less than the gain needed to render the system passive according to criterion 3.79.

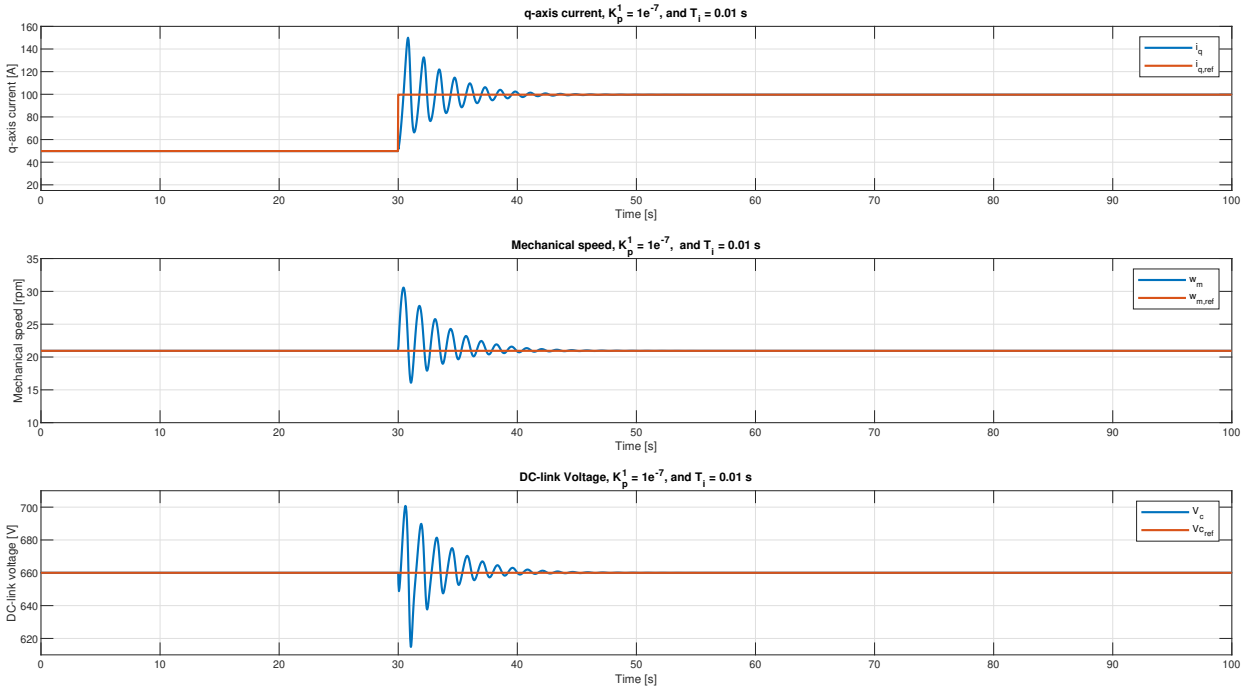

Figure 4.4: Step in torque input happens at t = 30 [s]. With $K_p = 1e^{-7} < \gamma$, the system preserves its stability regardless of the stability criterion 3.79 not being fulfilled.

From Figure 4.4, it is clear that the system is stable, even though K_p is chosen to be less than the calculated value of γ. There are some oscillations after the step, but the system's overall stability is preserved.

Passivity-based controllers for both converters

In the next simulations, both PBCs are included based on P(I) regulators, see Figure 4.1. The control variables u_1, u_2, u_3 and u_4 are calculated in the closed loop passivity-based controllers, as opposed to the previous case where, u_3 and u_4 were constant values from the load flow calculation. The purpose of this simulation is to investigate if the stability of the system is affected by the tuning of the PBCs for the two converters. The previous section validated that stability can be achieved by satisfying the stability criteria developed in section 3.2 for the generator-connected

converter. It is interesting to investigate how the tuning of the second converter will impact the stability and if it is possible to stabilize the system using the grid-connected converter as opposed to the generator-connected converter. Therefore the simulation result shown in Figure 4.5 displays two scenarios, where in the first scenario, the stability criteria 3.47 is not satisfied for the grid converter as opposed to the second scenario. A step in torque- and angular velocity is applied at $t = 30$ [s].

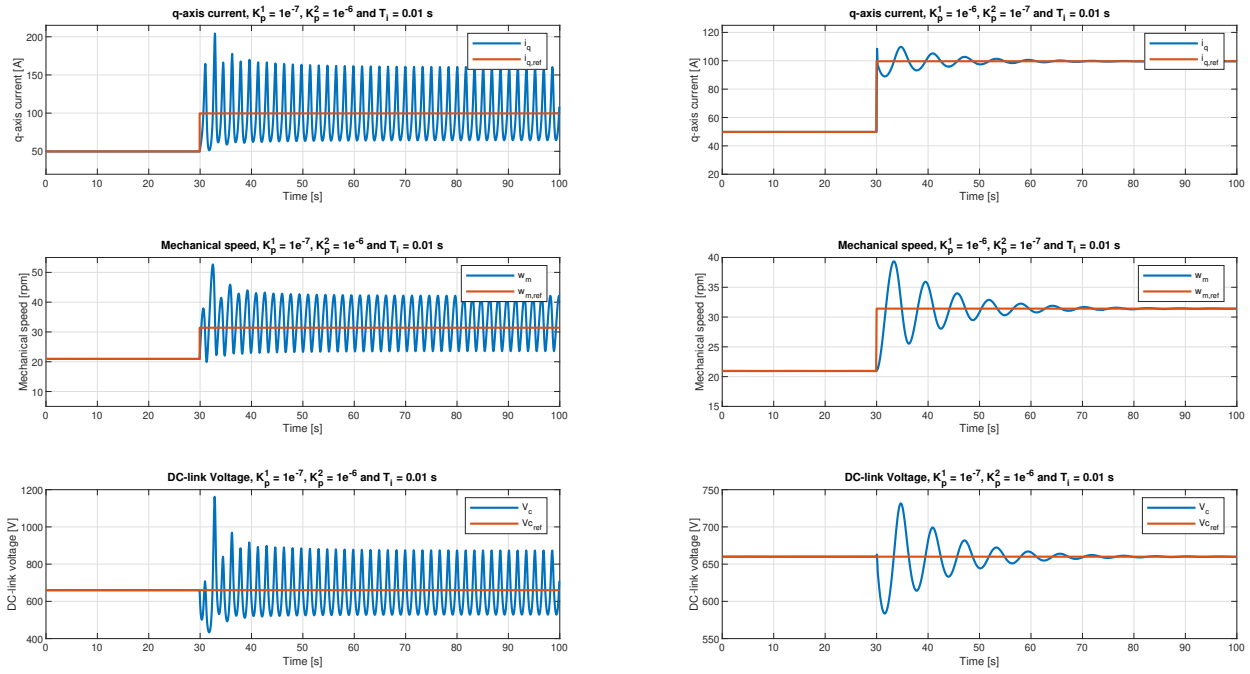

Figure 4.5: Initially the system is stable, and then a step in torque input and angular velocity happens at t = 30 [s]. When $K_p^1 = 1e^{-7}$ and $K_p^2 = 1e^{-6}$ [left], the system becomes unstable. When $K_p^1 = 1e^{-6}$ and $K_p^2 = 1e^{-7}$ [right], the system preserves it stability regardless of the step.

From Figure 4.5 one can see how the system's stability is more concerned with the tuning of the machine-side PBC (controller 1) than the gird-side PBC (controller 2). Choosing $K_p^1 < \gamma$ in controller 1 and K_p^2 slightly bigger than γ in controller 2 yields an unstable system. By interchanging the two values for K_p, a stable system was observed. The simulation thereby show that the best strategy for stability is to ensure that the stability criteria is fulfilled for the generator connected converter.

The criteria (3.47) is only concerned with the tuning of controller 1. To render the system passive, the criterion must only be fulfilled for controller 1. For controller 2, no similar criterion is found to guarantee stability. Making sure $K_p^2 > 0$, whilst $K_p^1 > \gamma$ is enough to guarantee stability. Not shown here, but from simulations, it is indicated that the tuning of controller 2 may compensate somewhat for controller 1 when K_p^2 is chosen sufficiently high. By, for instance choosing $K_p^1 = 1e^{-7}$ and $K_p^2 = 1$, the system's stability was preserved after the same disturbances as in the simulation shown in Figure 4.5 was applied. Simulations also indicate that the performance of the system could be improved by a strategic tuning of controller 2. This topic is not investigated further in this thesis, as this thesis is mainly concerned with stability.

4.2.2 Inclusion of Outer loops

In the previous simulation, Figure 4.5, the control variables u_1, u_2, u_3, u_4 are calculated in two PBCs. The passive input controller has three input variables but only two output variables. It is, therefore, actually not possible to control all three states. Especially if the model is an imperfect representation of a real system, the controllers will not be able to control all three states to the desired operating point. A practical solution to this challenge is to have one of the states calculated by an outer loop.

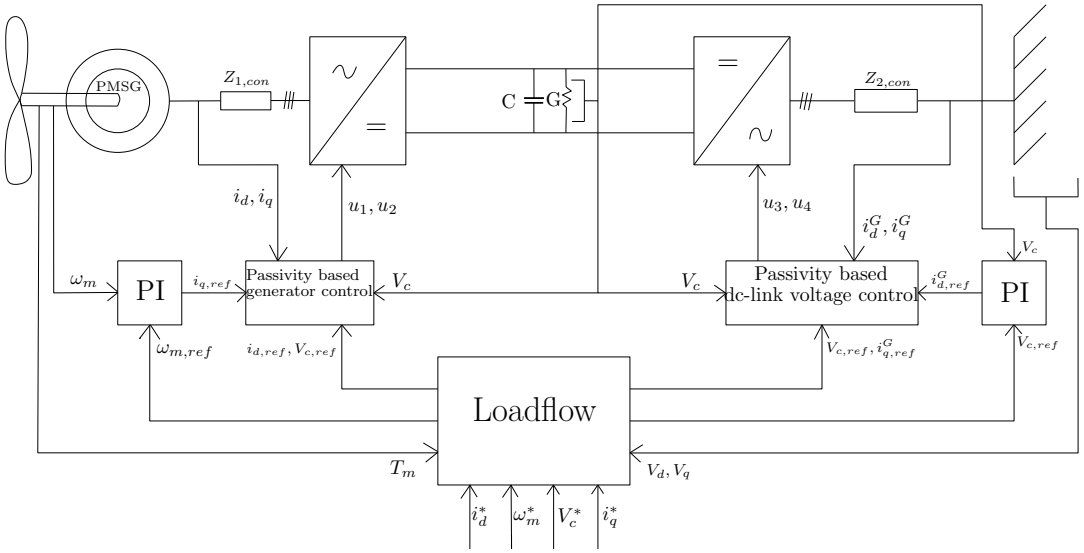

Figure 4.6: Control structure with outer loops

For the converter closest to the PMSG, the wind is chosen to be calculated by an outer loop based on a standard PI- controller. As the dynamics in the wind can be assumed to be sufficiently slower than the dynamics of the converter, the input to the PBCs is viewed as constant. Under this approximation, the stability certificate may arguably still be valid to a certain extent, particularly if one adopts a practical viewpoint. This is less the case for the second converter, where an outer loop calculates the DC link voltage reference. To check for stability and performance, we are forced to rely exclusively on our simulation results. The system is subjected to a step-change in the mechanical torque from 200 Nm to 400 Nm. The desired angular velocity is at the same time increased from 200 rpm to 270 rpm, and the desired voltage at the DC link is increased from 660 V to 800 V [2]. Two simulations are conducted where one includes the outer loops and the other without outer loops. The tuning of the P(I)-PBCs is the same in both cases.

[2]The reason for changing the torque input and the two references simultaneously is that during simulation it was found that the system had to experience quite strong disturbances to challenge the stability even without satisfying the stability criteria.

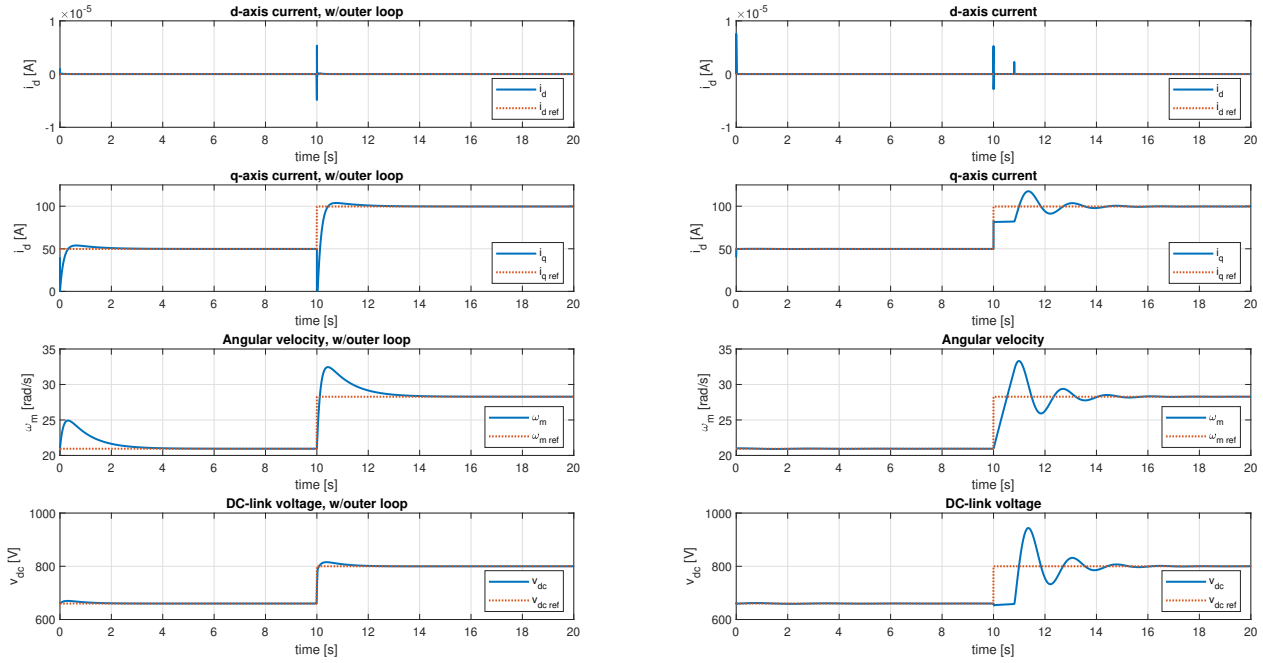

Figure 4.7: A step in mechanical torque, angular velocity, and dc-link voltage happens at t = 10 [s]. Simulation results are presented for a system with [left] and without [right] outer loops.

From Figure 4.7, it is apparent that having an outer loop improves the control system's performance. The system is able to achieve the desired operating point faster and without oscillations.

Disconnection of outer loops in case of instability

The stability certificate developed in section 3.2 is without outer loops. If the outer loops are tuned in such a way that the inputs to the PBCs will not be viewed as constant, then the system will be at risk of instability. However, as seen in the previous section, the control performance was faster and better, with outer loops to control the angular velocity and the DC-link voltage. Therefore, it is desirable to both have the improved performance provided by the outer loops and the stability guaranteed for the system without outer loops. In this section, a method for combining these desired qualities is suggested. Outer loops are included to increase performance, but in a case where the system is becoming unstable, the outer loops are disconnected. The motivation behind this is that the system is guaranteed to be stable if the stability criteria provided in section 3.2 is satisfied. As the system is detected to become unstable, the outer loops are disconnected such that the stability criteria are satisfied, and the system will become stable again. When the system is in stable operation, the outer loops can again be included to improve the control performance for the system.

A simulation was performed to test this. A disturbance in the torque occurs after five seconds, and the reference of the angular velocity is increased simultaneously. When the system is detected as being unstable, the outer loops are disconnected, which happens after 10 seconds.

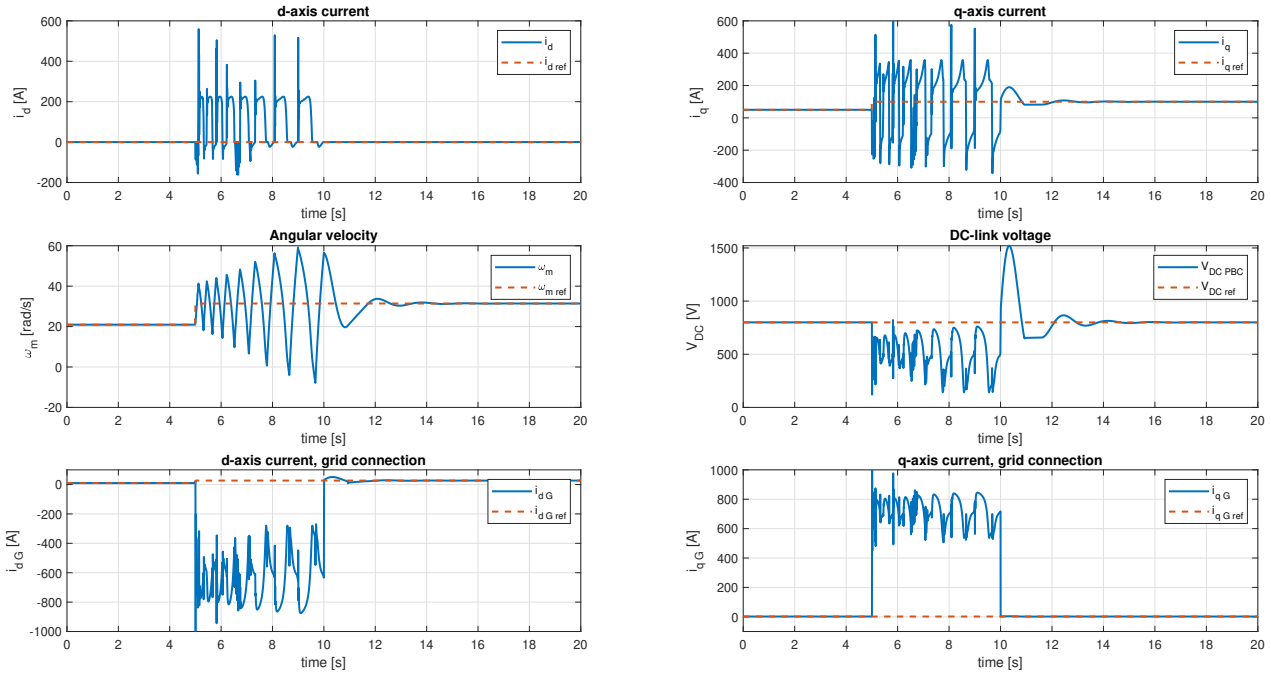

Figure 4.8: Simulation result for the coenergy variables where one disconnects the outer loops when the system is becoming unstable.

In Figure 4.8, it is apparent that the system is turning unstable after the system is subjected to disturbances after 5 seconds. The instability is detected, and the outer loops are disconnected after 10 seconds. The system then quickly regains stability. This is in line with the *stability certificate* developed in section 3.2. As a result of the disturbance, a new equilibrium calculation has to be performed for the system to become stable again. Unfortunately, due to the outer loops being tuned too fast, the system is not able to regain its stability. The reasoning for this is that in a cascaded control structure, it is important that the inner control loop is significantly faster than the outer loop [46]. The rule of thumb is that the inner loop should be roughly ten times faster than the outer loop. This is because the inner loop should view the inputs from the outer loop as constant, thereby avoiding the constant recalculation needed if this is not the case.

Comparison with traditional current control

In industry, the norm is to use PI current controllers as opposed to P(I)-PBCs. This technology is well tested and is much used due to its simplicity, and good performance [47]. In this section, the PBCs are compared to regular current control. For both the current control case and the PBC-case, the same outer loops shown in Figure 4.6 are used. The disturbance and the reference change the system is subjected to are the same as in the previous simulations.

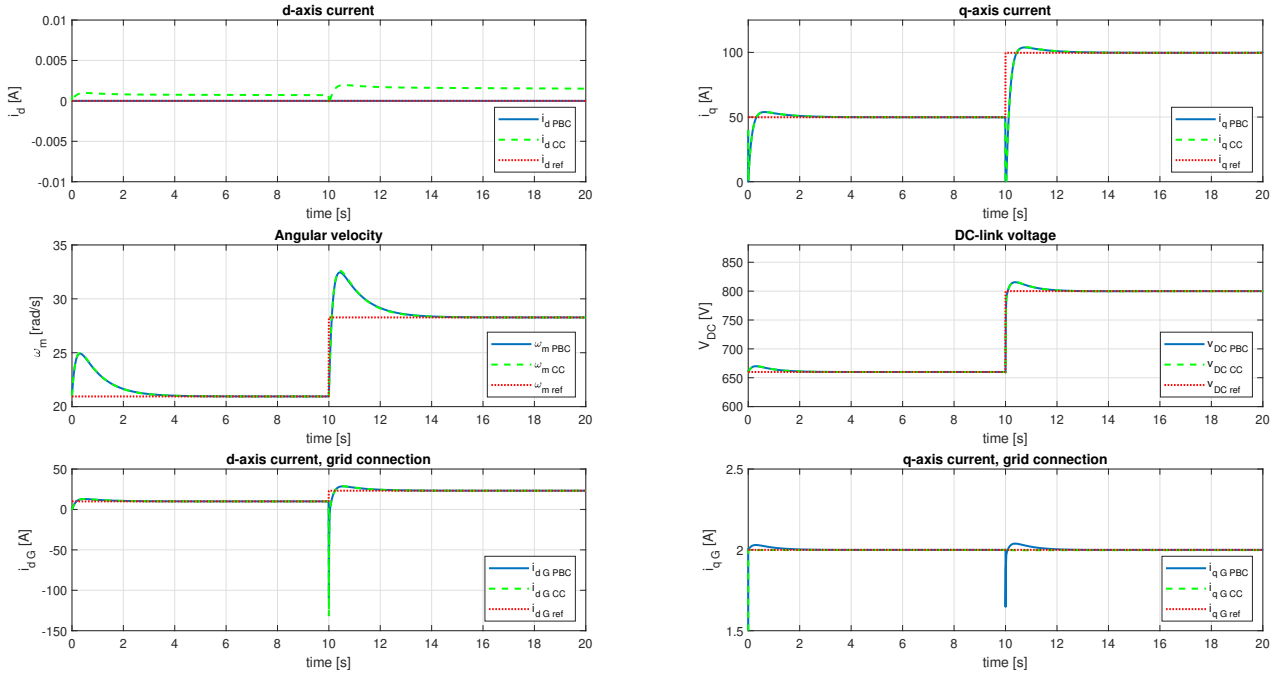

Figure 4.9: Comparison between passivity-based control [blue line] and PI current control [green dotted line], when subjected to a step in angular velocity, mechanical torque, and dc-link voltage at t = 10 [s].

From Figure 4.9, it is apparent that the performance is very similar for the PBC and the current controller. It must be noted that in this simulation, the same values were used in the tuning of both types of controllers. For a different tuning, the two controllers might have different performances compared to each other. Based on this simulation, the result is that the PBC has a similar performance to the traditional PI current controllers. The advantage of using the PBC is that the stability of the system is guaranteed even for large disturbances, as shown in section 3.2. In industry performance is often more important than guaranteed stable operation, but is ofcorse a desired property. The comparable performance for the PBCs and PI-current control, in this simulation, implies a bright future for passivity based control.

4.3 Improved Performance due to Damping in the Synchronous Generator

In both [23] and [48], which investigate modeling and control of multi-terminal HVDC systems, poor control performance by the P(I)-PBCs is observed. A potential explanation for this is that the system lack damping, and the convergence of the system is slow. To improve the performance, outer loops are included invoking the assumption of time-scale separation[3] and thereby not jeopardizing the stability guaranteed by using the passivity-based control. However this is not an ideal solution as the outer loops are not a part of the stability proof, and could therefore potentially jeopardize the stability.

By simulation shown in Figure 4.10 it is apparent that increasing the damping d in the PMSG does improve the convergence speed of the system. Although the systems analyzed in [23] and [48] have significant differences from the system analyzed in this thesis, the result in Figure 4.10 might have appliances for these multi-terminal HVDC systems. By including PMSGs in the HVDC system, the control performance could be improved without the need for outer loops due to the damping provided by the PMSGs. PMSG could then be designed such that the damping gave a sufficient improvement to the control of the HVDC system. The improved convergence due to higher damping indicates that the inclusion of PMSGs in the HVDC systems in [23] and [48] would be beneficial. However, this suggested improvement must be implemented in a replicated system described in these two papers to evaluate its effect.

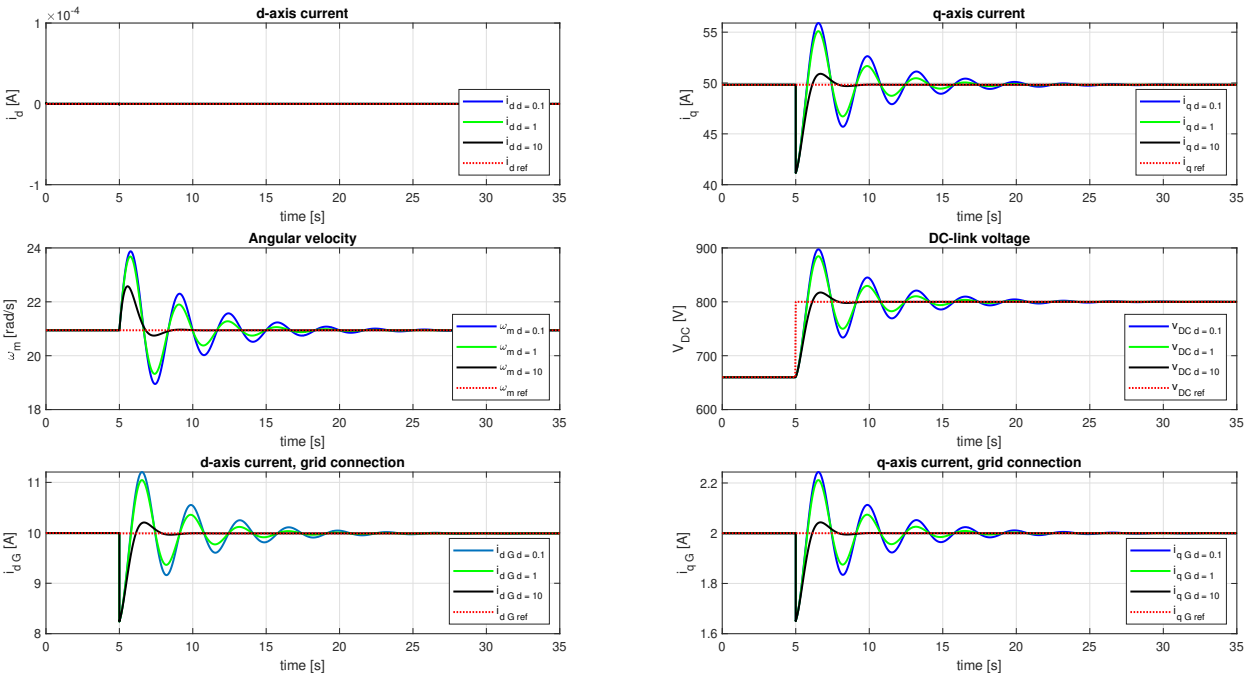

Figure 4.10: Comparison of the response of a voltage reference step for different damping values. As expected, an increase in damping results in a faster convergence.

[3]The assumption of time-scale separation means that the dynamics controlled in the outer loop are sufficiently much slower than the inner loop dynamics, such that the inner loop observes the output from the outer loop as constant.

End Note

This chapter presented the control objectives, equilibrium calculation, design of PBCs and the simulation results for the full back-to-back wind power system. The simulations validated the stability certificate developed in chapter 3 and suggested measures of practical solutions for improved performance. These are promising results, however the demand for wind power systems is greater than a single turbine. It is therefore time to expand the stability certificate to be valid for a wind park.

Chapter 5

Expanding to a Wind Park

The stability criteria found in chapter 3 is for a single wind energy conversion system. Wind turbines rarely appear alone and are usually a part of a larger wind park. Expanding the stability criteria to be valid for a wind park where the turbines are interconnected at the point of common coupling is, therefore, far more beneficial for real-world applications. The expansion of the stability certificate is achieved through modeling an electrical grid interconnected with multiple wind turbines. The modeling of the grid and connection with the wind energy conversion system is done by using graph theory following the methodology in [23]. A stability certificate *for an entire wind park guaranteeing large signal stability which also allows for a plug − and − play interconnection method could potentially have huge implications. Wind power is expected to be a cornerstone in the future power grid, and such a certificate could be central in the timely-needed transition from a centralized to a distributed power system.*

In this chapter, we aim to expand the *stability certificate* for a larger system containing an offshore wind park with multiple turbines connected via an HVDC connection to the continental grid. The *turbine string* will first be modified to allow for a more convenient interconnection to the power grid. In this thesis, a turbine string (TS) defines a system containing a permanent magnet synchronous generator and two 2L-VSC connected to an electrical grid in a back-to-back configuration. These TSs are connected in an electrical grid connected to the continental grid through an HVDC-link. The HVDC converter will be modeled as a constant voltage source. The complete system containing the TSs and the grid will be modeled using the pH formalism. With the help of graph theory, and specifically the incidence matrix B, the objective of showing the *scalability* of the *stability certificate* is achieved.

5.1 A Remodeling of the Turbine String

A TS is shown in Figure 5.1. Comparing this system to the system in section 3.2, the difference is that a capacitor is added to the system, and the grid connection is modeled as a current source instead of a constant voltage source. The addition of the capacitor will introduce two new states to the TS. Therefore, the system model for a TS must be modified and investigated if this modification will impact the stability criteria found in chapter 3.

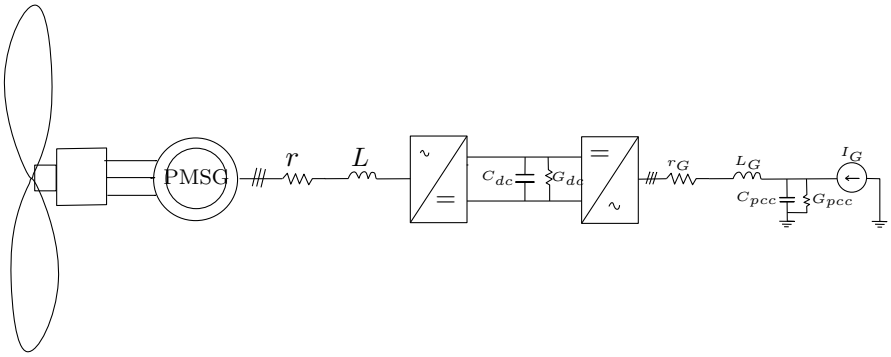

Figure 5.1: Turbine String

The equations describing a turbine string are:

$$\dot{\psi}_d = L\dot{i}_d = -r_s i_d + L i_q \frac{P}{2}\omega_m - u_1 V_c \tag{5.1}$$

$$\dot{\psi}_q = L\dot{i}_q = -r_s i_q - L i_d \frac{P}{2}\omega_m + \phi\frac{P}{2}\omega_m - u_2 V_c \tag{5.2}$$

$$\dot{\rho} = J\dot{\omega}_m = T_m(\omega_m) - \frac{P}{2}\phi i_q + d(\omega_{ref} - \omega_m) \tag{5.3}$$

$$\dot{q_c} = C_{dc}\dot{V}_c = u_1 i_d + u_2 i_q - u_3 i_d^G - u_4 i_q^G - G_{dc} V_c \tag{5.4}$$

$$\dot{\psi}_d^G = L_G\dot{i}_d^G = -r_G i_d^G + \omega_G L_G i_q^G + u_3 V_c - V_{pcc}^d \tag{5.5}$$

$$\dot{\psi}_d^G = L_G\dot{i}_q^G = -r_G i_q^G - \omega_G L_G i_d^G + u_4 V_c - V_{pcc}^q \tag{5.6}$$

$$\dot{q}_{pcc}^d = C_{pcc}V_{pcc}^d = i_d^G - G_{pcc}V_{pcc}^d + I_G^d \tag{5.7}$$

$$\dot{q}_{pcc}^q = C_{pcc}V_{pcc}^q = i_q^G - G_{pcc}V_{pcc}^q + I_G^q \tag{5.8}$$

The two new states that are introduced are modeling the grid connection as a current source and consist of the d and q component of the electrical charge q_{pcc} in the point of common coupling (PCC). C_{pcc} is the capacitance in the capacitor at PCC, and G_{pcc} is the conductance at PCC representing the losses in the capacitor. V_{pcc} is the voltage at PCC. I_G^d and I_G^q are the currents in the d and q axis modeling the external grid. G_{dc} and C_{dc} are the conductance and capacitance in the dc-link, respectively.

The Hamiltonian function describing the energy in the TS is defined as follows:

$$\begin{aligned}\mathcal{H}(x) &= \frac{1}{2}x^\top Qx \\ &= \frac{1}{2}\begin{bmatrix}\psi_d & \psi_q & \rho & q_c & \psi_d^G & \psi_q^G & q_{pcc}^d & q_{pcc}^q\end{bmatrix}\begin{bmatrix}\frac{1}{L} & 0 & 0 & 0 & 0 & 0 & 0 & 0 \\ 0 & \frac{1}{L} & 0 & 0 & 0 & 0 & 0 & 0 \\ 0 & 0 & \frac{1}{J} & 0 & 0 & 0 & 0 & 0 \\ 0 & 0 & 0 & \frac{1}{C_{dc}} & 0 & 0 & 0 & 0 \\ 0 & 0 & 0 & 0 & \frac{1}{L_G} & 0 & 0 & 0 \\ 0 & 0 & 0 & 0 & 0 & \frac{1}{L_G} & 0 & 0 \\ 0 & 0 & 0 & 0 & 0 & 0 & \frac{1}{C_{pcc}} & 0 \\ 0 & 0 & 0 & 0 & 0 & 0 & 0 & \frac{1}{C_{pcc}}\end{bmatrix}\begin{bmatrix}\psi_d \\ \psi_q \\ \rho \\ q_c \\ \psi_d^G \\ \psi_q^G \\ q_{pcc}^d \\ q_{pcc}^q\end{bmatrix} \\ &= \frac{1}{2}\left(\frac{1}{L}\psi_d^2 + \frac{1}{L}\psi_q^2 + \frac{1}{J}\rho^2 + \frac{1}{C_{dc}}q_c^2 + \frac{1}{L_G}\psi_d^{G^2} + \frac{1}{L_G}\psi_q^{G^2} + \frac{1}{C_{pcc}}{q_{pcc}^d}^2 + \frac{1}{C_{pcc}}{q_{pcc}^q}^2\right)\end{aligned} \tag{5.9}$$

The port-Hamiltonian representation of the turbine string becomes:

$$\underbrace{\begin{bmatrix}\dot{\psi}_d \\ \dot{\psi}_q \\ \dot{\rho} \\ \dot{q}_c \\ \dot{\psi}_d^G \\ \dot{\psi}_q^G \\ \dot{q}_{pcc}^d \\ \dot{q}_{pcc}^q\end{bmatrix}}_{x} = \begin{bmatrix}-r & \omega_m\frac{P}{2}L & 0 & -u_1 & 0 & 0 & 0 & 0 \\ -\omega_m & -r & \frac{P}{2}\phi & -u_2 & 0 & 0 & 0 & 0 \\ 0 & -\frac{P}{2}\phi & -d + \frac{T_m(\omega_m)}{\omega_m} & 0 & 0 & 0 & 0 & 0 \\ u_1 & u_2 & 0 & -G_{dc} & -u_3 & -u_4 & 0 & 0 \\ 0 & 0 & 0 & u_3 & -r_G & \omega_G L_G & -1 & 0 \\ 0 & 0 & 0 & u_4 & -\omega_G L_G & -r_G & 0 & -1 \\ 0 & 0 & 0 & 0 & 1 & 0 & -G_{pcc} & 0 \\ 0 & 0 & 0 & 0 & 0 & 1 & 0 & -G_{pcc}\end{bmatrix}\underbrace{\begin{bmatrix}i_d \\ i_q \\ \omega_m \\ V_c \\ i_d^G \\ i_q^G \\ V_{pcc}^d \\ V_{pcc}^q\end{bmatrix}}_{\nabla\mathcal{H}(x)} + \begin{bmatrix}0 \\ 0 \\ d\omega_{ref} \\ 0 \\ 0 \\ 0 \\ I_G^d \\ I_G^q\end{bmatrix} \tag{5.10}$$

which can be written on the abbreviated form:

$$\dot{x} = \underbrace{\left(\mathcal{J}(\omega_m) + \mathcal{J}_0 + \mathcal{J}_5 + \mathcal{J}_6 + \mathcal{J}_7 - \mathcal{R}(\omega_m)\right)\nabla\mathcal{H}(x) + E}_{f(x)} + \underbrace{\left[\mathcal{J}_1\nabla\mathcal{H}(x)\ \mathcal{J}_2\nabla\mathcal{H}(x)\ \mathcal{J}_3\nabla\mathcal{H}(x)\ \mathcal{J}_4\nabla\mathcal{H}(x)\right]}_{g(x)}\underbrace{\begin{bmatrix}u_1 \\ u_2 \\ u_3 \\ u_4\end{bmatrix}}_{u} \tag{5.11}$$

where

$$\mathcal{J}(\omega) = \frac{P}{2}L \begin{bmatrix} 0 & \omega_m & 0 & 0 & 0 & 0 & 0 & 0 \\ -\omega_m & 0 & 0 & 0 & 0 & 0 & 0 & 0 \\ 0 & 0 & 0 & 0 & 0 & 0 & 0 & 0 \\ 0 & 0 & 0 & 0 & 0 & 0 & 0 & 0 \\ 0 & 0 & 0 & 0 & 0 & 0 & 0 & 0 \\ 0 & 0 & 0 & 0 & 0 & 0 & 0 & 0 \\ 0 & 0 & 0 & 0 & 0 & 0 & 0 & 0 \\ 0 & 0 & 0 & 0 & 0 & 0 & 0 & 0 \end{bmatrix}, \quad \mathcal{J}_0 = \frac{P}{2}\phi \begin{bmatrix} 0 & 0 & 0 & 0 & 0 & 0 & 0 & 0 \\ 0 & 0 & 1 & 0 & 0 & 0 & 0 & 0 \\ 0 & -1 & 0 & 0 & 0 & 0 & 0 & 0 \\ 0 & 0 & 0 & 0 & 0 & 0 & 0 & 0 \\ 0 & 0 & 0 & 0 & 0 & 0 & 0 & 0 \\ 0 & 0 & 0 & 0 & 0 & 0 & 0 & 0 \\ 0 & 0 & 0 & 0 & 0 & 0 & 0 & 0 \\ 0 & 0 & 0 & 0 & 0 & 0 & 0 & 0 \end{bmatrix}, \quad \mathcal{J}_1 = \begin{bmatrix} 0 & 0 & 0 & -1 & 0 & 0 & 0 & 0 \\ 0 & 0 & 0 & 0 & 0 & 0 & 0 & 0 \\ 0 & 0 & 0 & 0 & 0 & 0 & 0 & 0 \\ 1 & 0 & 0 & 0 & 0 & 0 & 0 & 0 \\ 0 & 0 & 0 & 0 & 0 & 0 & 0 & 0 \\ 0 & 0 & 0 & 0 & 0 & 0 & 0 & 0 \\ 0 & 0 & 0 & 0 & 0 & 0 & 0 & 0 \\ 0 & 0 & 0 & 0 & 0 & 0 & 0 & 0 \end{bmatrix}$$

$$\mathcal{J}_2 = \begin{bmatrix} 0 & 0 & 0 & 0 & 0 & 0 & 0 & 0 \\ 0 & 0 & 0 & -1 & 0 & 0 & 0 & 0 \\ 0 & 0 & 0 & 0 & 0 & 0 & 0 & 0 \\ 0 & 1 & 0 & 0 & 0 & 0 & 0 & 0 \\ 0 & 0 & 0 & 0 & 0 & 0 & 0 & 0 \\ 0 & 0 & 0 & 0 & 0 & 0 & 0 & 0 \\ 0 & 0 & 0 & 0 & 0 & 0 & 0 & 0 \\ 0 & 0 & 0 & 0 & 0 & 0 & 0 & 0 \end{bmatrix}, \quad \mathcal{J}_3 = \begin{bmatrix} 0 & 0 & 0 & 0 & 0 & 0 & 0 & 0 \\ 0 & 0 & 0 & 0 & 0 & 0 & 0 & 0 \\ 0 & 0 & 0 & 0 & 0 & 0 & 0 & 0 \\ 0 & 0 & 0 & 0 & -1 & 0 & 0 & 0 \\ 0 & 0 & 0 & 1 & 0 & 0 & 0 & 0 \\ 0 & 0 & 0 & 0 & 0 & 0 & 0 & 0 \\ 0 & 0 & 0 & 0 & 0 & 0 & 0 & 0 \\ 0 & 0 & 0 & 0 & 0 & 0 & 0 & 0 \end{bmatrix}, \quad \mathcal{J}_4 = \begin{bmatrix} 0 & 0 & 0 & 0 & 0 & 0 & 0 & 0 \\ 0 & 0 & 0 & 0 & 0 & 0 & 0 & 0 \\ 0 & 0 & 0 & 0 & 0 & 0 & 0 & 0 \\ 0 & 0 & 0 & 0 & 0 & -1 & 0 & 0 \\ 0 & 0 & 0 & 0 & 0 & 0 & 0 & 0 \\ 0 & 0 & 0 & 1 & 0 & 0 & 0 & 0 \\ 0 & 0 & 0 & 0 & 0 & 0 & 0 & 0 \\ 0 & 0 & 0 & 0 & 0 & 0 & 0 & 0 \end{bmatrix}$$

$$\mathcal{J}_5 = \omega_G L_G \begin{bmatrix} 0 & 0 & 0 & 0 & 0 & 0 & 0 & 0 \\ 0 & 0 & 0 & 0 & 0 & 0 & 0 & 0 \\ 0 & 0 & 0 & 0 & 0 & 0 & 0 & 0 \\ 0 & 0 & 0 & 0 & 0 & 0 & 0 & 0 \\ 0 & 0 & 0 & 0 & 0 & 1 & 0 & 0 \\ 0 & 0 & 0 & 0 & -1 & 0 & 0 & 0 \\ 0 & 0 & 0 & 0 & 0 & 0 & 0 & 0 \\ 0 & 0 & 0 & 0 & 0 & 0 & 0 & 0 \end{bmatrix}, \quad \mathcal{J}_6 = \begin{bmatrix} 0 & 0 & 0 & 0 & 0 & 0 & 0 & 0 \\ 0 & 0 & 0 & 0 & 0 & 0 & 0 & 0 \\ 0 & 0 & 0 & 0 & 0 & 0 & 0 & 0 \\ 0 & 0 & 0 & 0 & 0 & 0 & 0 & 0 \\ 0 & 0 & 0 & 0 & 0 & 0 & -1 & 0 \\ 0 & 0 & 0 & 0 & 0 & 0 & 0 & 0 \\ 0 & 0 & 0 & 0 & 0 & 1 & 0 & 0 \\ 0 & 0 & 0 & 0 & 0 & 0 & 0 & 0 \end{bmatrix}, \quad \mathcal{J}_7 = \begin{bmatrix} 0 & 0 & 0 & 0 & 0 & 0 & 0 & 0 \\ 0 & 0 & 0 & 0 & 0 & 0 & 0 & 0 \\ 0 & 0 & 0 & 0 & 0 & 0 & 0 & 0 \\ 0 & 0 & 0 & 0 & 0 & 0 & 0 & 0 \\ 0 & 0 & 0 & 0 & 0 & 0 & 0 & 0 \\ 0 & 0 & 0 & 0 & 0 & 0 & 0 & -1 \\ 0 & 0 & 0 & 0 & 0 & 0 & 0 & 0 \\ 0 & 0 & 0 & 0 & 0 & 1 & 0 & 0 \end{bmatrix}$$

$$\mathcal{R}(\omega_m) = \begin{bmatrix} r & 0 & 0 & 0 & 0 & 0 & 0 & 0 \\ 0 & r & 0 & 0 & 0 & 0 & 0 & 0 \\ 0 & 0 & d - \frac{T_m(\omega_m)}{\omega_m} & 0 & 0 & 0 & 0 & 0 \\ 0 & 0 & 0 & G_{dc} & 0 & 0 & 0 & 0 \\ 0 & 0 & 0 & 0 & r_G & 0 & 0 & 0 \\ 0 & 0 & 0 & 0 & 0 & r_G & 0 & 0 \\ 0 & 0 & 0 & 0 & 0 & 0 & G_{pcc} & 0 \\ 0 & 0 & 0 & 0 & 0 & 0 & 0 & G_{pcc} \end{bmatrix}, \quad E = \begin{bmatrix} 0 \\ 0 \\ d\omega_{ref} \\ 0 \\ 0 \\ 0 \\ I_G^d \\ I_G^q \end{bmatrix}$$

The addition of the capacitor is a linear interconnection to an inductor on the grid side of the turbine string. It is shown in section 3.3 that stability can be ensured by having sufficient damping in the PMSG and by satisfying the tuning condition for the P(I)-PBC on the generator side of the DC-link. Therefore, it is easy to prove that including the capacitor through a linear interconnection does not alter the stability conditions. The proof is included in Appendix D.

5.2 The grid model

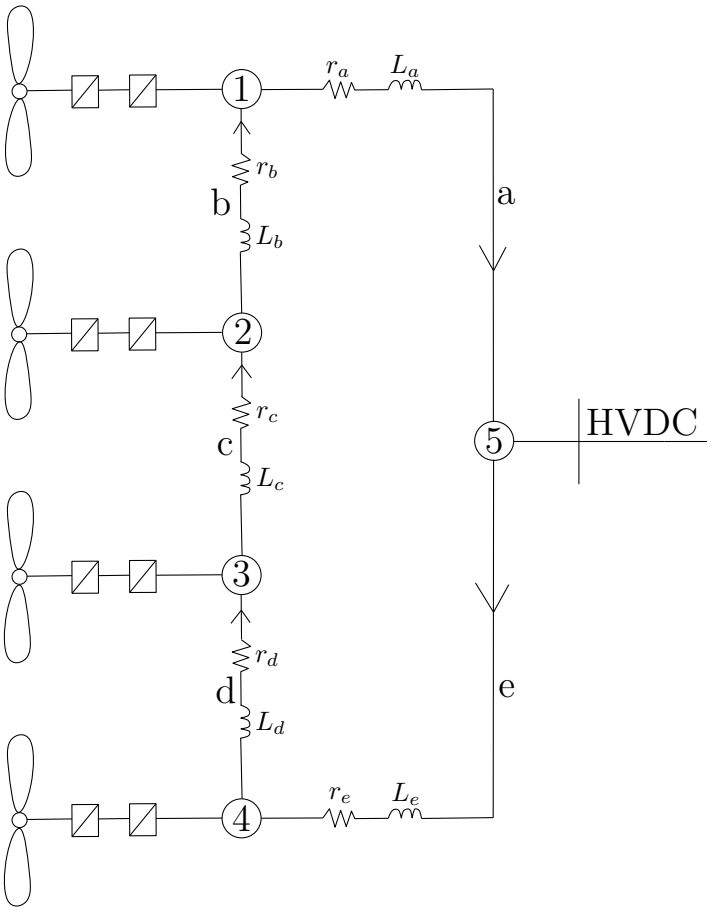

Figure 5.2: Wind park model

Graph theory is a powerful mathematical tool used to study the interactions of systems. A *directed* graph $\mathcal{G} = (\mathcal{V}, \epsilon)$ consists of a finite set $\mathcal{V}$ of vertices (nodes) and a finite set ϵ of directed edges (branches or links), together with a mapping from ϵ to the set of ordered pairs of $\mathcal{V}$ [49].
Figure 5.2 depicts an arbitrary topology for a simplified wind farm. The wind turbines are represented as vertices or nodes, and the transmission lines represent the edges. Because of the specified direction of the flows indicated by the arrow, Figure 5.2 depicts a directed graph.

A directed graph is completely specified by its incidence matrix. The incidence matrix $\mathcal{B}$ is a $N \times M$ matrix, where N is the number of vertices and M is the number of edges. In this thesis an element $\mathcal{B}_{i,j}$ is defined as positive if edge e_j leaves vertex v_i and the element $\mathcal{B}_{i,j}$ is defined as negative if edge e_j enters vertex v_i. If edge e_j is not connected to vertex v_i the element element $\mathcal{B}_{i,j}$ is zero. In other words, the element $\mathcal{B}_{i,j}$ is positive if the current flow in line j leaves node i and defined as negative if the current in line j enters node i. If line j is not connected to node i, the element element $\mathcal{B}_{i,j}$ is zero.
The incidence matrix for the arbitrary topology depicted in Figure 5.2 becomes:

$$\mathcal{B} = \begin{bmatrix} 1 & -1 & 0 & 0 & 0 \\ 0 & 1 & -1 & 0 & 0 \\ 0 & 0 & 1 & -1 & 0 \\ 0 & 0 & 0 & 1 & -1 \\ -1 & 0 & 0 & 0 & 1 \end{bmatrix} \tag{5.12}$$

In combination with graph theory, pH modeling allows for the modeling of multi-agent systems where the desired *plug-and-play* characteristics of the pH modeling formalism are preserved. The underlying dirac structures in the Hamiltonian modeling are directly defined by the incidence

matrix $\mathcal{B}$, and the conservation laws are thus captured [49].
The incidence matrix can be split up into two parts. One part contains the flow between the turbine strings, and the other contains the flow between the turbine strings and the HVDC-connection node (node 5 in Figure 5.2).

$$\mathcal{B} = \begin{bmatrix} \mathcal{B}_{\text{TS}} \\ \mathcal{B}_{\text{source}} \end{bmatrix} = \left[\begin{array}{ccccc} 1 & -1 & 0 & 0 & 0 \\ 0 & 1 & -1 & 0 & 0 \\ 0 & 0 & 1 & -1 & 0 \\ 0 & 0 & 0 & 1 & -1 \\ \hdashline -1 & 0 & 0 & 0 & 1 \end{array}\right]$$

The voltage in all the nodes except for the HVDC-connection node are the variables depending on the output of the turbine strings. The dq voltages in the HVDC-connection are assumed to be constant for simplicity and can be justified since the HVDC-converter is imposing the voltage at the node. Let U be a vector that contains the voltages in all the nodes. More precisely $U = \text{col}(U_{p,grid}, U_{source})$, where $U_{p,grid}$ is a vector of the voltages in the nodes that are connected to a turbine string and U_{source} is the voltage in the HVDC-connection (node 5).

An important property that will be utilized later is that the voltage difference between the nodes can be expressed using the transpose of the incidence matrix.

$$\mathcal{B}^\top U = \left[\begin{array}{ccccc} 1 & 0 & 0 & 0 & -1 \\ -1 & 1 & 0 & 0 & 0 \\ 0 & -1 & 1 & 0 & 0 \\ 0 & 0 & -1 & 1 & 0 \\ 0 & 0 & 0 & -1 & 1 \end{array}\right] \left[\begin{array}{c} V_1^{dq} \\ V_2^{dq} \\ V_3^{dq} \\ V_4^{dq} \\ \hdashline V_5^{dq} \end{array}\right] = \underbrace{\begin{bmatrix} V_1^{dq} \\ -V_1^{dq} + V_2^{dq} \\ -V_2^{dq} + V_3^{dq} \\ -V_3^{dq} + V_4^{dq} \\ -V_4^{dq} \end{bmatrix}}_{\mathcal{B}_{TS} U_{p,grid}} + \underbrace{\begin{bmatrix} -V_5^{dq} \\ 0 \\ 0 \\ 0 \\ V_5^{dq} \end{bmatrix}}_{\mathcal{B}_{source} U_{source}} \tag{5.13}$$

The equations describing the transmission line, exemplified as the line between node 1 and 2, is found with the help of Kirchhoff's voltage law.

$$\begin{aligned} L_b \frac{di_b^a}{dt} &= -r_b i_b^a + (V_2^a - V_1^a) \\ L_b \frac{di_b^b}{dt} &= -r_b i_b^b + (V_2^b - V_1^b) \\ L_b \frac{di_b^c}{dt} &= -r_b i_b^c + (V_2^c - V_1^c) \end{aligned} \tag{5.14}$$

with i_m^i is the current in phase i in transmission line $m \in M$. V_n^i is the voltage in phase i in node $n \in N$. r_m is the resistance in line m. To use a synchronous reference frame, a d-q transformation is applied.

$$\begin{aligned} L_b \frac{di_b^d}{dt} &= -r_b i_b^d + \omega_s i_b^q + (V_2^d - V_1^d) \\ L_b \frac{di_b^q}{dt} &= -r_b i_b^q - \omega_s i_b^d + (V_2^q - V_1^q) \end{aligned} \tag{5.15}$$

where the zero component is assumed to be zero.
Written on a port-Hamiltonian form, the transmission system can be expressed as:

$$\underbrace{\begin{bmatrix} \dot{\psi}_b^d \\ \dot{\psi}_b^q \end{bmatrix}}_{\dot{x}_b} = \left(\underbrace{\begin{bmatrix} 0 & \omega_s \\ -\omega_s & 0 \end{bmatrix}}_{J_{\omega_s}} - \underbrace{\begin{bmatrix} r_b & 0 \\ 0 & r_b \end{bmatrix}}_{R_b} \right) \underbrace{\begin{bmatrix} i_b^d \\ i_b^q \end{bmatrix}}_{\nabla \mathcal{H}(x_b)} + \underbrace{\begin{bmatrix} V_2^d - V_1^d \\ V_2^q - V_1^q \end{bmatrix}}_{\mathcal{B}_{TS,2.row} U_{p,grid}} \tag{5.16}$$

In the last term, and to preserve the generality in our analysis, the incidence matrix is used to express the voltage drop in the transmission line b. $U_{p,grid}$ can be viewed as an input to the system

at the nodes. This is useful when making a port-Hamiltonian model consisting of both the turbine strings and the grid. This is done in section 5.4.

A port-Hamiltonian representation of the complete grid shown in Figure 5.2 becomes:

$$\begin{aligned}
\dot{\psi}_a^d &= -r_a i_a^d + \omega_s i_a^q + (V_1^d - V_5^d) \\
\dot{\psi}_a^q &= -r_a i_a^q - \omega_s i_a^d + (V_1^q - V_5^q) \\
\dot{\psi}_b^d &= -r_b i_b^d + \omega_s i_b^q + (V_2^d - V_1^d) \\
\dot{\psi}_b^q &= -r_b i_b^q - \omega_s i_b^d + (V_2^q - V_1^q) \\
\dot{\psi}_c^d &= -r_c i_c^d + \omega_s i_c^q + (V_3^d - V_2^d) \\
\dot{\psi}_c^q &= -r_c i_c^q - \omega_s i_c^d + (V_3^q - V_2^q) \\
\dot{\psi}_d^d &= -r_d i_d^d + \omega_s i_d^q + (V_4^d - V_3^d) \\
\dot{\psi}_d^q &= -r_d i_d^q - \omega_s i_d^d + (V_4^q - V_3^q) \\
\dot{\psi}_e^d &= -r_e i_e^d + \omega_s i_e^q + (V_5^d - V_4^d) \\
\dot{\psi}_e^q &= -r_e i_e^q - \omega_s i_e^d + (V_5^q - V_4^q)
\end{aligned}$$

Abbreviated the port-Hamiltonian representation becomes:

$$\dot{x}_{grid} = F_{grid}\nabla\mathcal{H}(x_{grid}) + \mathcal{B}_{TS}^{\top}U_{p,grid} + \underbrace{\mathcal{B}_{source}^{\top}U_{source}}_{E} \tag{5.17}$$

where $F_{grid} = \mathcal{J}(\omega_s) - \mathcal{R}_{grid}$. The term "$\mathcal{B}_{source}^{\top}U_{source}$" is constant and can be viewed as disturbance to the system and denoted as E.

The Hamiltonian function is defined as:

$$\begin{aligned}
\mathcal{H}_{grid}(x) &= \frac{1}{2}x_{grid}^{\top}Q_{grid}x_{grid} \\
&= \frac{1}{2}\begin{bmatrix}\psi_a^d & \psi_a^q & \psi_b^d & \psi_b^q & \psi_c^d & \psi_c^q & \psi_d^d & \psi_d^q & \psi_e^d & \psi_e^q\end{bmatrix}
\begin{bmatrix}
\frac{1}{L_a} & 0 & 0 & 0 & 0 & 0 & 0 & 0 & 0 & 0 \\
0 & \frac{1}{L_a} & 0 & 0 & 0 & 0 & 0 & 0 & 0 & 0 \\
0 & 0 & \frac{1}{L_b} & 0 & 0 & 0 & 0 & 0 & 0 & 0 \\
0 & 0 & 0 & \frac{1}{L_b} & 0 & 0 & 0 & 0 & 0 & 0 \\
0 & 0 & 0 & 0 & \frac{1}{L_c} & 0 & 0 & 0 & 0 & 0 \\
0 & 0 & 0 & 0 & 0 & \frac{1}{L_c} & 0 & 0 & 0 & 0 \\
0 & 0 & 0 & 0 & 0 & 0 & \frac{1}{L_d} & 0 & 0 & 0 \\
0 & 0 & 0 & 0 & 0 & 0 & 0 & \frac{1}{L_d} & 0 & 0 \\
0 & 0 & 0 & 0 & 0 & 0 & 0 & 0 & \frac{1}{L_e} & 0 \\
0 & 0 & 0 & 0 & 0 & 0 & 0 & 0 & 0 & \frac{1}{L_e}
\end{bmatrix}
\begin{bmatrix}\psi_a^d \\ \psi_a^q \\ \psi_b^d \\ \psi_b^q \\ \psi_c^d \\ \psi_c^q \\ \psi_d^d \\ \psi_d^q \\ \psi_e^d \\ \psi_e^q\end{bmatrix} \\
&= \frac{1}{2}\left(\frac{1}{L}\psi_a^{d^2} + \frac{1}{L}\psi_a^{q^2} + \frac{1}{L}\psi_b^{d^2} + \frac{1}{L}\psi_b^{q^2} + \frac{1}{L}\psi_c^{d^2} + \frac{1}{L}\psi_c^{q^2} + \frac{1}{L}\psi_d^{d^2} + \frac{1}{L}\psi_d^{q^2} + \frac{1}{L}\psi_e^{d^2} + \frac{1}{L}\psi_e^{q^2}\right)
\end{aligned}$$

$\nabla\mathcal{H}(x_{grid})$ thus contains the d- and q component of the currents flowing in the transmission lines.

$$\nabla\mathcal{H}(x_{grid}) = \begin{bmatrix}
i_a^d \\ i_a^q \\ i_b^d \\ i_b^q \\ i_c^d \\ i_c^q \\ i_d^d \\ i_d^q \\ i_e^d \\ i_e^q
\end{bmatrix}$$

Written out $\mathcal{J}(\omega_s)$ and $\mathcal{R}_{grid}$ becomes:

$$\mathcal{J}(\omega_s) = \begin{bmatrix} \begin{bmatrix} 0 & \omega_s^a \\ -\omega_s^a & 0 \end{bmatrix} & 0_{2\times2} & 0_{2\times2} & 0_{2\times2} & 0_{2\times2} \\ 0_{2\times2} & \begin{bmatrix} 0 & \omega_s^b \\ -\omega_s^b & 0 \end{bmatrix} & 0_{2\times2} & 0_{2\times2} & 0_{2\times2} \\ 0_{2\times2} & 0_{2\times2} & \begin{bmatrix} 0 & \omega_s^c \\ -\omega_s^c & 0 \end{bmatrix} & 0_{2\times2} & 0_{2\times2} \\ 0_{2\times2} & 0_{2\times2} & 0_{2\times2} & \begin{bmatrix} 0 & \omega_s^d \\ -\omega_s^d & 0 \end{bmatrix} & 0_{2\times2} \\ 0_{2\times2} & 0_{2\times2} & 0_{2\times2} & 0_{2\times2} & \begin{bmatrix} 0 & \omega_s^e \\ -\omega_s^e & 0 \end{bmatrix} \end{bmatrix} \tag{5.18}$$

$$R_{grid} = \begin{bmatrix} r_a & 0 & 0 & 0 & 0 & 0 & 0 & 0 & 0 & 0 \\ 0 & r_a & 0 & 0 & 0 & 0 & 0 & 0 & 0 & 0 \\ 0 & 0 & r_b & 0 & 0 & 0 & 0 & 0 & 0 & 0 \\ 0 & 0 & 0 & r_b & 0 & 0 & 0 & 0 & 0 & 0 \\ 0 & 0 & 0 & 0 & r_c & 0 & 0 & 0 & 0 & 0 \\ 0 & 0 & 0 & 0 & 0 & r_c & 0 & 0 & 0 & 0 \\ 0 & 0 & 0 & 0 & 0 & 0 & r_d & 0 & 0 & 0 \\ 0 & 0 & 0 & 0 & 0 & 0 & 0 & r_d & 0 & 0 \\ 0 & 0 & 0 & 0 & 0 & 0 & 0 & 0 & r_e & 0 \\ 0 & 0 & 0 & 0 & 0 & 0 & 0 & 0 & 0 & r_e \end{bmatrix} \tag{5.19}$$

The grid model is represented on a port-Hamiltonian form using the incidence matrix as shown in 5.17. The grid is now modeled on a form suited for connecting the turbine strings. Before connecting them together, a complete model for all the turbine strings must be created.

5.3 The Complete Model of the Turbine Strings

In order to make a complete model of the grid and the TS, it is beneficial to make a port-Hamiltonian representation of all the TSs. The model for a single TS is shown in section 5.1.

$$\dot{x}_i = \underbrace{\left(\mathcal{J}(\omega_{m,i}) + \mathcal{J}_0 + u_i^1\mathcal{J}_1 + u_i^2\mathcal{J}_2 + u_i^3\mathcal{J}_3 + u_i^4\mathcal{J}_4 + \mathcal{J}_5 + \mathcal{J}_6 + \mathcal{J}_7 - \mathcal{R}(\omega_{m,i})\right)}_{F_i(\omega_{m,i},u_i)} \nabla\mathcal{H}(x_i) + G_{p,i}u_{p,i} + E_i \tag{5.20}$$

where $u_{p,i}$ is the current flowing from the grid at node i and into the turbine string at that node. The "p" stands for port. The disturbance matrix E_i does not contain these currents, as they did in the model in section 5.1, as they now are viewed as input to the turbine string.

$$G_1 = \begin{bmatrix} 0 & 0 \\ 0 & 0 \\ 0 & 0 \\ 0 & 0 \\ 0 & 0 \\ 0 & 0 \\ 0 & 0 \\ 1 & 0 \\ 0 & 1 \end{bmatrix}, \quad u_{p,1} = \begin{bmatrix} I_d^{G,1} \\ I_q^{G,1} \end{bmatrix}, \quad E = \begin{bmatrix} 0 \\ 0 \\ d\omega_{ref,1} \\ 0 \\ 0 \\ 0 \\ 0 \\ 0 \end{bmatrix}$$

The port-Hamiltonian representation of all the turbine strings for the system in Figure 5.2 are:

$$\begin{aligned}
\dot{x}_1 &= \left(\mathcal{J}(\omega_{m,1}) + \mathcal{J}_0 + u_1^1\mathcal{J}_1 + u_1^2\mathcal{J}_2 + u_1^3\mathcal{J}_3 + u_1^4\mathcal{J}_4 + \mathcal{J}_5 + \mathcal{J}_6 + \mathcal{J}_7 - \mathcal{R}(\omega_{m,1})\right)\nabla\mathcal{H}(x_1) + G_{p_1}u_{p,1} + E_1 \\
\dot{x}_2 &= \left(\mathcal{J}(\omega_{m,2}) + \mathcal{J}_0 + u_2^1\mathcal{J}_1 + u_2^2\mathcal{J}_2 + u_2^3\mathcal{J}_3 + u_2^4\mathcal{J}_4 + \mathcal{J}_5 + \mathcal{J}_6 + \mathcal{J}_7 - \mathcal{R}(\omega_{m,2})\right)\nabla\mathcal{H}(x_2) + G_{p,2}u_{p,2} + E_2 \\
\dot{x}_3 &= \left(\mathcal{J}(\omega_{m,3}) + \mathcal{J}_0 + u_3^1\mathcal{J}_1 + u_3^2\mathcal{J}_2 + u_3^3\mathcal{J}_3 + u_3^4\mathcal{J}_4 + \mathcal{J}_5 + \mathcal{J}_6 + \mathcal{J}_7 - \mathcal{R}(\omega_{m,3})\right)\nabla\mathcal{H}(x_3) + G_{p,3}u_{p,3} + E_3 \\
\dot{x}_4 &= \left(\mathcal{J}(\omega_{m,4}) + \mathcal{J}_0 + u_4^1\mathcal{J}_1 + u_4^2\mathcal{J}_2 + u_4^3\mathcal{J}_3 + u_4^4\mathcal{J}_4 + \mathcal{J}_5 + \mathcal{J}_6 + \mathcal{J}_7 - \mathcal{R}(\omega_{m,4})\right)\nabla\mathcal{H}(x_4) + G_{p,4}u_{p,4} + E_4
\end{aligned}$$

which can be written as:

$$\begin{aligned}
\underbrace{\begin{bmatrix} \dot{x}_1 \\ \dot{x}_2 \\ \dot{x}_3 \\ \dot{x}_4 \end{bmatrix}}_{x_{TS}} &= \underbrace{\begin{bmatrix} F(\omega_{m,1},u_1) & 0_{8x8} & 0_{8x8} & 0_{8x8} \\ 0_{8x8} & F(\omega_{m,2},u_2) & 0_{8x8} & 0_{8x8} \\ 0_{8x8} & 0_{8x8} & F(\omega_{m,3},u_3) & 0_{8x8} \\ 0_{8x8} & 0_{8x8} & 0_{8x8} & F(\omega_{m,4},u_4) \end{bmatrix}}_{F_{TS}(\omega_m,u)} \underbrace{\begin{bmatrix} \nabla\mathcal{H}(x_1) \\ \nabla\mathcal{H}(x_2) \\ \nabla\mathcal{H}(x_3) \\ \nabla\mathcal{H}(x_4) \end{bmatrix}}_{\nabla H(x_{TS})} \\
&+ \underbrace{\begin{bmatrix} G_{p,1} & 0_{8x2} & 0_{8x2} & 0_{8x2} \\ 0_{8x2} & G_{p,2} & 0_{8x2} & 0_{8x2} \\ 0_{8x2} & 0_{8x2} & G_{p,3} & 0_{8x2} \\ 0_{8x2} & 0_{8x2} & 0_{8x2} & G_{p,4} \end{bmatrix}}_{G_{p,TS}} \underbrace{\begin{bmatrix} u_{p,1} \\ u_{p,2} \\ u_{p,3} \\ u_{p,4} \end{bmatrix}}_{U_{p,TS}} + \underbrace{\begin{bmatrix} E_1 \\ E_2 \\ E_3 \\ E_4 \end{bmatrix}}_{E_{TS}}
\end{aligned} \tag{5.21}$$

and written in compact form as:

$$\dot{x}_{TS} = F_{TS}(\omega_m, u)\nabla\mathcal{H}(x_{TS}) + G_{p,TS}U_{p,TS} + E_{TS} \tag{5.22}$$

The Hamiltonian for all the turbine strings is the sum of the Hamiltonians for each turbine string.

$$\mathcal{H}(x_{TS}) = \frac{1}{2}x_{TS}^\top \mathcal{Q}_{TS}x_{TS}, \mathcal{Q}_{TS} = \text{bdiag}\{Q_i\} \tag{5.23}$$

The notation $\mathcal{Q}_{TS} = bdiagQ_i$ means that $\mathcal{Q}$ is a block diagonal matrix with the matrices Q_i along the diagonal. 5.22 is on a form suited for connecting the turbine strings as a grid together.

5.4 The interconnection

The port-Hamiltonian systems for the grid and the turbine strings are combined to make a complete model of the wind park. This section investigates the interconnections between the grid and the turbine strings, and the result is a port-Hamiltonian model for the wind park.

The input to the turbine strings are currents flowing from the grid into the turbine strings, which can be found using Kirchhoff's current law in the nodes.

Input Turbine string

$$U_{p,TS} = \begin{bmatrix} I_{dq}^{G,1} \\ I_{dq}^{G,2} \\ I_{dq}^{G,3} \\ I_{dq}^{G,4} \end{bmatrix} = \begin{bmatrix} i_b^{dq} - i_a^{dq} \\ i_c^{dq} - i_b^{dq} \\ i_d^{dq} - i_c^{dq} \\ i_e^{dq} - i_d^{dq} \end{bmatrix} \text{(From kirchoff's current law at the nodes)}$$

Output grid

$$y_{grid} = \mathcal{B}_{TS} \nabla \mathcal{H}(x_{grid}) = \begin{bmatrix} i_a^{dq} - i_b^{dq} \\ i_b^{dq} - i_c^{dq} \\ i_c^{dq} - i_d^{dq} \\ i_d^{dq} - i_e^{dq} \end{bmatrix} = - \begin{bmatrix} I_{dq}^{G,1} \\ I_{dq}^{G,2} \\ I_{dq}^{G,3} \\ I_{dq}^{G,4} \end{bmatrix}$$

Thereby;

$$U_{p,TS} = -\mathcal{B}_{TS} \nabla \mathcal{H}(x_{grid}) = -y_{grid} \tag{5.24}$$

The inputs to the grid are the node voltages, which means that the output from the turbine strings is also voltages.

Input grid:

$$U_{p.grid} = \begin{bmatrix} V_1^{dq} \\ V_2^{dq} \\ V_3^{dq} \\ V_4^{dq} \end{bmatrix}$$

Output Turbine string

$$y_{TS} = G_{p,TS}^{\top} \nabla \mathcal{H}(x_{TS}) = \begin{bmatrix} V_1^{dq} \\ V_2^{dq} \\ V_3^{dq} \\ V_4^{dq} \end{bmatrix}$$

Thereby;

$$U_{p,grid} = G_{p,TS}^{\top} \nabla \mathcal{H}(x_{TS}) = y_{TS} \tag{5.25}$$

Combining 5.24 and 5.25, the interconnection between the grid and the turbine strings can be expressed as:

$$\begin{bmatrix} U_{p,TS} \\ U_{p,grid} \end{bmatrix} = \begin{bmatrix} 0 & -1 \\ 1 & 0 \end{bmatrix} \begin{bmatrix} y_{TS} \\ y_{grid} \end{bmatrix} \tag{5.26}$$

Equation 5.26 shown that the TSs and the grid are connected through a power conserving interconnection.

To create the complete port-Hamiltonian representation of the system, 5.17 and 5.22 are combined with interconnection relation between the two subsystems shown in 5.26.

$$\begin{aligned} \dot{x}_{TS} &= F_{TS}(\omega_m, u) \nabla \mathcal{H}(x_{TS}) - G_{p,TS} \mathcal{B}_{TS} \nabla \mathcal{H}(x_{grid}) + E_{TS} \\ \dot{x}_{grid} &= F_{grid} \nabla \mathcal{H} + \mathcal{B}_{TS}^{\top} G_{p,TS} \nabla \mathcal{H}(x_{TS}) + E_{grid} \end{aligned}$$

$$\underbrace{\begin{bmatrix}\dot{x}_{TS}\\ \dot{x}_{grid}\end{bmatrix}}_{\dot{x}_{tot}} = \underbrace{\begin{bmatrix}F_{TS}(\omega_m,u) & -G_{p,TS}\mathcal{B}_{TS}\\ \mathcal{B}_{TS}^{\top}G_{p,TS}^{\top} & F_{grid}\end{bmatrix}}_{F_{tot}(x_{TS},u)}\underbrace{\begin{bmatrix}\nabla\mathcal{H}(x_{TS})\\ \nabla\mathcal{H}(x_{grid})\end{bmatrix}}_{\nabla\mathcal{H}(x_{tot})} + \underbrace{\begin{bmatrix}E_{TS}\\ E_{grid}\end{bmatrix}}_{E_{tot}} \tag{5.27}$$
$$\dot{x}_{tot} = F_{tot}(x_{TS},u)\nabla\mathcal{H}(x_{tot}) + E_{tot}$$

Equation (5.27) shows the port-Hamiltonian representation of the complete system. The Hamiltonian of the complete system is the sum of the Hamiltonians for the turbine strings and for the grid $\mathcal{H}_{tot} = \mathcal{H}_{TS} + \mathcal{H}_{grid}$

$$\mathcal{H}_{tot} = \frac{1}{2}x_{tot}^{\top}\mathcal{Q}_{tot}x_{tot}, \text{where } \mathcal{Q}_{tot} = \begin{bmatrix}\mathcal{Q}_{TS} & 0\\ 0 & Q_{grid}\end{bmatrix} \tag{5.28}$$

5.5 Stability analysis

To analyse the stability of the wind park, an incremental model is used.

$$\begin{array}{rrl} & \dot{x}_{tot} = & F_{tot}(x_{TS},u)\nabla\mathcal{H}(x_{tot}) + E_{tot} \\ - & 0 = & F_{tot}(\bar{x}_{TS},\bar{u})\nabla\mathcal{H}(\bar{x}_{tot}) + E_{tot} \\ \hline & \dot{\widetilde{x}}_{tot} = & F_{tot}(x_{TS},u)\nabla\mathcal{H}(x_{tot}) - F_{tot}(\bar{x}_{TS},\bar{u})\nabla\mathcal{H}(\bar{x}_{tot}) \end{array} \tag{5.29}$$

$$\begin{bmatrix}\dot{\widetilde{x}}_{TS}\\ \dot{\widetilde{x}}_{grid}\end{bmatrix} = \begin{bmatrix}F_{TS}(\omega_m,u) & -G_{p,TS}\mathcal{B}_{TS}\\ \mathcal{B}_{TS}^\top G_{p,TS}^\top & F_{grid}\end{bmatrix}\begin{bmatrix}\nabla\mathcal{H}(x_{TS})\\ \nabla\mathcal{H}(x_{grid})\end{bmatrix} - \begin{bmatrix}F_{TS}(\bar{\omega}_m,\bar{u}) & -G_{p,TS}\mathcal{B}_{TS}\\ \mathcal{B}_{TS}^\top G_{p,TS}^\top & F_{grid}\end{bmatrix}\begin{bmatrix}\nabla\mathcal{H}(\bar{x}_{TS})\\ \nabla\mathcal{H}(\bar{x}_{grid})\end{bmatrix} \tag{5.30}$$

As before a LCF is chosen as, $\mathcal{V} = \frac{1}{2}\widetilde{x}_{tot}^\top \mathcal{Q}_{tot}\widetilde{x}_{tot}$ and $\dot{\mathcal{V}} = \widetilde{x}_{tot}^\top \mathcal{Q}_{tot}\dot{\widetilde{x}}_{tot}$. This definition of the LCF satisfies the first two conditions for a Lyapunov function, this is shown in section 3.1.

$$I: \quad \dot{\mathcal{V}} = \widetilde{x}_{tot}^\top \mathcal{Q}_{tot}F_{tot}(x_{TS},u)\nabla H(x_{tot}) - \widetilde{x}_{tot}^\top \mathcal{Q}_{tot}F_{tot}(\bar{x}_{TS},\bar{u})\nabla H(\bar{x}_{tot})$$

$$\begin{aligned} II: \quad \dot{\mathcal{V}} &= \begin{bmatrix}\widetilde{x}_{TS}^\top \mathcal{Q}_{TS} & \widetilde{x}_{grid}^\top Q_{grid}\end{bmatrix}\begin{bmatrix}F_{TS}(\omega_m,u) & -G_{p,TS}\mathcal{B}_{TS}\\ \mathcal{B}_{TS}^\top G_{p,TS}^\top & F_{grid}\end{bmatrix}\begin{bmatrix}\mathcal{Q}_{TS}x_{TS}\\ Q_{grid}x_{grid}\end{bmatrix} \\ &\quad - \begin{bmatrix}\widetilde{x}_{TS}^\top \mathcal{Q}_{TS} & \widetilde{x}_{grid}^\top Q_{grid}\end{bmatrix}\begin{bmatrix}F_{TS}(\bar{\omega}_m,\bar{u}) & -G_{p,TS}\mathcal{B}_{TS}\\ \mathcal{B}_{TS}^\top G_{p,TS}^\top & F_{grid}\end{bmatrix}\begin{bmatrix}\mathcal{Q}_{TS}\bar{x}_{TS}\\ Q_{grid}\bar{x}_{grid}\end{bmatrix} \end{aligned}$$

$$\begin{aligned} III: \quad \dot{\mathcal{V}} &= \widetilde{x}_{TS}^\top \mathcal{Q}_{TS}F_{TS}(\omega_m,u)\mathcal{Q}_{TS}x_{TS} - \widetilde{x}_{TS}^\top \mathcal{Q}_{TS}G_{p,TS}\mathcal{B}_{TS}Q_{grid}x_{grid} + \widetilde{x}_{grid}^\top Q_{grid}\mathcal{B}_{TS}^\top G_{p,TS}^\top \mathcal{Q}_{TS}x_{TS} \\ &\quad + \widetilde{x}_{grid}^\top Q_{grid}F_{grid}Q_{grid}x_{grid} - \widetilde{x}_{TS}^\top \mathcal{Q}_{TS}F_{TS}(\bar{\omega}_m,\bar{u})\mathcal{Q}_{TS}\bar{x}_{TS} + \widetilde{x}_{TS}^\top \mathcal{Q}_{TS}G_{p,TS}\mathcal{B}_{TS}Q_{grid}\bar{x}_{grid} \\ &\quad - \widetilde{x}_{grid}^\top Q_{grid}\mathcal{B}_{TS}^\top G_{p,TS}^\top \mathcal{Q}_{TS}\bar{x}_{TS} - \widetilde{x}_{grid}^\top Q_{grid}F_{grid}Q_{grid}\bar{x}_{grid} \end{aligned}$$

$$\begin{aligned} IV: \quad \dot{\mathcal{V}} &= \widetilde{x}_{TS}^\top \mathcal{Q}_{TS}F_{TS}(\omega_m,u)\mathcal{Q}_{TS}x_{TS} - \widetilde{x}_{TS}^\top \mathcal{Q}_{TS}F_{TS}(\bar{\omega}_m,\bar{u})\mathcal{Q}_{TS}\bar{x}_{TS} + \widetilde{x}_{grid}^\top Q_{grid}F_{grid}Q_{grid}\widetilde{x}_{grid} \\ &\quad \underbrace{- \widetilde{x}_{TS}^\top \mathcal{Q}_{TS}G_{p,TS}\mathcal{B}_{TS}Q_{grid}\widetilde{x}_{grid} + \widetilde{x}_{grid}^\top Q_{grid}\mathcal{B}_{TS}^\top G_{p,TS}^\top \mathcal{Q}_{TS}\widetilde{x}_{TS}}_{=0} \end{aligned}$$

$$V: \quad \dot{\mathcal{V}} = \widetilde{x}_{TS}^\top \mathcal{Q}_{TS}F_{TS}(\omega_m,u)\mathcal{Q}_{TS}x_{TS} - \widetilde{x}_{TS}^\top \mathcal{Q}_{TS}F_{TS}(\bar{\omega}_m,\bar{u})\mathcal{Q}_{TS}\bar{x}_{TS} + \widetilde{x}_{grid}^\top Q_{grid}F_{grid}Q_{grid}\widetilde{x}_{grid}$$

$$\begin{aligned} VI: \quad \dot{\mathcal{V}} &= \widetilde{x}_{TS}^\top \mathcal{Q}_{TS}\Big(\text{bdiag}\Big\{\left(\mathcal{J}(\omega_{m,i}) + \mathcal{J}_0 + \mathcal{J}_5 + \mathcal{J}_6 + \mathcal{J}_7 - \mathcal{R}(\omega_{m,i})\right)Q_{TS}x_{TS,i} + g(x_{TS,i})u_i\Big\} \\ &\quad - \text{bdiag}\Big\{\left(\mathcal{J}(\bar{\omega}_{m,i}) + \mathcal{J}_0 + \mathcal{J}_5 + \mathcal{J}_6 + \mathcal{J}_7 - \mathcal{R}(\bar{\omega}_{m,i})\right)Q_{TS}\bar{x}_{TS,i} + g(\bar{x}_{TS,i})\bar{u}_i\Big\}\Big) \\ &\quad + \widetilde{x}_{grid}^\top Q_{grid}\big(\mathcal{J}(\omega_s) - \mathcal{R}_{grid}\big)Q_{grid}\widetilde{x}_{grid} \end{aligned}$$

$$\begin{aligned} VII: \quad \dot{\mathcal{V}} &= \widetilde{x}_{TS}^\top \mathcal{Q}_{TS}\ \text{bdiag}\Big\{\mathcal{J}(\omega_{m,i}) - \mathcal{R}(\omega_{m,i})\Big\}\mathcal{Q}_{TS}x_{TS} + \widetilde{x}_{TS}^\top \mathcal{Q}_{TS}\ \text{bdiag}\Big\{g(x_{TS,i})u_i\Big\} \\ &\quad - \widetilde{x}_{TS}^\top \mathcal{Q}_{TS}\ \text{bdiag}\Big\{\mathcal{J}(\bar{\omega}_{m,i}) - \mathcal{R}(\bar{\omega}_{m,i})\Big\}\mathcal{Q}_{TS}\bar{x}_{TS} - \widetilde{x}_{TS}^\top \mathcal{Q}_{TS}\ \text{bdiag}\Big\{g(\bar{x}_{TS,i})\bar{u}_i\Big\} \\ &\quad - \widetilde{x}_{grid}^\top Q_{grid}R_{grid}Q_{grid}\widetilde{x}_{grid} \end{aligned}$$

$$\begin{aligned} VIII: \quad \dot{\mathcal{V}} &= \widetilde{x}_{TS}^\top \mathcal{Q}_{TS}\ \text{bdiag}\Big\{\mathcal{J}(\omega_{m,i}) - \mathcal{R}(\omega_{m,i})\Big\}\mathcal{Q}_{TS}x_{TS} - \widetilde{x}_{TS}^\top \mathcal{Q}_{TS}\ \text{bdiag}\Big\{\mathcal{J}(\bar{\omega}_{m,i}) - \mathcal{R}(\bar{\omega}_{m,i})\Big\}\mathcal{Q}_{TS}\bar{x}_{TS} \\ &\quad - \widetilde{x}_{grid}^\top Q_{grid}\mathcal{R}_{grid}Q_{grid}\widetilde{x}_{grid} + \underbrace{\widetilde{x}_{TS}^\top \mathcal{Q}_{TS}\ \text{bdiag}\Big\{g(x_{TS,i})u_i - g(\bar{x}_{TS,i})\bar{u}_i\Big\}}_{*} \end{aligned}$$

Taking a closer look at the term *:

$$
\begin{aligned}
* &= \widetilde{x}_{TS}^{\top}\mathcal{Q}_{TS}\ \text{bdiag}\Big\{g(x_{TS,i})u_i - g(\bar{x}_{TS,i})\bar{u}_i\Big\} \\
&= \widetilde{x}_{TS}^{\top}\mathcal{Q}_{TS}\ \text{bdiag}\Big\{g(\widetilde{x}_{TS,i}+\bar{x}_{TS,i})u_i - g(\bar{x}_{TS,i})\bar{u}_i\Big\} \\
&= \widetilde{x}_{TS}^{\top}\mathcal{Q}_{TS}\ \text{bdiag}\Big\{g(\widetilde{x}_{TS,i})u_i + g(\bar{x}_{TS,i})u_i - g(\bar{x}_{TS,i})\bar{u}_i\Big\} \\
&= \widetilde{x}_{TS}^{\top}\mathcal{Q}_{TS}\ \text{bdiag}\Big\{g(\widetilde{x}_{TS,i})u_i + g(\bar{x}_{TS,i})\widetilde{u}_i\Big\} \\
&= \underbrace{\widetilde{x}_{TS}^{\top}\mathcal{Q}_{TS}\ \text{bdiag}\Big\{u_i^1\mathcal{J}_1 + u_i^2\mathcal{J}_2 + u_i^3\mathcal{J}_3 + u_i^4\mathcal{J}_4\Big\}\mathcal{Q}_{TS}\widetilde{x}_{TS}}_{=0} + \widetilde{x}_{TS}^{\top}\mathcal{Q}_{TS}\ \text{bdiag}\Big\{g(\bar{x}_{TS,i})\widetilde{u}_i\Big\} \\
&= \underbrace{\widetilde{x}_{TS}^{\top}\mathcal{Q}_{TS}\ \text{bdiag}\Big\{g(\bar{x}_{TS,i})\Big\}}_{\widetilde{y}^{\top}}\widetilde{U} \\
&= \widetilde{y}^{\top}\widetilde{U}
\end{aligned}
$$

Where, $\widetilde{U} = \begin{bmatrix}\widetilde{u}_1\\ \widetilde{u}_2\\ \widetilde{u}_3\\ \widetilde{u}_4\end{bmatrix}$ and $\widetilde{u}_i = \begin{bmatrix}\widetilde{u}_i^1\\ \widetilde{u}_i^2\\ \widetilde{u}_i^3\\ \widetilde{u}_i^4\end{bmatrix}$

$$
\begin{aligned}
IX: \quad \dot{\mathcal{V}} &= \widetilde{x}_{TS}^{\top}\mathcal{Q}_{TS}\ \text{bdiag}\Big\{\mathcal{J}(\omega_{m,i}) - \mathcal{R}(\omega_{m,i})\Big\}\mathcal{Q}_{TS}x_{TS} - \widetilde{x}_{TS}^{\top}\mathcal{Q}_{TS}\ \text{bdiag}\Big\{\mathcal{J}(\bar{\omega}_{m,i}) - \mathcal{R}(\bar{\omega}_{m,i})\Big\}\mathcal{Q}_{TS}\bar{x}_{TS} \\
&\quad - \widetilde{x}_{grid}^{\top}Q_{grid}\mathcal{R}_{grid}Q_{grid}\widetilde{x}_{grid} + \widetilde{y}^{\top}\widetilde{U} \\
X: \quad \dot{\mathcal{V}} &= \widetilde{y}^{\top}\widetilde{U} + \widetilde{x}_{TS}^{\top}\mathcal{Q}_{TS}\ \text{bdiag}\Big\{\mathcal{J}(\omega_{m,i}) - \mathcal{R}(\omega_{m,i})\Big\}\mathcal{Q}_{TS}x_{TS} - \widetilde{x}_{TS}^{\top}\mathcal{Q}_{TS}\ \text{bdiag}\Big\{\mathcal{J}(\bar{\omega}_{m,i}) - \mathcal{R}(\bar{\omega}_{m,i})\Big\}\mathcal{Q}_{TS}\bar{x}_{TS} \\
&\quad - \widetilde{x}_{grid}^{\top}Q_{grid}\mathcal{R}_{grid}Q_{grid}\widetilde{x}_{grid} + \underbrace{\widetilde{x}_{TS}^{\top}\mathcal{Q}_{TS}\ \text{bdiag}\Big\{\mathcal{J}(\omega_{m,i})\Big\}\mathcal{Q}_{TS}\bar{x}_{TS} - \widetilde{x}_{TS}^{\top}\mathcal{Q}_{TS}\ \text{bdiag}\Big\{\mathcal{J}(\omega_{m,i})\Big\}\mathcal{Q}_{TS}\bar{x}_{TS}}_{=0} \\
XI: \quad \dot{\mathcal{V}} &= \widetilde{y}^{\top}\widetilde{U} + \widetilde{x}_{TS}^{\top}\mathcal{Q}_{TS}\Bigg[\Big(\ \text{bdiag}\big\{\mathcal{J}(\omega_{m,i})\big\} - \text{bdiag}\big\{\mathcal{J}(\bar{\omega}_{m,i})\big\}\Big)\mathcal{Q}_{TS}\bar{x}_{TS} - \text{bdiag}\big\{-\mathcal{R}(\omega_{m,i})\big\}\mathcal{Q}_{TS}x_{TS} \\
&\quad + \text{bdiag}\big\{-\mathcal{R}(\bar{\omega}_{m,i})\big\}\mathcal{Q}_{TS}\bar{x}_{TS}\Bigg] - \widetilde{x}_{grid}^{\top}Q_{grid}\mathcal{R}_{grid}Q_{grid}\widetilde{x}_{grid} \\
XII: \quad \dot{\mathcal{V}} &= \widetilde{y}^{\top}\widetilde{U} + \widetilde{z}^{\top}\Big[M(z) - M(\bar{z})\Big] - \widetilde{x}_{grid}^{\top}Q_{grid}\mathcal{R}_{grid}Q_{grid}\widetilde{x}_{grid} + \widetilde{z}^{\top}\Big[\gamma\ \text{bdiag}\big\{g(\bar{x}_{TS,i})^{PMSG}g(\bar{x}_{TS,i})^{PMSG^{\top}}\big\} \\
&\quad - \gamma\ \text{bdiag}\big\{g(\bar{x}_{TS,i})^{PMSG}g(\bar{x}_{TS,i})^{PMSG^{\top}}\big\}\Big]\widetilde{z} \\
XIII: \quad \dot{\mathcal{V}} &= \underbrace{\widetilde{y}^{\top}\widetilde{U}}_{Term\ I} + \underbrace{\widetilde{y}^{PMSG^{\top}}\gamma\widetilde{y}^{PMSG}}_{Term\ II} + \underbrace{\widetilde{z}^{\top}\Big[M(z) - M(\bar{z}) - \gamma\ \text{bdiag}\big\{g(\bar{x}_{TS,i})^{PMSG}g(\bar{x}_{TS,i})^{PMSG^{\top}}\widetilde{z}\big\}\Big]}_{Term\ III} \\
&\quad - \underbrace{\widetilde{x}_{grid}^{\top}Q_{grid}\mathcal{R}_{grid}Q_{grid}\widetilde{x}_{grid}}_{Term\ IV}
\end{aligned}
$$

Step explanation

- I: The time derivative for the LCF for the complete wind park.
- II: The time derivative of the LCF is written on matrix form.
- III: Expression is expanded writing out the matrices.
- IV: Rearranging and grouping six terms into three by utilizing $\widetilde{x} = x - \bar{x}$. Last two terms cancels with each other due to the power preserving interconnection.
- V: After the rearranging and cancellation of term six in step [IV], the time derivative of the LCF becomes the expression in [V].

VI: $F_{TS}(\omega_m, u)$ and $F_{TS}(\bar{\omega}_m, \bar{u})$ are written on a block diagonal from.

VII: In each block diagonal term, $\mathcal{J}_0, \mathcal{J}_5, \mathcal{J}_6$ and $\mathcal{J}_7$ are canceled due to skew-symmetry. The same happens with $\widetilde{x}_{grid}^{\top} Q_{grid} J(\omega_s) Q_{grid} \widetilde{x}_{grid}$, where the skew symmetric term $\mathcal{J}(\omega_s)$ is canceled.

VIII: Rearranging and grouping of $g(x_{TS,i}u_i)$ and $g(\bar{x}_{TS,i}\bar{u}_i)$ to term denoted with *. It is shown that term * can be written as $\widetilde{y}^{\top}\widetilde{U}$ where $\widetilde{y}^{\top}$ is the passive output from each turbine string.

IX: The terms are re-written and the new definition of the passive output is included. $\widetilde{y}^{\top} = \widetilde{x}_{TS}^{\top} \mathcal{Q}_{TS} \text{bdiag}\{g(\bar{x}_{TS,i})\}$

X: Zero is added to the equation by adding and subtracting the term, $\widetilde{x}_{TS}^{\top} \mathcal{Q}_{TS}$ $\text{bdiag}\{\mathcal{J}(\omega_{m,i})\} \mathcal{Q}_{TS} \bar{x}_{TS}$

XI: Term three and five in [X] are grouped together, while the parts including $\mathcal{J}(\omega_{m,i})$ in term 2 and 6 in [X] are canceled due to skew-symmetry.

XII: Two new definitions are introduced, $z \triangleq Q_{TS} x_{TS}$ and $M(z) \triangleq \text{bdiag}\{\mathcal{J}(\omega_{m,i})\bar{z} - \mathcal{R}(\omega_{m,i})z\}$. A term containing the passive output feedback is included to help render the system passive. The term is added and subtracted such that the system does not change properties. As shown in section 3.2 it is possible to render the system passive only using the output feedback from the converter closest to the generator.

XIII: Terms are grouped together and the final expression for the time derivative of the LCF is presented

Term III is investigated to see if it is negative semidefinite, and as before this is equivalent to $\nabla M(z) + \nabla^{\top} M(z) - 2\gamma \text{ bdiag}\{g(\bar{x}_{TS,i})^{PMSG} g(\bar{x}_{TS,i})^{PMSG^{\top}}\} \leq 0$. $\nabla M(z)$ must then be found for the entire system.

$$
\begin{aligned}
M(z) &= \text{bdiag}\{\mathcal{J}(\omega_{m,i})\bar{z} - \mathcal{R}(\omega_{m,i})z\} \\
&= \begin{bmatrix} \mathcal{J}(\omega_{m,1}) & 0_{8x8} & 0_{8x8} & 0_{8x8} \\ 0_{8x8} & \mathcal{J}(\omega_{m,2}) & 0_{8x8} & 0_{8x8} \\ 0_{8x8} & 0_{8x8} & \mathcal{J}(\omega_{m,3}) & 0_{8x8} \\ 0_{8x8} & 0_{8x8} & 0_{8x8} & \mathcal{J}(\omega_{m,4}) \end{bmatrix} \begin{bmatrix} Q_1\bar{x}_{TS,1} \\ Q_2\bar{x}_{TS,2} \\ Q_3\bar{x}_{TS,3} \\ Q_4\bar{x}_{TS,4} \end{bmatrix} - \begin{bmatrix} \mathcal{R}(\omega_{m,1}) & 0_{8x8} & 0_{8x8} & 0_{8x8} \\ 0_{8x8} & \mathcal{R}(\omega_{m,2}) & 0_{8x8} & 0_{8x8} \\ 0_{8x8} & 0_{8x8} & \mathcal{R}(\omega_{m,3}) & 0_{8x8} \\ 0_{8x8} & 0_{8x8} & 0_{8x8} & \mathcal{R}(\omega_{m,4}) \end{bmatrix} \begin{bmatrix} Q_1 x_{TS,1} \\ Q_1 x_{TS,2} \\ Q_1 x_{TS,3} \\ Q_1 x_{TS,4} \end{bmatrix} \\
&= \begin{bmatrix} \mathcal{J}(\omega_{m,1})Q_1\bar{x}_{TS,1} - \mathcal{R}(\omega_{m,1})Q_1 x_{TS,1} \\ \mathcal{J}(\omega_{m,2})Q_2\bar{x}_{TS,2} - \mathcal{R}(\omega_{m,2})Q_2 x_{TS,2} \\ \mathcal{J}(\omega_{m,3})Q_3\bar{x}_{TS,3} - \mathcal{R}(\omega_{m,3})Q_3 x_{TS,3} \\ \mathcal{J}(\omega_{m,4})Q_4\bar{x}_{TS,4} - \mathcal{R}(\omega_{m,4})Q_4 x_{TS,4} \end{bmatrix} = \begin{bmatrix} M_1(z_1) \\ M_2(z_2) \\ M_3(z_3) \\ M_4(z_4) \end{bmatrix}
\end{aligned}
$$

$$
\nabla M(z) = \begin{bmatrix} \nabla M_1(z_1) & 0_{8x8} & 0_{8x8} & 0_{8x8} \\ 0_{8x8} & \nabla M_2(z_2) & 0_{8x8} & 0_{8x8} \\ 0_{8x8} & 0_{8x8} & \nabla M_3(z_3) & 0_{8x8} \\ 0_{8x8} & 0_{8x8} & 0_{8x8} & \nabla M_4(z_4) \end{bmatrix} = \text{bdiag}\{M_i(z_i)\} \tag{5.31}
$$

It is apparent that $\nabla M(z)$ for the entire system is a diagonal matrix with the $\nabla M(z)$ of each turbine string along the diagonal. Term III is thereby monotonically decreasing if the criterion 3.106 and 3.107 are satisfied for each turbine string in the wind park *independently*.

$$
\begin{aligned}
&\nabla M(z) + \nabla^{\top} M(z) - 2\gamma \text{ bdiag}\{g(\bar{x}_{TS,i})^{PMSG} g(\bar{x}_{TS,i})^{PMSG^{\top}}\} \\
&= \text{bdiag}\big\{\nabla M_i(z_i) + \nabla^{\top} M_i(z_i) - 2\gamma g(\bar{x}_{TS,i})^{PMSG} g(\bar{x}_{TS,i})^{PMSG^{\top}}\big\}
\end{aligned} \tag{5.32}
$$

Assuming that stability criteria are satisfied in each turbine string, Term III is negative semi-definite. Term IV is positive definite as $R_{grid} \geq 0$. The time derivative of the LCF can be written

as:

$$\dot{\mathcal{V}} \leq \widetilde{y}^{\top}\widetilde{U} + \widetilde{y}^{PMSG^{\top}}\gamma\widetilde{y}^{PMSG}$$
$$\dot{\mathcal{V}} \leq -\widetilde{y}^{\top}K_P\widetilde{y} + \widetilde{y}^{PMSG^{\top}}\gamma\widetilde{y}^{PMSG}$$
$$\dot{\mathcal{V}} \leq -\Big(\sum_{i=1}^{4}\widetilde{y}_i^{PMSG^{\top}}\left(K_{P,i}^{PMSG} - \gamma_i I_{2x2}\right)\widetilde{y}_i^{PMSG} + \sum_{i=1}^{4}\widetilde{y}_i^{G^{\top}}K_{P,i}^{G}\widetilde{y}_i^{G}\Big) \leq 0$$

where $y_i^{\top} = \widetilde{x}_{TS,i}^{\top}Q_i g(\bar{x}_{TS,i})$.

It can thereby be concluded that if the following criteria are satisfied for each turbine string, and the converters are tuned such that $K_{P,i} > \gamma$ at each turbine, then the overall interconnected wind park is guaranteed to be stable for large disturbances with a local decentralized tuning.

$$2d_i - 2\frac{\partial T_{m,i}(\omega_{m,i})}{\partial \omega_m, i} - \frac{\left(\bar{i}_{q,i}\frac{P_i}{2}L_i\right)^2}{2(r+\gamma\bar{V}_{c,i}^2)} \geq 0$$
$$2\left(G_i + \gamma\bar{i}_{q,i}^2\right) - \frac{\left(2\gamma\bar{i}_{q,i}\bar{V}_{c,i}\right)}{2(r_i+\gamma\bar{V}_{c,i}^2)} \geq 0$$

5.6 Conclusion

In this chapter, a *stability certificate* for a wind park with four wind turbines is developed. The stability proof will hold for a wind park with n turbines as it is enough to satisfy the criterion at each wind turbine. In conclusion, a *scalable stability certificate* for a wind park of size n has been developed.

The *stability certificate* for the wind park states that stability for the entire system is guaranteed when the stability criteria for each turbine string are satisfied locally. The stability criteria for a single turbine string are developed in Appendix D and shown to be the same as found in section 3.3.

$$2d - 2\frac{\partial T_m(\omega_m)}{\partial \omega_m} - \frac{\left(\bar{i}_q\frac{P}{2}L\right)^2}{2(r+\gamma\bar{V}_c^2)} \geq 0 \tag{5.33}$$
$$2\left(G + \gamma\bar{i}_q^2\right) - \frac{\left(2\gamma\bar{i}_q\bar{V}_c\right)}{2(r+\gamma\bar{V}_c^2)} \geq 0 \tag{5.34}$$

Chapter 6

Conclusion and Future Work

6.1 Conclusion

This master thesis presents a *stability certificate* to guarantee large signal stability for a wind park. With the help of non-linear control theory concepts such as passivity in combination with Lyapunov stability and port-Hamiltonian modeling, stability criteria are derived for a wind energy conversion system consisting of a wind turbine, a permanent magnet synchronous generator, and a full scale back-to-back 2L-VSCs. The *stability certificate* is generalized for any number of wind turbines by utilizing graph theory and its connection to port-Hamiltonian modeling through the incidence matrix $\mathcal{B}$.

6.1.1 Scalable Stability Certificate for a Wind Park

The major result of this master thesis is a scalable certificate for a wind park that guarantees large signal stability. To ensure the stability of the entire wind park, it is sufficient to satisfy the local stability criteria at each turbine string. Such decentralized control is beneficial in multiple ways. It does not require an exchange of information between turbine strings and the grid, nor the need for communication between the turbine strings. The control structure for the wind park is, therefore, simple, as each turbine can be controlled independently from the others. From a commercial viewpoint, it is beneficial for the companies delivering the different components in the wind park to avoid sharing their company secrets as it is unnecessary to ensure stability. Another great advantage of decentralized control is that it allows for unlimited expansion as long the stability is satisfied at each turbine string. Such a *scalable stability certificate* with a *plug-and-play* feature can allow for needed continuous expansion of distributed renewable resources without risking jeopardizing the stability of the power grid.

6.1.2 PMSG Design to Guarantee Stability

In criterion 3.106, one can see how the PI controller only affects the last term. As a consequence, the damping d must be designed such that it counteracts the second term to fulfill the stability criterion. The damper windings in the rotor are a part of the design process of the machine; hence, the stability certificate should therefore ideally be a part of the design process as well to guarantee large signal stability. Including the certificate in the design process also minimizes the risk of sacrificing too much performance by having over-dimensioned damper windings.

6.1.3 Competitive Performance for PI-PBC

In section 4.2.2 the industry standard PI current controllers are compared with the PI-PBCs designed in this thesis. The performance is very similar when the two controller types are tuned identically. The simplicity of the PI current controllers might seem appealing to some. However, unlike the PI-PBCs, which can guarantee large signal stability, the current controllers do not have that feature. Therefore, the PI-PBCs are the preferred controller type of the two when they are tuned identically and subjected to the disturbances explained in subsection 4.2.2.

6.1.4 Practical use of Stability Certificate Without Compromising Performance

The stability certificates for the systems developed in this master thesis consist of a turbine string of increasing complexity with passive feedback loops. In subsection 4.2.2, it is shown that the control performance is greatly improved when PI-controlled outer loops are implemented. Implementing outer loops ultimately does jeopardize the stability guarantee provided by the stability certificate as the system is altered, even though it is possible to argue that stability still can be guaranteed by invoking the assumption of time scale separation. A practical solution is proposed to combine the desired large signal stability guarantee provided by the stability certificate and the improved performance of implementing a cascaded control structure. The outer loops are used to have the turbine operating at maximum efficiency, thereby extracting the maximum power from the wind. When instability is detected, the outer loops are disconnected. As the stability is guaranteed by the now valid stability certificate, the system will regain a stable operation. The outer loops can now be reconnected to increase performance.

6.1.5 The effect of damping in a PMSG

In section 4.3 it was briefly discussed the impact of increasing the damping had on the control performance of the WECS. The result was that higher damping led to faster convergence. This result could be relevant for power systems controlled with PBCs as it has been reported to give poor control performance without the help of outer loops. The inclusion of PMSG is in this thesis shown to be unproblematic if the stability criteria are satisfied and could therefore potentially be used to improve performance in power systems without jeopardizing the stability guarantee by reducing –potentially removing– the need for including outer loops.

6.2 Future work

6.2.1 Damping

The damping in the synchronous generator that in this thesis is represented by the coefficient d is essential to ensure stable operation, as seen by the stability criteria developed. It is therefore of great interest to be able to measure, calculate and design the damping in the generator. In subsection 3.3.3 a method for designing the damping by adjusting the resistance in the damper windings was proposed. It is not delved deeper into whether this method of adjusting the damping is a good one or not. This topic should be further explored, as sufficient damping guarantees stable operation for a single wind energy conversion system and an entire wind park.

6.2.2 Robustness Issues

As briefly discussed in subsection 4.2.2, the simulated system has some robustness issues. The new equilibrium points must be recalculated when subjected to a constantly changing wind. For smaller systems, the computational processing power needed is limited, but as the system expands, likewise

does the computational power needed. The calculation of the equilibrium points also require a perfect model of the system. Creating a perfect model of the system is a close to impossible task, therefore, different methods to solve the equilibrium calculations could be a topic for future research.

6.2.3 Comparison of PI-PBC and PI Current Controller

An interesting research topic could also be a more comprehensive comparison of the PI-PBC and the PI current controller. When the two controllers are tuned identically, the performance is very similar. Tuning them separately from stability- and a performance perspective could be interesting. While the PI-PBC is able to guarantee large signal stability, the PI current controller might result in a better performance. How to decide the trade-off between the two is, therefore, an interesting topic that could be investigated.

6.2.4 Virtual Controllable Damping

By choice of Lyapunov candidate function in this master thesis, it is shown that a certain damping is needed to ensure the stability of the system. This damping is provided by the damper windings in the PMSG. The PMSG must therefore be designed with sufficient damping. In chapter 2, it is shown that during the rotor's acceleration to the desired working condition is where the highest amount of damping is needed. This means that most of the time, having designed the PMSG with advanced damper windings to provide sufficient damping is unnecessary. It could therefore be advantageous to replace the physical damping with a virtual controllable damping. A topic for future work is to find a Lyapunov function that, by use of the energy in the controller, can render the system passive. If such a Lyapunov function exists, it would be a superior solution to only providing damping by damper windings. A controllable damping is much more flexible and most likely less expensive as it does not depend on physical components.

6.2.5 Passive Controller that Directly Controls the Rotor Speed

In this master thesis, the rotors angular velocity is indirectly controlled through the PI-PBCs. With some exceptions, a cascaded control structure is utilized. To extract maximal energy from the wind, it is essential to have the ideal tip speed ratio. It is therefore desired to control the speed of the wind turbine directly. A topic for future work is to design a passive controller that directly controls the rotor speed of the wind turbine.

6.2.6 Simulation of the wind park

Due to time constraints, simulations of the wind park to test the *stability certificate* has been left for future work.

Bibliography

[1] Melanee Thomas et al. 'Great expectations: Public opinion about energy transition'. In: *Energy Policy* 162 (2022), p. 112777. ISSN: 0301-4215. DOI: https://doi.org/10.1016/j.enpol.2022.112777. URL: https://www.sciencedirect.com/science/article/pii/S0301421522000027.

[2] Norwegian Water Resources and Energy Directorate. *Opprinnelsesgarantier og varedeklarasjon for strømleverandører*. URL: https://www.nve.no/energi/virkemidler/opprinnelsesgarantier-og-varedeklarasjon-for-stromleverandorer/#:~:text=Opprinnelsesgarantier%5C%20er%5C%20en%5C%20merkeordning%5C%20for,kraft%5C%20og%5C%20ikke%5C%2Dfornybar%5C%20kraft. (visited on 8th June 2022).

[3] International Energy Agency. *World Energy Outlook 2021*. 2021.

[4] Ritchie H., Roser M. and Rosado P. 'Energy'. In: *Our World in Data* (2020). URL: https://ourworldindata.org/energy.

[5] Ritchie H., Roser M. and Rosado P. 'CO and Greenhouse Gas Emissions'. In: *Our World in Data* (2020). URL: https://ourworldindata.org/co2-and-other-greenhouse-gas-emissions.

[6] Salvatore D'Arco, Jon Are Suul and Olav B. Fosso. 'A Virtual Synchronous Machine implementation for distributed control of power converters in SmartGrids'. In: *Electric Power Systems Research* 122 (2015), pp. 180–197. DOI: 10.1016/j.epsr.2015.01.001..

[7] Pieter Tielens and Dirk Van Hertem. 'The relevance of inertia in power systems'. In: *Renewable and Sustainable Energy Reviews* 55 (2016), pp. 999–1009. ISSN: 1364-0321.

[8] International Energy Agency. *Renewables 2021, analysis and forecast to 2026*. 2021.

[9] Global Wind Energy Council. *GWEC — GLOBAL WIND REPORT 2021*. 2021.

[10] MUSIAL W. et al. *Offshore Wind Market Report: 2021 Edition*. 2021.

[11] Norwegian Government. *Major initiative to promote offshore wind power*. URL: https://www.regjeringen.no/en/aktuelt/major-initiative-to-promote-offshore-wind-power/id2900436/ (visited on 23rd May 2022).

[12] O. Anaya-Lara et al. *Offshore Wind Energy Generation*. Vol. 1. Wiley, 2014, pp. 73–153.

[13] Devonie mcCamey. *What We Know—and Do Not Know—About Achieving a National-Scale 100% Renewable Electric Grid*. URL: https://www.nrel.gov/news/features/2021/what-we-know-and-dont-know-about-achieving-a-national-scale-100-renewable-electric-grid.html (visited on 12th Apr. 2022).

[14] Johan Morren, Jan Pierik and Sjoerd W.H. de Haan. 'Comparison between linear and non-linear control strategies for variable speed wind turbines'. In: *Control Engineering Practice* 18.12 (2010), pp. 1357–1368.

[15] Rafael Cisneros et al. 'An adaptive passivity-based controller for a wind energy conversion system'. In: (2019), pp. 4852–4857.

[16] J.M. Carrasco et al. 'Power-Electronic Systems for the Grid Integration of Renewable Energy Sources: A Survey'. In: *IEEE Transactions on Industrial Electronics* 53.4 (2006), pp. 1002–1016. DOI: 10.1109/TIE.2006.878356.

[17] Shafiullah Md., Ahmed Shakir D. and Al-Sulaiman Fahad A. 'Grid Integration Challenges and Solution Strategies for Solar PV Systems: A Review'. In: *IEEE Access* 10 (2022), pp. 52233–52257. DOI: 10.1109/ACCESS.2022.3174555.

[18] Shakir D. Ahmed et al. 'Grid Integration Challenges of Wind Energy: A Review'. In: *IEEE Access* 8 (2020), pp. 10857–10878. DOI: 10.1109/ACCESS.2020.2964896.

[19] A. van der Schaft and D. Jeltsema. *Port-Hamiltonian Systems Theory: An Introductory Overview*. Vol. 1. 2014, pp. 173–378.

[20] Qing-Chang Zhong and Márcio Stefanello. 'Port-Hamiltonian control of power electronic converters to achieve passivity'. In: (2017), pp. 5092–5097. DOI: 10.1109/CDC.2017.8264413.

[21] Gilbert Bergna-Diaz, Santiago Sanchez and Elisabetta Tedeschi. 'Port Hamiltonian Modelling of Modular Multilevel Converters with Fixed Equilibrium Point'. In: *Twelfth International Conference on Ecological Vehicles and Renewable Energies (EVER)* (2017). DOI: 10.1109/EVER.2017.7935911.

[22] S. Fiaz et al. 'On port-Hamiltonian Modeling of the Synchronous Generator and Ultimate Boundedness of its solutions'. In: *IFAC Proceedings Volumes* (2012), pp. 30–35. ISSN: 1474-6670. DOI: 10.3182/20120829-3-IT-4022.00042.

[23] Daniele Zonetti, Romeo Ortega and Abdelkrim Benchaib. 'Modeling and control of HVDC transmission systems from theory to practice and back'. In: *Control Engineering Practice* 45 (2015), pp. 133–146. ISSN: 0967-0661. DOI: https://doi.org/10.1016/j.conengprac.2015.09.012. URL: https://www.sciencedirect.com/science/article/pii/S096706611530023X.

[24] Hassan Khalil. *Nonlinear Systems*. Vol. 3. 2001, pp. 111–259.

[25] Sh Zare, A.R. Tavakolpour-Saleh and T. Binazadeh. 'Passivity based-control technique incorporating genetic algorithm for design of a free piston Stirling engine'. In: *Renewable Energy Focus* 28 (2019), pp. 66–77. ISSN: 1755-0084. DOI: https://doi.org/10.1016/j.ref.2018.11.003. URL: https://www.sciencedirect.com/science/article/pii/S1755008418303569.

[26] Kelly R., Carelli R. and Ortega R. 'Adaptive motion control design of robot manipulators: an input-output approach'. In: *International Journal of Control* 50.6 (1989), pp. 2563–2581. DOI: 10.1080/00207178908953515.

[27] R. Ortega et al. 'Control by Interconnection and Standard Passivity-Based Control of Port-Hamiltonian Systems'. In: *IEEE Transactions on Automatic Control* 53.11 (2008), pp. 2527–2542. DOI: 10.1109/TAC.2008.2006930.

[28] S. Fiaz et al. 'A port-Hamiltonian approach to power network modeling and analysis'. In: *European Journal of Control* 19.6 (2013), pp. 477–485. ISSN: 0947-3580. DOI: https://doi.org/10.1016/j.ejcon.2013.09.002. URL: https://www.sciencedirect.com/science/article/pii/S094735801300157X.

[29] Nandhini Sayeekumar et al. 'Graph theory and its applications in power systems - a review'. In: (2015), pp. 154–157. DOI: 10.1109/ICCICCT.2015.7475267.

[30] Felix Strehle et al. 'Towards Port-Hamiltonian Modeling of Multi-Carrier Energy Systems: A Case Study for a Coupled Electricity and Gas Distribution System'. In: *IFAC-PapersOnLine* 51.2 (2018). 9th Vienna International Conference on Mathematical Modelling, pp. 463–468. ISSN: 2405-8963. DOI: https://doi.org/10.1016/j.ifacol.2018.03.078. URL: https://www.sciencedirect.com/science/article/pii/S240589631830082X,.

[31] N. Monshizadeh et al. 'Conditions on Shifted Passivity of Port-Hamiltonian Systems'. In: *Syst. Control. Lett.* 123 (2019), pp. 55–61.

[32] V.I Arnold. *Mathematical Methods of Classical Mechanics*. Vol. 60. Springer Science Business Media, 2013.

[33] Simo Puntanen, George P. H. Styan (auth.) and Fuzhen Zhang (eds.) *The Schur complement and its applications*. Vol. 4. Springer, 2015.

[34] Edward Wilson Kimbark. 'Damper Windings and Damping'. In: *Power System Stability*. 1995, pp. 214–246. DOI: 10.1109/9780470545614.ch14.

[35] E. Schlemmer. 'Damping of synchronous machines -analytical estimations versus finite element results'. In: (2009), pp. 751–754. DOI: 10.1109/ICCEP.2009.5211969.

[36] P.S. Bimbhra. *Generalized Theory of Electrical Machines*. Vol. 5th ed. Khanna Publisher, 1995, p. 303.

[37] Siegfried Heier. *Grid integration of wind energy. Onshore and offshore conversion systems.* Vol. Third edition. Wiley, 2014.

[38] Chee-Mun Ong. *Dynamic Simulation of Electric Machinery.* Vol. vol. 1. Prentice Hall, 1998.

[39] Ling S. J., Moebs W. and Sanny. J. *University Physics Volume 2.* Vol. 2. "OpenStax", 2016. URL: https://openstax.org/books/university-physics-volume-2/pages/1-introduction.

[40] Tianfu Sun, Jiabin Wang and Xiao Chen. 'Maximum Torque Per Ampere (MTPA) Control for Interior Permanent Magnet Synchronous Machine Drives Based on Virtual Signal Injection'. In: *IEEE Transactions on Power Electronics* 30.9 (2015), pp. 5036–5045. DOI: 10.1109/TPEL.2014.2365814.

[41] Ned Mohan, Tore M. Undeland and William P.Robbins. *Power Electronics Converters, Applications and Design.* Vol. 3. John Wiley Sons, Inc, 2003.

[42] Nagwa F. Ibrahim and Sobshy S Dessouky. *Design and Implementation of Voltage Soruce Converters in HVDC Systems.* Vol. 1. Springer, 2021.

[43] Xiaodong Liang. 'Emerging Power Quality Challenges Due to Integration of Renewable Energy Sources'. In: *IEEE Transactions on Industry Applications* 53.2 (2017), pp. 855–866. DOI: 10.1109/TIA.2016.2626253.

[44] Hunyár M. and Veszprémi K. 'Reactive power control of wind turbines'. In: *2014 16th International Power Electronics and Motion Control Conference and Exposition* (2014), pp. 348–352. DOI: 10.1109/EPEPEMC.2014.6980517.

[45] Wei Gan, Hongchao Ji and Xingwu Yang. 'A three-phase PWM rectifier with reactive power compensation function'. In: (2014), pp. 1–4. DOI: 10.1109/APPEEC.2014.7066073.

[46] Balchen J. G., Andresen T. and Foss B. A. *Reguleringsteknikk.* Vol. 6. 2016.

[47] Gulur Srinivas, Iyer Vishnu Mahadeva and Bhattacharya Subhashish. 'A Dual-Loop Current Control Structure With Improved Disturbance Rejection for Grid-Connected Converters'. In: *IEEE Transactions on Power Electronics* 34.10 (2019), pp. 10233–10244. DOI: 10.1109/TPEL.2019.2891686.

[48] Gilbert Bergna-Diaz et al. 'PI Passivity-Based Control and Performance Analysis of MMC Multiterminal HVDC Systems'. In: *IEEE Journal of Emerging and Selected Topics in Power Electronics* 7.4 (2019), pp. 2453–2466. DOI: 10.1109/JESTPE.2018.2889152.

[49] Arjan Schaft and Bernhard Maschke. 'Port-Hamiltonian Systems on Open Graphs'. In: *SIAM Journal on Control and Optimization* 51 (Jan. 2010). DOI: 10.1137/110840091.

[50] Brandon N. Cassimere, Scott D. Sudhoff and Doug H. Sudhoff. 'Analytical Design Model for Surface-Mounted Permanent-Magnet Synchronous Machines'. In: *IEEE Transactions on Energy Conversion* 24.2 (2009), pp. 347–357. DOI: 10.1109/TEC.2009.2016139.

[51] P. Krause et al. *Analysis of Electric Machinery and Drive Systems.* Vol. 3. 2013, pp. 86–210.

[52] J. Kinnunen et al. 'Design of damper windings for permanent magnet synchronous machines'. In: *International Review of Electrical Engineering* 2 (Mar. 2007), pp. 260–272.

Appendix A

Complete back-to-back Wind Power System

In section 3.2, the hypothesis, "Only using the converter closest to the PMSG is enough to compensate for the lack of monotonicity inherent to the machine, and thus to render the rest of the system passive." was investigated and proved to be true. In this part of the appendix, we use both converters to render the system passive.

Equation 3.65 is repeated here for ease.

$$\dot{x} = \underbrace{\big(J(\omega_m) + J_0 + J_5 - R)\big)\nabla\mathcal{H}(x) + E}_{f(x)} + \underbrace{\big[J_1\nabla\mathcal{H}(x)\ J_2\nabla\mathcal{H}(x)\ J_3\nabla\mathcal{H}(x)\ J_4\nabla\mathcal{H}(x)\big]}_{g(x)} \underbrace{\begin{bmatrix} u_1 \\ u_2 \\ u_3 \\ u_4 \end{bmatrix}}_{\boldsymbol{u}} \tag{A.1}$$

From the equation it's clear that the $g(x)$ matrix contains the control input from both converters. Written out g(x) becomes

$$\underbrace{\begin{bmatrix} 0&0&0&-1&0&0 \\ 0&0&0&0&0&0 \\ 0&0&0&0&0&0 \\ 1&0&0&0&0&0 \\ 0&0&0&0&0&0 \\ 0&0&0&0&0&0 \end{bmatrix}}_{J_1} \underbrace{\begin{bmatrix} i_d \\ i_q \\ \omega_m \\ V_c \\ i_d^G \\ i_q^G \end{bmatrix}}_{\nabla\mathcal{H}(x)} \underbrace{\begin{bmatrix} 0&0&0&0&0&0 \\ 0&0&0&-1&0&0 \\ 0&0&0&0&0&0 \\ 0&1&0&0&0&0 \\ 0&0&0&0&0&0 \\ 0&0&0&0&0&0 \end{bmatrix}}_{J_2} \underbrace{\begin{bmatrix} i_d \\ i_q \\ \omega_m \\ V_c \\ i_d^G \\ i_q^G \end{bmatrix}}_{\nabla\mathcal{H}(x)} \underbrace{\begin{bmatrix} 0&0&0&0&0&0 \\ 0&0&0&0&0&0 \\ 0&0&0&0&0&0 \\ 0&0&0&0&-1&0 \\ 0&0&0&1&0&0 \\ 0&0&0&0&0&0 \end{bmatrix}}_{J_3} \underbrace{\begin{bmatrix} i_d \\ i_q \\ \omega_m \\ V_c \\ i_d^G \\ i_q^G \end{bmatrix}}_{\nabla\mathcal{H}(x)} \underbrace{\begin{bmatrix} 0&0&0&0&0&0 \\ 0&0&0&0&0&0 \\ 0&0&0&0&0&0 \\ 0&0&0&0&0&-1 \\ 0&0&0&0&0&0 \\ 0&0&0&1&0&0 \end{bmatrix}}_{J_4} \underbrace{\begin{bmatrix} i_d \\ i_q \\ \omega_m \\ V_c \\ i_d^G \\ i_q^G \end{bmatrix}}_{\nabla\mathcal{H}(x)}$$

$$g(x) = \begin{bmatrix} -V_c & 0 & 0 & 0 \\ 0 & -V_c & 0 & 0 \\ 0 & 0 & 0 & 0 \\ i_d & i_q & -i_d^G & -i_q^G \\ 0 & 0 & V_c & 0 \\ 0 & 0 & 0 & V_c \end{bmatrix} \tag{A.2}$$

Checking for monotonicity
To check if the expression

$$\nabla^\top M(z) + \nabla M(z) - 2\gamma g(\bar{x})g^\top(\bar{x}) \leq 0 \tag{A.3}$$

is negative semidefinite, the term $g(\bar{x})g^\top(\bar{x})$ needs to be computed

$$g(\bar{x})g^\top(\bar{x}) = \underbrace{\begin{bmatrix} -\bar{V}_c & 0 & 0 & 0 \\ 0 & -\bar{V}_c & 0 & 0 \\ 0 & 0 & 0 & 0 \\ \bar{i}_d & \bar{i}_q & -\bar{i}_d^G & -\bar{i}_q^G \\ 0 & 0 & \bar{V}_c & 0 \\ 0 & 0 & 0 & \bar{V}_c \end{bmatrix}}_{g(\bar{x})} \underbrace{\begin{bmatrix} -\bar{V}_c & 0 & 0 & \bar{i}_d & 0 & 0 \\ 0 & -\bar{V}_c & 0 & \bar{i}_q & 0 & 0 \\ 0 & 0 & 0 & -\bar{i}_d^G & \bar{V}_c & 0 \\ 0 & 0 & 0 & -\bar{i}_q^G & 0 & \bar{V}_c \end{bmatrix}}_{g^\top(\bar{x})}$$

$$g(\bar{x})g^\top(\bar{x}) = \begin{bmatrix} \bar{V}_c^2 & 0 & 0 & -\bar{i}_d\bar{V}_c & 0 & 0 \\ 0 & \bar{V}_c^2 & 0 & -\bar{i}_q\bar{V}_c & 0 & 0 \\ 0 & 0 & 0 & 0 & 0 & 0 \\ -\bar{i}_d\bar{V}_c & -\bar{i}_q\bar{V}_c & 0 & \bar{i}_d^2+\bar{i}_q^2+\bar{i}_d^{G2}+\bar{i}_q^{G2} & -\bar{i}_d^G\bar{V}_c & -\bar{i}_q^G\bar{V}_c \\ 0 & 0 & 0 & -\bar{i}_d^G\bar{V}_c & \bar{V}_c^2 & 0 \\ 0 & 0 & 0 & -\bar{i}_q^G\bar{V}_c & 0 & \bar{V}_c^2 \end{bmatrix} \tag{A.4}$$

The expression for $\nabla M(z)$ is equal to 3.74, and by setting $\bar{i}_d = 0$, the total expression becomes:

$$\underbrace{\begin{bmatrix} -r & 0 & 0 & 0 & 0 & 0 \\ 0 & -r & 0 & 0 & 0 & 0 \\ L\frac{P}{2}\bar{i}_q & 0 & -d & 0 & 0 & 0 \\ 0 & 0 & 0 & -G & 0 & 0 \\ 0 & 0 & 0 & 0 & -r_G & 0 \\ 0 & 0 & 0 & 0 & 0 & -r_G \end{bmatrix}}_{\nabla^\top M(z)} + \underbrace{\begin{bmatrix} -r & 0 & L\frac{P}{2}\bar{i}_q & 0 & 0 & 0 \\ 0 & -r & 0 & 0 & 0 & 0 \\ 0 & 0 & -d & 0 & 0 & 0 \\ 0 & 0 & 0 & -G & 0 & 0 \\ 0 & 0 & 0 & 0 & -r_G & 0 \\ 0 & 0 & 0 & 0 & 0 & -r_G \end{bmatrix}}_{\nabla M(z)} - 2\gamma \underbrace{\begin{bmatrix} \bar{V}_c^2 & 0 & 0 & 0 & 0 & 0 \\ 0 & \bar{V}_c^2 & 0 & -\bar{i}_q\bar{V}_c & 0 & 0 \\ 0 & 0 & 0 & 0 & 0 & 0 \\ 0 & -\bar{i}_q\bar{V}_c & 0 & \bar{i}_q^2+\bar{i}_d^{G2}+\bar{i}_q^{G2} & -\bar{i}_d^G\bar{V}_c & -\bar{i}_q^G\bar{V}_c \\ 0 & 0 & 0 & -\bar{i}_d^G\bar{V}_c & \bar{V}_c^2 & 0 \\ 0 & 0 & 0 & -\bar{i}_q^G\bar{V}_c & 0 & \bar{V}_c^2 \end{bmatrix}}_{g(\bar{x})g^\top(\bar{x})} \leq 0$$

$$\begin{bmatrix} -2(r+\gamma\bar{V}_c^2) & 0 & L\frac{P}{2}\bar{i}_q & 0 & 0 & 0 \\ 0 & -2(r+\gamma\bar{V}_c^2) & 0 & 2\gamma\bar{i}_q\bar{V}_c & 0 & 0 \\ L\frac{P}{2}\bar{i}_q & 0 & -2d & 0 & 0 & 0 \\ 0 & 2\gamma\bar{i}_q\bar{V}_c & 0 & -2G-2\gamma(\bar{i}_q^2+\bar{i}_d^{G2}+\bar{i}_q^{G2}) & 2\gamma\bar{i}_d\bar{V}_c & 2\gamma\bar{i}_q^G\bar{V}_c \\ 0 & 0 & 0 & 2\gamma\bar{i}_d\bar{V}_c & -2(r_G+\gamma\bar{V}_c^2) & 0 \\ 0 & 0 & 0 & 2\gamma\bar{i}_q^G\bar{V}_c & 0 & -2(r_G+\gamma\bar{V}_c^2) \end{bmatrix} \leq 0 \tag{A.5}$$

To show that matrix A.5 is negative semi-definite, the Schur complement is utilized

$$-X = \begin{bmatrix} A & B \\ B^\top & C \end{bmatrix} \tag{A.6}$$

As before, to say that X is negative semi-definite, is the same as -X is positive semi-definite

Matrix A, B and C are defined as follows:

$$\begin{aligned} A &= \begin{bmatrix} 2(r+\gamma\bar{V}_c^2) & 0 \\ 0 & 2(r+\gamma\bar{V}_c^2) \end{bmatrix} \\ B &= \begin{bmatrix} -L\frac{P}{2}\bar{i}_q & 0 & 0 & 0 \\ 0 & -2\gamma\bar{i}_q\bar{V}_c & 0 & 0 \end{bmatrix} \\ C &= \begin{bmatrix} 2d & 0 & 0 & 0 \\ 0 & 2G+2\gamma(\bar{i}_q^2+\bar{i}_d^{G2}+\bar{i}_q^{G2}) & -2\gamma\bar{i}_d\bar{V}_c & -2\gamma\bar{i}_q^G\bar{V}_c \\ 0 & -2\gamma\bar{i}_d\bar{V}_c & 2(r_G+\gamma\bar{V}_c^2) & 0 \\ 0 & -2\gamma\bar{i}_q^G\bar{V}_c & 0 & 2(r_G+\gamma\bar{V}_c^2) \end{bmatrix} \end{aligned} \tag{A.7}$$

$$\frac{X}{A} = C - B^\top A^{-1} B$$

$$C - B^\top A^{-1} B = \begin{bmatrix} 2d & 0 & 0 & 0 \\ 0 & 2G + 2\gamma(\bar{i}_d^2 + \bar{i}_q^2 + \bar{i}_q^{G2}) & -2\gamma \bar{i}_d \bar{V}_c & -2\gamma \bar{i}_q^G \bar{V}_c \\ 0 & -2\gamma \bar{i}_d \bar{V}_c & 2(r_G + \gamma \bar{V}_c^2) & 0 \\ 0 & -2\gamma \bar{i}_q^G \bar{V}_c & 0 & 2(r_G + \gamma \bar{V}_c^2) \end{bmatrix}$$
$$- \begin{bmatrix} -L\frac{P}{2}\bar{i}_q & 0 & 0 & 0 \\ 0 & -2\gamma \bar{i}_q \bar{V}_c & 0 & 0 \end{bmatrix} \begin{bmatrix} -\frac{1}{2(r+\gamma \bar{V}_c^2)} & 0 \\ 0 & -\frac{1}{2(r+\gamma \bar{V}_c^2)} \end{bmatrix} \begin{bmatrix} -L\frac{P}{2}\bar{i}_q & 0 \\ 0 & -2\gamma \bar{i}_q \bar{V}_c \\ 0 & 0 \\ 0 & 0 \end{bmatrix}$$
$$= \begin{bmatrix} 2d - \frac{L^2 P^2 i_q^{G2}}{8(\gamma \bar{V}_c^2 + r)} & 0 & 0 & 0 \\ 0 & 2G + 2\gamma(\bar{i}_d^2 + \bar{i}_q^2 + \bar{i}_q^{G2}) - \frac{2\bar{V}_c^2 \bar{i}_q^2 \gamma^2}{\gamma \bar{V}_c^2 + r} & -2\bar{V}_c \bar{i}_d \gamma & -2\bar{V}_c \bar{i}_q^G \gamma \\ 0 & -2\bar{V}_c \bar{i}_d \gamma & 2(r_G + \gamma \bar{V}_c^2) & 0 \\ 0 & -2\bar{V}_c \bar{i}_q^G \gamma & 0 & 2(r_G + \gamma \bar{V}_c^2) \end{bmatrix} \tag{A.8}$$

From the expression above, it's not clear whether the matrix is positive- or negative semi-definite. To make it more obvious, the Schur complement is utilized again, resulting in a 2×2 matrix instead

The following choice of A_2, B_2 and C_2 is made:

$$A_2 = \begin{bmatrix} 2d - \frac{L^2 P^2 \bar{i}_q^{G2}}{8(\gamma \bar{V}_c^2 + r)} & 0 \\ 0 & 2G + 2\gamma(\bar{i}_d^2 + \bar{i}_q^2 + \bar{i}_q^{G2}) - \frac{2\bar{V}_c^2 \bar{i}_q^2 \gamma^2}{\gamma \bar{V}_c^2 + r} \end{bmatrix} = \begin{bmatrix} A_{2,11} & A_{2,12} \\ A_{2,21} & A_{2,22} \end{bmatrix}$$
$$B_2 = \begin{bmatrix} 0 & 0 \\ -2\bar{V}_c \bar{i}_d \gamma & -2\bar{V}_c \bar{i}_q^G \gamma \end{bmatrix} \tag{A.9}$$
$$C_2 = \begin{bmatrix} 2(r_G + \gamma \bar{V}_c^2) & 0 \\ 0 & 2(r_G + \gamma \bar{V}_c^2) \end{bmatrix}$$

$$\frac{X_2}{A_2} = C_2 - B_2^\top A_2^{-1} B_2 = \begin{bmatrix} a_{11} & a_{12} \\ a_{21} & a_{22} \end{bmatrix} \tag{A.10}$$

where

$$a_{11} = 2(r_G + \gamma \bar{V}_c^2) - \frac{2\bar{V}_c^2 \bar{i}_d^2 \gamma^2 (r + \gamma \bar{V}_c^2)}{\bar{V}_c^2 \bar{i}_q^{G2} \gamma^2 + \bar{V}_c^2 \bar{i}_d^2 \gamma^2 + G\bar{V}_c^2 \gamma + r\bar{i}_q^{G2} \gamma + r\bar{i}_q^2 \gamma + r\bar{i}_d^2 \gamma + Gr}$$
$$a_{12} = -\frac{2\bar{V}_c^2 \bar{i}_d \bar{i}_q^G \gamma^2 (r + \gamma \bar{V}_c^2)}{\bar{V}_c^2 \bar{i}_q^{G2} \gamma^2 + \bar{V}_c^2 \bar{i}_d^2 \gamma^2 + G\bar{V}_c^2 \gamma + r\bar{i}_q^{G2} \gamma + r\bar{i}_q^2 \gamma + r\bar{i}_d^2 \gamma + Gr}$$
$$a_{21} = -\frac{2\bar{V}_c^2 \bar{i}_d \bar{i}_q^G \gamma^2 (r + \gamma \bar{V}_c^2)}{\bar{V}_c^2 \bar{i}_q^{G2} \gamma^2 + \bar{V}_c^2 \bar{i}_d^2 \gamma^2 + G\bar{V}_c^2 \gamma + r\bar{i}_q^{G2} \gamma + r\bar{i}_q^2 \gamma + r\bar{i}_d^2 \gamma + Gr}$$
$$a_{22} = 2(r_G + \gamma \bar{V}_c^2) - \frac{2\bar{V}_c^2 \bar{i}_q^{G2} \gamma^2 (r + \gamma \bar{V}_c^2)}{\bar{V}_c^2 \bar{i}_q^{G2} \gamma^2 + \bar{V}_c^2 \bar{i}_d^2 \gamma^2 + G\bar{V}_c^2 \gamma + r\bar{i}_q^{G2} \gamma + r\bar{i}_q^2 \gamma + r\bar{i}_d^2 \gamma + Gr}$$

Just as before, it is not clear whether the matrix is positive- or negative semi-definite. With the help of the Schur complement one last time and by choosing $A_3 = a_{11}$, $B_3 = a_{12}$ and $C_3 = a_{22}$ one gets:

$$\frac{2(r_G + \gamma \bar{V}_c)(G\bar{V}^4 \gamma^2 + Grr_G + \bar{V}_c \bar{i}_d^2 r_G \gamma^2 + \bar{V}_c \bar{i}_q^{G2} r_G \gamma^2 + \bar{V}_c \bar{i}_q^2 r \gamma^2 + G\bar{V}_c^2 r\gamma + G\bar{V}_c^2 r_G \gamma + \bar{i}_d^2 r r_G \gamma + \bar{i}_q^{G2} r r_G \gamma + \bar{i}_q^{G2} r r_G \gamma)}{G\bar{V}_c^4 \gamma^2 + Grr_G + \bar{V}_c^4 \bar{i}_q^{G2} \gamma^3 + \bar{V}_c^2 \bar{i}_d^2 r_G \gamma^2 + \bar{V}_c^2 \bar{i}_q^{G2} r\gamma^2 + \bar{V}_c^2 \bar{i}_q^{G2} r_G \gamma^2 + \bar{V}_c^2 \bar{i}_q^2 r\gamma^2 + G\bar{V}_c^2 r\gamma + G\bar{V}_c^2 r_G \gamma + \bar{i}_d^2 r r_G \gamma + \bar{i}_q^{G2} r r_G \gamma + \bar{i}_q^2 r r_G \gamma} \tag{A.11}$$

The expression could be further simplified to:

$$\frac{2(\bar{V}_c^2 \gamma + r_G)(G\bar{V}_c^4 \gamma^2 + Grr_G + \bar{V}_c^2 \gamma^2 (\bar{i}_d^2 r_G + \bar{i}_q^{G2} r_G + \bar{i}_q^2 r) + G\bar{V}_c^2 \gamma (r + r_G) + r r_G \gamma (\bar{i}_d^2 + \bar{i}_q^{G2} + \bar{i}_q^2))}{G\bar{V}_c^4 \gamma^2 + Grr_G + \bar{V}_c^4 \bar{i}_q^{G2} \gamma^3 + \bar{V}_c^2 \gamma^2 (\bar{i}_d^2 r_G + i_q^{G2} r + i_q^{G2} r_G + i_q^2 r) + G\bar{V}_c^2 \gamma (r + r_G) + r r_G \gamma (\bar{i}_d^2 + i_q^{G2} + i_q^2)} \tag{A.12}$$

From the expression one could observe that it is always positive semi-definite with a choice of a positive γ. The Schur complement also demands that all choices of A is positive semi-definite, i.e., the choice of A, A_2 and A_3 all have to be positive semi-definite. By choosing γ according to 3.45, A.7 is guaranteed to be positive definite. From the A_2 matrix in A.9, one can see that it is similar to 3.43. By choosing a suitable γ and making sure the damping is sufficiently high one is able to make $A_{2,11}$ positive. By expanding $A_{2,22}$ one is able to see that it is always positive, with a positive choice of γ

$$A_{2,22} = 2G + 2\gamma(\bar{i}_d^2 + \bar{i}_q^2 + \bar{i}_q^{G2}) - \frac{2\bar{V}_c^2\bar{i}_q^2\gamma^2}{\gamma\bar{V}_c^2 + r}$$

$$2G\gamma\bar{V}_c^2 + 2Gr + 2\gamma\bar{V}_c^2(\bar{i}_d^2 + \bar{i}_q^{g2}) + 2\gamma r(\bar{i}_d^2 + \bar{i}_q^2 + \bar{i}_q^{G2}) \geq 0 \tag{A.13}$$

Expanding a_{11} in Equation A.10 results in

$$\begin{aligned} a_{11} = {} & \bar{V}_c^2\gamma^2\bar{i}_q^{G2}(r_G + \gamma\bar{V}_c^2) + r_G\bar{V}_c^2\bar{i}_d^2\gamma^2 + r_gG\bar{V}_c^2\gamma + G\bar{V}_c^4\gamma^2 \\ & + r_gr\gamma(\bar{i}_q^{G2} + \bar{i}_q^2 + \bar{i}_d^2) + \bar{V}_c^2\gamma^2r(\bar{i}_q^{G2} + \bar{i}_q^2) + Gr(r_G + \bar{V}_c^2\gamma) \end{aligned} \tag{A.14}$$

From the expression one can see that it is positive semi-definite.

Conclusion
As before, the choice of LCF is chosen as the Hamiltonian of the shifted system, i.e. the Hamiltonian of the incremental model.

$$\mathcal{V}(\widetilde{x}) = \mathcal{H}(\widetilde{x}) = \frac{1}{2}\widetilde{x}^\top Q\widetilde{x} \tag{A.15}$$

Condition I and II for this LCF, are by definition satisfied as shown in section 3.1

Condition IV is satisfied as well, since

$$\nabla^\top M(z) + \nabla M(z) - 2\gamma g(\bar{x})g^\top(\bar{x}) \leq 0 \tag{A.16}$$

Condition III is also satisfied, and a similar procedure as in section 3.2 can be used to show this.

All conditions are therefore satisfied, i.e., a wind energy conversion system with back-to-back 2L-VSCs can be made asymptotically stable using passive feedback for control of both converters.

Appendix B

Derivation of Model Equations

This part of the appendix is concerned with the model derivation of the wind energy conversion system from the specialization project, and is included for the sake of completeness.

To be able to get an understanding of how the permanent magnet synchronous machine works, a mathematical model must be constructed.

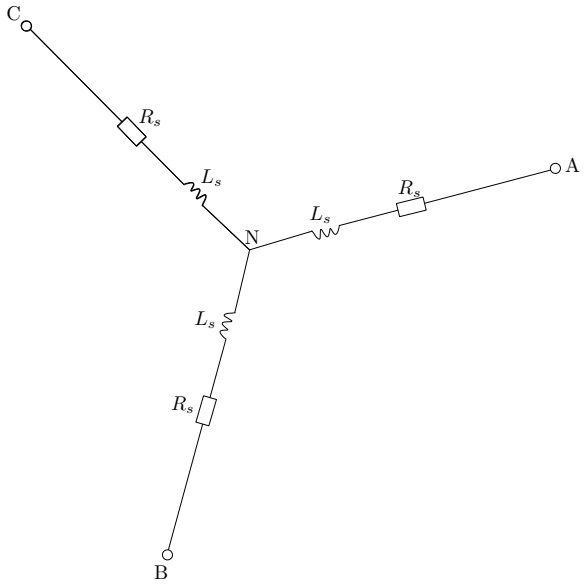

Figure B.1: PMSG electrical scheme

By looking at Figure B.1 above, the voltage equations for the three phases in the stator, measured between the respective phases and the neutral point can be found as:

$$V_s^a = R_s i_s^a + \frac{d\lambda_s^a}{dt} \tag{B.1}$$

$$V_s^b = R_s i_s^b + \frac{d\lambda_s^b}{dt} \tag{B.2}$$

$$V_s^c = R_s i_s^c + \frac{d\lambda_s^c}{dt} \tag{B.3}$$

The term $R_s i_s$ represents the losses in each phase, and is mainly heat dissipation due to the current flowing in the wires. The term $\frac{d\lambda_s}{dt}$ is the change of flux linkage in the stator. The flux linkage λ_s is composed of the flux generated in the stator, but also the permanent flux in the rotor, due to the permanent magnet.

$$\lambda_{abcs} = \phi_s * N + \phi_r * N = L_s i^s_{abc} + \lambda_r \tag{B.4}$$

ϕ_s and ϕ_r is the flux in the stator and rotor respectively. N is the number of turns in the stator windings. L_s is the inductance and i^s_{abc} is the current flowing in the phases. λ_r is the flux linkage due to the permanent magnets in the rotor.

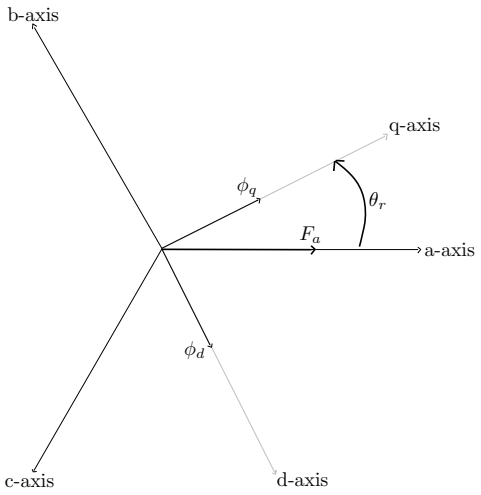

Figure B.2: Flux and mmf component

If one were to begin by considering the magnetic flux caused by the current flowing in the a-phase and decomposing it into its d- and q flux components it would result in

$$\phi_d = P_d F_a \sin(\theta_r) \tag{B.5}$$
$$\phi_q = P_q F_a \cos(\theta_r) \tag{B.6}$$

P_d and P_q are the permeance of the d and q-axis. F_a is the magnetomotive force in the a-phase stator winding. θ_r is the angle between the a-axis and the q-axis. See Figure B.2 for a detailed orientation of the axes

The flux linkage of these decomposed fluxes with the a-phase winding is expressed as

$$\lambda_{aa} = N_s(\phi_d \sin(\theta_r) + \phi_q \cos(\theta_r)) \tag{B.7}$$
$$\lambda_{aa} = N_s F_a(P_d \sin^2(\theta_r) + P_q \cos^2(\theta_r)) \tag{B.8}$$
$$\lambda_{aa} = N_s F_a(\frac{P_d + P_q}{2} - \frac{P_d - P_q}{2}\cos(2\theta_r)), \tag{B.9}$$

where N_s is the number of turns in the winding. The linkage of the dq flux components with the b-phase winding which leads the a-phase winding by $\frac{2\pi}{3}$ is then:

$$\lambda_{ba} = N_s F_a(P_d \sin(\theta_r)\sin(\theta_r - \frac{2\pi}{3}) + P_q \cos(\theta_r)\cos(\theta_r - \frac{2\pi}{3})) \tag{B.10}$$
$$\lambda_{ba} = N_s F_a(-\frac{P_d + P_q}{4} - \frac{P_d - P_q}{2}\cos 2(\theta_r - \frac{\pi}{3})) \tag{B.11}$$

By defining the new variables

$$L_0 = N_s F_a \frac{P_d + P_q}{2} \tag{B.12}$$
$$L_{ms} = N_s F_a \frac{P_d - P_q}{2} \tag{B.13}$$

one can now express the self inductance in the stator a-phase winding as

$$L_{aa} = L_0 - L_{ms}\cos(2\theta_r) \tag{B.14}$$

The equation above is the self inductance excluding the leakage inductance. The mutual inductance between the a-phase and b-phase then becomes

$$L_{ab} = L_{ba} = -\frac{L_0}{2} - L_{ms}\cos 2(\theta_r - \frac{\pi}{3}) \tag{B.15}$$

The deduction of the flux expressions are based on the works of [38]

Permanent magnets rotors could be salient or non-salient. If one were to study a salient PMSG, the assumption of equal P_d and P_q could be invoked. This is due to the symmetry and the fact that the airgap "seen" by the stator windings will be uniform, since the permeance of the magnets are very similar to the permeance of air. In a non-salient rotor, the airgap "seen" by the stator windings would not be uniform, and the assumptions of equal permeance would not be correct[50]. Setting $P_d = P_q$ in B.9 yields

$$\lambda_{aa} = N_s F_a(\frac{P_d + P_q}{2}) \tag{B.16}$$

The same simplification is also possible in B.11

$$\lambda_{ba} = N_s F_a(-\frac{P_d + P_q}{4}) \tag{B.17}$$

From the two expressions above, one can now see that the rotor dependence is gone and this simplifies the calculations significantly.
By utilizing the relationship between flux linkage and inductance, the resulting inductance matrix will take the form

$$L_{ss} = \begin{bmatrix} L_{ms} + L_0 & -\frac{1}{2}L_0 & -\frac{1}{2}L_0 \\ -\frac{1}{2}L_0 & L_{ms} + L_0 & -\frac{1}{2}L_0 \\ -\frac{1}{2}L_0 & -\frac{1}{2}L_0 & L_{ms} + L_0 \end{bmatrix} \tag{B.18}$$

L_{ms} is the magnetizing inductance and L_0 is the leakage inductance. To simplify the calculations even more, a transformations to the rotors $qd0$ reference frame is advised. This is done through the Park transformation.

$$P = \frac{2}{3}\begin{bmatrix} \cos(\theta) & \cos(\theta - \frac{2\pi}{3}) & \cos(\theta + \frac{2\pi}{3}) \\ \sin(\theta) & \sin(\theta - \frac{2\pi}{3}) & \sin(\theta + \frac{2\pi}{3}) \\ \frac{1}{2} & \frac{1}{2} & \frac{1}{2} \end{bmatrix} \tag{B.19}$$

In a three phase resistive circuit

$$\mathbf{V}^s_{abc} = \mathbf{r}_s \mathbf{i}^s_{abc} \tag{B.20}$$

The park transformation of B.20 then becomes

$$\mathbf{V}^s_{qd0} = P\mathbf{r}_s P^{-1}\mathbf{i}^s_{qd0} \tag{B.21}$$

If one were to assume that the resistances of the three stator windings are equal, which is something that is true due to the design of the machine, the expression simplifies to

$$\mathbf{V}^s_{qd0} = \mathbf{r}_s \mathbf{i}^s_{qd0} \tag{B.22}$$

since

$$P\mathbf{r}_s P^{-1} = \mathbf{r}_s \tag{B.23}$$

In a three phase inductive circuit one has

$$\mathbf{v}^s_{abc} = \frac{d\lambda^s_{abc}}{dt} \tag{B.24}$$

The park transformation then becomes

$$\mathbf{v}^s_{qd0} = P\frac{dP^{-1}\lambda^s_{qd0}}{dt} \tag{B.25}$$

Expanded, this becomes

$$\mathbf{v}_{qd0}^{s} = P\frac{dP^{-1}}{dt}\lambda_{qd0}^{s} + PP^{-1}\frac{d\lambda_{qd0}^{s}}{dt} \tag{B.26}$$

By the help of some trigonometric identities, one can write B.26

$$\mathbf{v}_{qd0}^{s} = \omega\lambda_{qd0}^{s} + \frac{d\lambda_{qd0}^{s}}{dt} \tag{B.27}$$

because

$$P\frac{dP^{-1}}{dt} = \omega\begin{bmatrix} 0 & 1 & 0 \\ -1 & 0 & 0 \\ 0 & 0 & 0 \end{bmatrix} \tag{B.28}$$

See [51] and equation (3.4-10) for more information.
The flux linkages in the new reference frame can be expressed as

$$\lambda_{qd0}^{s} = P\mathbf{L}_s P^{-1}\mathbf{i}_{qd0}^{s} \tag{B.29}$$

From the expression above, one can express $\mathbf{L}_s$ as

$$\mathbf{L}_s = P\mathbf{L}_s P^{-1} \tag{B.30}$$

In this case, one would get

$$\frac{2}{3}\begin{bmatrix} \cos(\theta) & \cos(\theta-\frac{2\pi}{3}) & \cos(\theta+\frac{2\pi}{3}) \\ \sin(\theta) & \sin(\theta-\frac{2\pi}{3}) & \sin(\theta+\frac{2\pi}{3}) \\ \frac{1}{2} & \frac{1}{2} & \frac{1}{2} \end{bmatrix}\begin{bmatrix} L_{ls}+L_0 & -\frac{1}{2}L_0 & -\frac{1}{2}L_0 \\ -\frac{1}{2}L_0 & L_{ls}+L_0 & -\frac{1}{2}L_0 \\ -\frac{1}{2}L_0 & -\frac{1}{2}L_0 & L_{ls}+L_0 \end{bmatrix}\begin{bmatrix} \cos(\theta) & \sin(\theta) & 1 \\ \cos(\theta-\frac{2\pi}{3}) & \sin(\theta-\frac{2\pi}{3}) & 1 \\ \cos(\theta+\frac{2\pi}{3}) & \sin(\theta+\frac{2\pi}{3}) & 1 \end{bmatrix} \tag{B.31}$$

$$\mathbf{L}_s = \begin{bmatrix} \frac{3}{2}L_{ms}+L_0 & 0 & 0 \\ 0 & \frac{3}{2}L_{ms}+L_0 & 0 \\ 0 & 0 & L_0 \end{bmatrix} = \begin{bmatrix} L_q & 0 & 0 \\ 0 & L_d & 0 \\ 0 & 0 & L_{ms} \end{bmatrix} \tag{B.32}$$

The flux linkage established by the permanent magnet is a sinusoidal wave displaced by 120° between the phases

$$\lambda^{r} = \begin{bmatrix} \sin(\theta_r) \\ \sin(\theta_r-\frac{2\pi}{3}) \\ \sin(\theta_r+\frac{2\pi}{3}) \end{bmatrix} \tag{B.33}$$

The complete flux linkage is then

$$\lambda_{qd0}^{s,r} = \lambda_{qd0}^{s} + \lambda^{r} \tag{B.34}$$

The complete voltage equations referred to the rotating dq-frame thus becomes

$$\mathbf{v}_{qd0}^{s} = \mathbf{r}_s\mathbf{i}_{qd0}^{s} + \omega_r\lambda_{qd0}^{s,r} + \frac{d\lambda_{qd0}^{s,r}}{dt} \tag{B.35}$$

If one were to expand the expression

$$v_q = r_s i_q^{s} + \omega_r\lambda_d + \frac{d\lambda_q}{dt} \tag{B.36}$$

$$v_d = r_s i_d^{s} - \omega_r\lambda_q + \frac{d\lambda_d}{dt} \tag{B.37}$$

$$v_0 = r_s i_0^{s} + \frac{d\lambda_0}{dt} \tag{B.38}$$

By utilizing the relationship between the inductance and current, and also the relationship between mechanical- and electrical angular velocity the following model could be found.

$$L_q\dot{i}_q = -r_s i_q - L_d i_d\frac{P}{2}\omega_m + \lambda_d^{r}\frac{P}{2}\omega_m - v_{qs} \tag{B.39}$$

$$L_d\dot{i}_d = -r_s i_d + L_q i_q\frac{P}{2}\omega_m - v_{ds} \tag{B.40}$$

where

$$\omega_e = \frac{P}{2}\omega_m, \tag{B.41}$$

and P is the number of magnetic poles in the machine.
The sign of v_{qs} and v_{ds} is negative due to the fact that the machine of interest is a generator, not a motor. Assuming no demagnetization, λ_d^r is constant and will be denoted by ϕ hereafter. A assumption of equal permeance in the q- and d axis was made earlier in the development of the inductance matrix, this leads to the next assumptions which is that the inductance in the q- and d axis is also roughly the same. By considering all the new assumptions, the final equations becomes

$$L\dot{i}_q = -r_s i_q - Li_d\frac{P}{2}\omega_m + \phi\frac{P}{2}\omega_m - v_q \tag{B.42}$$

$$L\dot{i}_d = -r_s i_d + Li_q\frac{P}{2}\omega_m - v_d \tag{B.43}$$

The two equations above describes the electrical relationship in the generator, and will be the starting point for the port-Hamiltonian analysis to come. The only thing left now, is therefore an equation describing the mechanical relationship of the machine.
The well know torque relationship in an electrical machine, based on Newton's law of rotation states that

$$J\dot{\omega}_m = T_m - T_e \tag{B.44}$$

J is the inertia of the machine. ω_m is the angular velocity, T_m is the mechanical torque, and T_e is the electrical torque.
The total power of a three-phase machine is

$$P^s_{abc} = v^s_a i^s_a + v^s_b i^s_b + v^s_c i^s_c \tag{B.45}$$

The total power have to be equal in both dq and abc variables, therefore

$$P^s_{qd0} = P^s_{abc} = \frac{3}{2}(v^s_q i^s_q + v^s_d i^s_d + 2v^s_0 i^s_0) \tag{B.46}$$

The factor $\frac{3}{2}$ is due to the park transformation. Utilizing the relationship $P = T\omega$ one would get

$$T_e\frac{2}{P}\omega_m = \frac{3}{2}(v^s_q i^s_q + v^s_d i^s_d + 2v^s_0 i^s_0) \tag{B.47}$$

Inserting equation B.36, B.37, B.38 into the above equation yields

$$T_e\frac{2}{P}\omega_m = \underbrace{\frac{3}{2}r_s(i^{s\,2}_q + i^{s\,2}_d + 2i^{s\,2}_0)}_{\text{Ohmic losses}} + \frac{3}{2}(\lambda^s_d i^s_q - \lambda^s_q i^s_d)\omega_m + \underbrace{\frac{3}{2}(i^s_q\frac{d\lambda^s_q}{dt} + i^s_d\frac{d\lambda^s_d}{dt} + 2i^s_0\frac{d\lambda^s_0}{dt})}_{\text{Change of stored magnetic energy}} \tag{B.48}$$

Equating the coefficients of ω_m gives

$$T_e = \frac{3}{2}\frac{P}{2}(\lambda^s_d i^s_q - \lambda^s_q i^s_d) \tag{B.49}$$

By utilizing the relationship between flux linkage λ, inductance and current, one would get

$$T_e = \frac{3}{2}\frac{P}{2}(\phi i^s_q + (L_d - L_q)i^s_q i^s_d) \tag{B.50}$$

Since $L_d = L_q$ in this case, the final expression for the electrical torque is

$$T_e = \frac{3}{2}\frac{P}{2}\phi i^s_q \tag{B.51}$$

The expression describing the relationship between electrical end mechanical torque is thus

$$J\dot{\omega}_m = T_m - T_e = T_m - \frac{3}{2}\frac{P}{2}\phi i^s_q \tag{B.52}$$

To make the model more realistic a damping term is also introduced in the mechanical torque expression

$$J\dot{\omega}_m = T_m - \frac{3}{2}\frac{P}{2}\phi i_q^s + d(\omega_{ref} - \omega_m) \tag{B.53}$$

The last term in Equation B.53 describes the damping in the system. d is the damping coefficient and is chosen in the design process of the machine. The damping term represents a damper winding, which in steady state does not affect the system, since in steady state $\omega_m = \omega_{ref}$, for a synchronous machine. When the reference speed, i.e angular velocity of the rotating magnetic field put up by the stator currents, ω_e, is different from the angular velocity of the magnetic field put up by the permanent magnets on the rotor, the damper winding influence the system. Damper windings in synchronous machines are included to damp the sub-transient oscillations that could occur during a fault. They are also used to develop what is called pull-in torque, which makes the machine go from asynchronous mode to synchronous mode. The torque produced by the damper winding is zero when the machine operates in synchronous mode [52]

Appendix C

PI Controller

The industry standard is a proportional integral controller, or abbreviated as PI controller. To find a similar criterion for a PI controller, one must first expand the Lyapunov function to include the "energy" from the controller. This is due to the fact that the Lyapunov function has to depend on all the states, including those representing the controller

$$W(x,z) = V(x) + \frac{1}{2}\tilde{z}K_I\tilde{z} \tag{C.1}$$

The second part of C.1 represents the energy stored in the PI controller, while $V(x)$ is the Lyapunov function representing the stored energy in the generator. The PI is expressed as

$$u = -K_P y + K_I z \tag{C.2}$$

$$\dot{z} = y \tag{C.3}$$

Expanding the new Lyapunov function results in

$$\dot{W} = \dot{V} + (K_I\tilde{z})^\top \dot{\tilde{z}} \tag{C.4}$$

$$\begin{aligned}
I: &\quad \dot{W} = y^\top\tilde{u} + \gamma y^\top y + (K_I\tilde{z})^\top\dot{\tilde{z}} \\
II: &\quad \dot{W} = y^\top\tilde{u} + \gamma y^\top y - \tilde{z}^\top K_I y \\
III: &\quad \dot{W} = y^\top\tilde{u} + \gamma y^\top y - y^\top K_I(z-\bar{z}) \\
IV: &\quad \dot{W} = y^\top\tilde{u} + \gamma y^\top y - y^\top K_I z + y^\top K_I\bar{z} \\
V: &\quad \dot{W} = y^\top(u-\bar{u}) + \gamma y^\top y - y^\top(u+K_P y) + y^\top K_I\bar{z} \\
VI: &\quad \dot{W} = -y^\top\bar{u} + \gamma y^\top y - y^\top K_P y + y^\top K_I\bar{z} \\
VII: &\quad \dot{W} = \gamma y^\top y - y^\top K_P y
\end{aligned} \tag{C.5}$$

Step explanations:

C.4 - I The expression for $\dot{V}(x)$, included the PI regulator is inserted

I - II $\dot{\tilde{z}} = \dot{z}$-$\dot{\bar{z}} = \dot{z} =$ -y

II - III Rearranging and $\tilde{z} = z$-$\bar{z}$

III - IV Expanding last term of [III]

IV - V $\tilde{u} = u$-$\bar{u}$ and $K_I z = u + K_P y$

V - VI Cancelling $y^\top u$ in first term with $-y^\top u$ in third term

VI - VII Cancelling $K_I\bar{z} = \bar{u}$ in last term with fist term in

The expression found above is equal to the one found for a proportional controller, i.e. the criterion becomes the same

$$\dot{W} = -y^\top[K_P - \gamma I]y \leq 0, \text{ if } K_P > \gamma \tag{C.6}$$

Appendix D

Stability Analysis of a Turbine String

To investigate the stability of the system, the incremental model is developed:

$$\begin{array}{lll} & \dot{x} = & \left(\mathcal{J}(\omega_m) + \mathcal{J}_0 + \mathcal{J}_5 + \mathcal{J}_6 + \mathcal{J}_7 - \mathcal{R}(\omega_m)\right) Qx + E + g(x)u \\ - & 0 = & \left(\mathcal{J}(\bar{\omega_m}) + \mathcal{J}_0 + \mathcal{J}_5 + \mathcal{J}_6 + \mathcal{J}_7 - \mathcal{R}(\bar{\omega}_m)\right) Q\bar{x} + E + g(\bar{x})\bar{u} \\ \hline & \dot{\widetilde{x}} = & (\mathcal{J}_0 + \mathcal{J}_5 + \mathcal{J}_6 + \mathcal{J}_7)Q\widetilde{x} + \mathcal{J}(\omega_m)Qx - \mathcal{R}(\omega_m)Qx - \mathcal{J}(\bar{\omega}_m)Q\bar{x} + \mathcal{R}(\bar{\omega}_m)Q\bar{x} + g(x)u - g(\bar{x})\bar{u} \end{array}$$

The term $g(x)u - g(\bar{x})\bar{u}$, can be reformulated to $g(\widetilde{x})u + g(\bar{x})\widetilde{u}$. The incremental model can then be formulated as:

$$\dot{\widetilde{x}} = \Big(\mathcal{J}_0 + \sum_{i=i}^{4} \mathcal{J}_i u_i + \sum_{i=5}^{7} \mathcal{J}_i\Big) Q\widetilde{x} + \mathcal{J}(\omega_m)Qx - \mathcal{R}(\omega_m)Qx - \mathcal{J}(\bar{\omega}_m)Q\bar{x} + \mathcal{R}(\bar{\omega}_m)Q\bar{x} + g(\bar{x})\widetilde{u} \quad \text{(D.1)}$$

As before the Lyapunov candidate function (LCF) is inspired by the Hamiltonian of the incremental model. $\mathcal{V} = \frac{1}{2}\widetilde{x}^\top Q\widetilde{x}$. As before condition I and II for such a Lyapunov function are always satisfied. To investigate the stability, condition III and IV must be tested. The time derivative of the LCF is, $\dot{\mathcal{V}}(x) = \widetilde{x}^\top Q\dot{\widetilde{x}}$:

$$\begin{aligned}
I: \quad \dot{\mathcal{V}}(x) &= \widetilde{x}^\top Q\Big(\mathcal{J}_0 + \sum_{i=i}^{4} \mathcal{J}_i u_i + \sum_{i=5}^{7} \mathcal{J}_i\Big) Q\widetilde{x} + \widetilde{x}^\top Q\mathcal{J}(\omega_m)Q - \widetilde{x}^\top Q\mathcal{R}(\omega_m)Qx - \widetilde{x}^\top Q\mathcal{J}(\bar{\omega}_m)Q\bar{x} \\
&\quad + \widetilde{x}^\top Q\mathcal{R}(\bar{\omega}_m)Q\bar{x} + \underbrace{\widetilde{x}^\top Qg(\bar{x})}_{y^\top}\widetilde{u} \\
II: \quad \dot{\mathcal{V}}(x) &= y^\top\widetilde{u} + \widetilde{x}^\top Q\mathcal{J}(\omega_m)Qx - \widetilde{x}^\top Q\mathcal{R}(\omega_m)Qx - \widetilde{x}^\top Q\mathcal{J}(\bar{\omega}_m)Q\bar{x} + \widetilde{x}^\top Q\mathcal{R}(\bar{\omega}_m)Q\bar{x} \\
&\quad + \underbrace{\widetilde{x}^\top Q\mathcal{J}(\omega_m)Q\bar{x} - \widetilde{x}^\top Q\mathcal{J}(\omega_m)Q\bar{x}}_{0} \\
III: \quad \dot{\mathcal{V}}(x) &= y^\top\widetilde{u} + \underbrace{\widetilde{x}^\top Q\mathcal{J}(\omega_m)(Qx - Q\bar{x})}_{0} - \widetilde{x}^\top Q\mathcal{R}(\omega_m)Qx - \widetilde{x}^\top Q\mathcal{J}(\bar{\omega}_m)Q\bar{x} + \widetilde{x}^\top Q\mathcal{R}(\bar{\omega}_m)Q\bar{x} \\
&\quad + \widetilde{x}^\top Q\mathcal{J}(\omega_m)Q\bar{x} \\
IV: \quad \dot{\mathcal{V}}(x) &= y^\top\widetilde{u} + \widetilde{x}^\top Q\Big[\big(\mathcal{J}(\omega_m) - \mathcal{J}(\bar{\omega}_m)\big)Q\bar{x} - \mathcal{R}(\omega_m)Qx + \mathcal{R}(\bar{\omega}_m)Q\bar{x}\Big] \\
V: \quad \dot{\mathcal{V}}(x) &= y^\top\widetilde{u} + \widetilde{x}^\top Q\Big[\big(\mathcal{J}(\omega_m) - \mathcal{J}(\bar{\omega}_m)\big)Q\bar{x} - \mathcal{R}(\omega_m)Qx + \mathcal{R}(\bar{\omega}_m)Q\bar{x}\Big] + \widetilde{x}^\top Q\left(\gamma g(\bar{x})^{PMSG} g(\bar{x})^{PMSG^\top}\right) Q\widetilde{x} \\
&\quad - \widetilde{x}^\top Q\left(\gamma g(\bar{x})^{PMSG} g(\bar{x})^{PMSG^\top}\right) Q\widetilde{x} \\
VI: \quad \dot{\mathcal{V}}(x) &= -y^\top\widetilde{u} + \widetilde{x}^\top Q\Big[\big(J(\omega_m) - \mathcal{J}(\bar{\omega}_m)\big)Q\bar{x} - \mathcal{R}(\omega_m)Qx + \mathcal{R}(\bar{\omega}_m)Q\bar{x} \\
&\quad - \gamma g(\bar{x})^{PMSG} g(\bar{x})^{PMSG^\top} Q\widetilde{x}\Big] + {y^{PMSG}}^\top \gamma y^{PMSG} \\
VII: \quad \dot{\mathcal{V}}(x) &= -y^\top\widetilde{u} + {y^{PMSG}}^\top \gamma y^{PMSG} + (z - \bar{z})^\top\Big[M(z) - M(\bar{z}) - \gamma g(\bar{x})^{PMSG} g(\bar{x})^{PMSG^\top}(z - \bar{z})\Big]
\end{aligned}$$

Step explanations:

I Due to skewsymetry the terms $\mathcal{J}_0, \mathcal{J}_1, \mathcal{J}_2, \mathcal{J}_3, \mathcal{J}_4, \mathcal{J}_5, \mathcal{J}_6$ and $\mathcal{J}_7$ are eliminated. The passive output, $\widetilde{x}^\top g(\bar{x})$, is collected to a term $y^\top$

II Zero is added to the equation by adding and subtracting the term, $\widetilde{x}^\top Q\mathcal{J}(\omega_m)Q\bar{x}$

III Due to skew symmetry $\widetilde{x}^\top Q\mathcal{J}(\omega_m)(Qx - Q\bar{x}) = 0$

IV The expression is factorised.

V A term containing the passive output feedback is included to help render the system passive. The term is added and subtracted such that system does not change properties. As shown in section 3.2 it is possible to render the system passive only using the output feedback from the converter closest to the generator.

VI Using the definition of the passive output from I

VII Two new definitions are introduced $z \triangleq Qx$ and $M(z) \triangleq \mathcal{J}(\omega_m)\bar{z} - \mathcal{R}(\omega_m)z$.

The time derivative of the LCF can be expressed as:

$$\dot{\mathcal{V}}(x) = -y^\top \widetilde{u} + y^{PMSG^\top}\gamma y^{PMSG} + \underbrace{(z-\bar{z})^\top\Big[M(z) - M(\bar{z}) - \gamma g(\bar{x})^{PMSG} g(\bar{x})^{PMSG^\top}(z-\bar{z})\Big]}_{TermIII} \tag{D.2}$$

Checking for monotonicity

In section 3.1 it is shown that if Term III is monotonically decreasing, condition III and IV can be satisfied by use of a PI controller when K_p is chosen greater than γ. As stated in section 3.1, to check if $M(z) - M(\widetilde{z}) - \gamma g(\bar{x})^{PMSG} g(\bar{x})^{PMSG^\top}\widetilde{z}$ is monotonically decreasing, is equivalent to checking whether the following term is negative semi-definite.

$$\nabla^\top M(z) + \nabla M(z) - 2\gamma g(\bar{x})^{PMSG} g(\bar{x})^{PMSG^\top} \leq 0$$

$M(z)$ is defined as:

$$\begin{aligned}
M(z) &= \mathcal{J}(\omega_m)\bar{z} - \mathcal{R}(\omega_m)z \\
&= \frac{P}{2}L \begin{bmatrix} 0 & \omega_m & 0&0&0&0&0&0 \\ -\omega_m & 0 & 0&0&0&0&0&0 \\ 0&0&0&0&0&0&0&0 \\ 0&0&0&0&0&0&0&0 \\ 0&0&0&0&0&0&0&0 \\ 0&0&0&0&0&0&0&0 \\ 0&0&0&0&0&0&0&0 \\ 0&0&0&0&0&0&0&0 \end{bmatrix} \begin{bmatrix} \bar{i}_d \\ \bar{i}_q \\ \bar{\omega}_m \\ \bar{V}_c \\ \bar{i}_d^G \\ \bar{i}_q^G \\ \bar{V}_{pcc}^d \\ \bar{V}_{pcc}^q \end{bmatrix} - \begin{bmatrix} r & 0 & 0 & 0 & 0 & 0 & 0 & 0 \\ 0 & r & 0 & 0 & 0 & 0 & 0 & 0 \\ 0 & 0 & d - \frac{T_m(\omega_m)}{\omega_m} & 0 & 0 & 0 & 0 & 0 \\ 0 & 0 & 0 & G_{dc} & 0 & 0 & 0 & 0 \\ 0 & 0 & 0 & 0 & r_G & 0 & 0 & 0 \\ 0 & 0 & 0 & 0 & 0 & r_G & 0 & 0 \\ 0 & 0 & 0 & 0 & 0 & 0 & G_{pcc} & 0 \\ 0 & 0 & 0 & 0 & 0 & 0 & 0 & G_{pcc} \end{bmatrix} \begin{bmatrix} i_d \\ i_q \\ \omega_m \\ V_c \\ i_d^G \\ i_q^G \\ V_{pcc}^d \\ V_{pcc}^q \end{bmatrix} \\
&= \begin{bmatrix} \frac{P}{2}L\omega_m\bar{i}_q - ri_d \\ -\frac{P}{2}L\omega_m\bar{i}_d - ri_q \\ -d\omega_m + T_m(\omega_m) \\ -G_{dc}V_c \\ -r_G i_d^G \\ -r_G i_q^G \\ -G_{_{pcc}V_{pcc}^d} \\ -G_{_{pcc}V_{pcc}^q} \end{bmatrix}
\end{aligned}$$

$$\nabla M(z) = \begin{bmatrix} -r & 0 & \bar{i}_q \frac{P}{2} L & 0 & 0 & 0 & 0 & 0 \\ 0 & -r & -\bar{i}_d \frac{P}{2} L & 0 & 0 & 0 & 0 & 0 \\ 0 & 0 & -d + \frac{\partial \bar{T}_m(\omega_m)}{\partial \omega_m} & 0 & 0 & 0 & 0 & 0 \\ 0 & 0 & 0 & -G_{dc} & 0 & 0 & 0 & 0 \\ 0 & 0 & 0 & 0 & -r_G & 0 & 0 & 0 \\ 0 & 0 & 0 & 0 & 0 & -r_G & 0 & 0 \\ 0 & 0 & 0 & 0 & 0 & 0 & -G_{pcc} & 0 \\ 0 & 0 & 0 & 0 & 0 & 0 & 0 & -G_{pcc} \end{bmatrix} \tag{D.3}$$

$$g(\bar{x})^{PMSG} g(\bar{x})^{PMSG^\top} = \begin{bmatrix} \bar{V}_c^2 & 0 & 0 & -\bar{i}_d \bar{V}_c & 0 & 0 & 0 & 0 \\ 0 & \bar{V}_c^2 & 0 & -\bar{i}_q \bar{V}_c & 0 & 0 & 0 & 0 \\ 0 & 0 & 0 & 0 & 0 & 0 & 0 & 0 \\ -\bar{V}_c \bar{i}_d & -\bar{V}_c \bar{i}_q & 0 & \bar{i}_d^2 + \bar{i}_q^2 & 0 & 0 & 0 & 0 \\ 0 & 0 & 0 & 0 & 0 & 0 & 0 & 0 \\ 0 & 0 & 0 & 0 & 0 & 0 & 0 & 0 \\ 0 & 0 & 0 & 0 & 0 & 0 & 0 & 0 \\ 0 & 0 & 0 & 0 & 0 & 0 & 0 & 0 \end{bmatrix} \tag{D.4}$$

At the equilibrium it is desired that the d-axis current component in the generator is zero, such that the generator is operating at maximum torque per ampere. $\bar{i}_d = 0$. Putting the expression together results in:

$$\nabla^\top M(z) + \nabla M(z) - 2\gamma g(\bar{x})^{PMSG} g(\bar{x})^{PMSG^\top} =$$

$$\begin{bmatrix} -2(r + \gamma \bar{V}_c^2) & 0 & \bar{i}_q \frac{P}{2} L & 0 & 0 & 0 & 0 & 0 \\ 0 & -2(r + \gamma \bar{V}_c^2) & 0 & 2\gamma \bar{i}_q \bar{V}_c & 0 & 0 & 0 & 0 \\ \bar{i}_q \frac{P}{2} L & 0 & -2d + 2\frac{\partial T_m(\omega_m)}{\partial \omega_m} & 0 & 0 & 0 & 0 & 0 \\ 0 & 2\gamma \bar{i}_q \bar{V}_c & 0 & -2\left(G_{dc} + \gamma \bar{i}_q^2\right) & 0 & 0 & 0 & 0 \\ 0 & 0 & 0 & 0 & -2r_G & 0 & 0 & 0 \\ 0 & 0 & 0 & 0 & 0 & -2r_G & 0 & 0 \\ 0 & 0 & 0 & 0 & 0 & 0 & -2G_{pcc} & 0 \\ 0 & 0 & 0 & 0 & 0 & 0 & 0 & -2G_{pcc} \end{bmatrix} \tag{D.5}$$

Using the Schur complement to investigate negative semi-definiteness of D.5. The matrices are chosen as:

$$A = \begin{bmatrix} -2(r + \gamma \bar{V}_c^2) & 0 & \bar{i}_q \frac{P}{2} L & 0 \\ 0 & -2(r + \gamma \bar{V}_c^2) & 0 & 2\gamma \bar{i}_q \bar{V}_c \\ \bar{i}_q \frac{P}{2} L & 0 & -2d + 2\frac{T_m(\omega_m)}{\omega_m} & 0 \\ 0 & 2\gamma \bar{i}_q \bar{V}_c & 0 & -2\left(G_{dc} + \gamma \bar{i}_q^2\right) \end{bmatrix} \tag{D.6}$$

$$B = B^\top = \begin{bmatrix} 0 & 0 & 0 & 0 \\ 0 & 0 & 0 & 0 \\ 0 & 0 & 0 & 0 \\ 0 & 0 & 0 & 0 \end{bmatrix} \tag{D.7}$$

$$C = \begin{bmatrix} -2r_G & 0 & 0 & 0 \\ 0 & -2r_G & 0 & 0 \\ 0 & 0 & -2G_{pcc} & 0 \\ 0 & 0 & 0 & -2G_{pcc} \end{bmatrix} \tag{D.8}$$

Matrix A is identical to 3.99 and is in section 3.3 shown to be negative semidefinite when criterion 3.106 and 3.107 are satisfied. As r_G, G_{pcc} both are greater than zero, that means matrix C is negative definite. D.5 is thereby negative definite when 3.106 and 3.107 are satisfied. Term III is then monotonically decreasing. All conditions for the Lyapunov function is therefore satisfied.

In conclusion, the modification of the turbine string, by changing the grid connection to a current source, did not alter the stability criteria. This is in line with the proposition from section 3.2 that says that stability can be achieved by using passive feedback control on the generator connected converter and sufficient damping in the generator. When altering the grid side of the DC-link, the stability is thereby not effected.

Tutturen, T and Nyhus-Solli, J

Towards Plug-and-Play control of Wind power systems

NTNU

Kunnskap for en bedre verden